POLITECNICO DI MILANO
Faculty of Systems Engineering
Department of Electronics, Information and Bioengineering
PhD Programme in Bioengineering – XXIX Course

DEVELOPMENT AND EVALUATION OF SMART-MATERIAL-BASED SOLUTIONS FOR THE MECHANICAL CONTROL OF MOVEMENT DISORDERS

Candidate
Lorenzo Garavaglia

Advisors
Dr. Simone Pittaccio
Prof. Andrea Aliverti

Tutor
Prof.ssa Chiara Guazzoni

Coordinator
Prof. Andrea Aliverti

Completed in the year 2017

Abstract

The thesis describes the process that led to the design, construction and testing of a new wearable orthotic device for supporting upper-limb rehabilitation in children affected by Childhood Dyskinesia. The work starts presenting an analysis of the solutions already implemented and in use to treat Movement Disorders, investigating more in detail the neurophysiological basis of these kinds of diseases, and hypothesising a new approach to offer a valid relief. The principal requirements of the new solution, are that the orthosis be dynamic and wearable, that it impart a sufficient force field to help repositioning, support and control the voluntary motion, and dampen the involuntary ones, but mild enough to avoid hindrance to movement, while still being perceived as a stimulating sensory feedback. Moreover, the device should be fully customised, to transfer correctly the forces and be comfortable, thus augmenting the efficacy.

The idea of this new approach led to the second step of the thesis, i.e. the study and the selection of some functional material, that could fulfil the technical requirements and the initial working hypothesis. In particular, the thesis presents the dynamic viscoelastic core of the orthosis, i.e. parts made of NiTi-based alloys, a class of metallic materials displaying nonlinear stress-strain relationships and damping capacity. The section about the materials finishes by illustrating the specific treatments to optimise the functional elements, and characterising their mechanical behaviour.

Another important point is personalisation. The process to fully customise the dynamic device requires to deal with the construction of all the parts of the orthosis and the interfaces between the device and the limb, in order to increase the comfort and the efficacy. To accomplish

this aim, in the thesis is presented an innovative method based on optoelectronic stereophotogrammetry for all-in-one-frame acquisition of upper-arm geometry and a process for the design and production of wearable orthoses. This section describes the entire procedure to acquire data from the subject, virtually design the device, and physically construct and assemble it. This method provides all the quantitative data necessary to construct the orthosis without constraining the affected limb or subjecting the patients to annoyingly long acquisition sessions. Furthermore the method allows to design and modify the device as much as needed to fulfil all the anatomical and functional requirements before it is delivered to the subject.

Once the new customised dynamic wearable orthoses for the upper limb have been developed, it has been necessary to devise a protocol to test them on the affected patients, and evaluate the performance of the devices. To achieve this, a specialised method to collect kinematic data from dyskinetic patients has been created, together with a dedicated acquisition protocol, a home-written MatLab code to extract relevant kinematic parameters, and a post-processing method to evaluate the patients' status and the results of a rehabilitation treatment. Normality data from healthy young volunteers have been obtained as well, and used first to test the whole experimental procedure and then as a baselines of comparison for the tracings measured from the patients.

To conclude the study, five children affected by Childhood Dyskinesia have been enrolled and the thesis presents the results of five single-case trials conducted on those patients. The clinical trials were aimed at assessing the effect of the pseudoelastic orthoses on posture and movement control, and include the evaluation of the patients in 2 different conditions (with and without orthosis) at 2 milestones: before and after a one-month's rehabilitation treatment. The methods comprised clinical scales, videos, interviews and the *ad-hoc* quantitative

kinematic analysis based on the home-written subroutines devised for this purpose. The orthoses have been well accepted by all the subjects; they reported to have used them for far more hours than the minimum suggested by the clinicians. The quantitative evaluations reported a positive effect in terms of repositioning for the more dystonic patients and a more functional help for the hyperkinetic patients.

On the whole, our findings give a fairly broad overview of all the aspects concerning the new orthotic treatment, from its design and construction to its use and effects. Finally we tried to suggest possible improvements and future perspectives.

Sommario

La tesi presenta il processo che ha condotto alla progettazione, alla costruzione e infine alla valutazione di un nuovo dispositivo ortesico indossabile per il supporto alla riabilitazione dell'arto superiore in bambini affetti da Discinesia Infantile. Il lavoro inizia presentando un'analisi delle soluzioni già sviluppate e ad oggi in uso per il trattamento dei Disturbi del Movimento, investigando nel dettaglio le basi neurofisiologiche di questa classe di malattie ed ipotizzando un nuovo approccio che possa offrire un valido aiuto. Sono stati così delineati i requisiti del nuovo dispositivo proposto e in particolare, che l'ortesi sia dinamica ed indossabile, fornisca una forza correttiva che aiuti nel riposizionamento, sia di supporto e controllo per i movimenti volontari e smorzi quelli involontari; tali forze dovranno essere altresì sufficientemente basse da evitare di impedire il movimento pur essendo percepite, inducendo così una stimolazione sensoriale. Inoltre il dispositivo dovrà essere totalmente personalizzato sulle caratteristiche anatomiche e funzionali del paziente, trasferendo correttamente le forze per essere al contempo confortevole e massimizzare l'efficacia del trattamento terapeutico.

L'idea di questo nuovo approccio porta alla seconda parte della tesi, che riguarda lo studio e la selezione dei materiali funzionali che possano esaudire i tecnici requisiti richiesti per tale applicazione. In particolare parte della tesi è focalizzata sullo studio delle leghe di NiTi, una classe di materiali metallici che possiedono caratteristiche sforzo-deformazioni non lineari e una elevata capacità di smorzamento, potendo pertanto essere utilizzate come nucleo dinamico viscoelastico delle ortesi progettate. La sezione sui materiali si conclude illustrando i trattamenti termomeccanici specifici volti all'ottimizzazione della lega e alla

caratterizzazione del suo comportamento meccanico per la presente applicazione.

Un altro aspetto fondamentale del nuovo dispositivo proposto è rappresentato dalla personalizzazione. Il processo di personalizzazione dell'ortesi dinamica ha preso in considerazione non solo tutte le parti dell'ortesi stessa, ma anche l'interfaccia tra il dispositivo e l'arto al fine di incrementarne il comfort e l'efficacia. A tale scopo è stato messo a punto un metodo innovativo basato sulla stereofotogrammetria optoelettronica per l'acquisizione delle superfici corporee e quindi la ricostruzione della geometria dell'arto superiore, e il processo necessario per la progettazione e la costruzione delle ortesi indossabili. Questa sezione della tesi descrive l'intera procedura per acquisire i dati dai soggetti, progettare il dispositivo, costruirlo in tutte le sue parti ed assemblarlo, senza richiedere una partecipazione continuativa e spesso fastidiosa per il paziente. Il metodo inoltre consente di progettare e modificare variamente il dispositivo al fine di adattarlo perfettamente alle caratteristiche anatomiche del soggetto e ai requisiti funzionali prima di consegnarlo per l'uso.

Dopo aver sviluppato il nuovo dispositivo indossabile per l'arto superiore, è stato necessario sviluppare il protocollo sperimentale per testarlo sui pazienti al fine di valutarne l'efficacia. A tale scopo, è stato creato un metodo per l'acquisizione dei dati di cinematica ottenuti tramite uso del sistema optoelettronico, una serie di programmi MatLab per l'estrazione dei parametri di cinematica e il relativo metodo per la valutazione dello stato del paziente prima e dopo il trattamento. Sono stati acquisiti altresì dei soggetti sani con lo scopo di testare e validare l'intera procedura sperimentale prima della prova sui pazienti discinetici e per poter disporre dei tracciati da usare come riferimento per i pazienti.

La tesi presenta poi, come ultima parte, una serie di 5 single-case trial clinici per valutare l'effetto delle ortesi pseudoelastiche su 5 pazienti pediatrici discinetici. Lo studio prevedeva 2 differenti condizioni (*con* e *senza* ortesi) in due tempi differenti: *prima* e *dopo* un mese di trattamento con il dispositivo. Il protocollo comprendeva la valutazione tramite scale cliniche, video, commenti dei genitori e dei terapisti e l'analisi cinematica preparata *ad hoc*. L'ortesi è stata ben accettata da tutti i pazienti: hanno riportato di averla utilizzata per molte più ore rispetto a quelle suggerite dai medici di riferimento. Le valutazioni quantitative hanno mostrato un effetto positivo in termini di riposizionamento dell'arto paretico per i pazienti maggiormente distonici, mentre i soggetti maggiormente ipercinetici hanno riportato un miglioramento funzionale nell'arto testato.

In conclusione lo studio offre un'ampia osservazione di tutti gli aspetti riguardanti il nuovo trattamento ortesico dinamico funzionale, dalla sua progettazione fino all'utilizzo e i suoi effetti.

Table of contents

Introduction

The present thesis arises from the interest in understanding the relative current inefficacy in the general management of some neurophysiological diseases. Nowadays many patients, in particular children, are affected by Movement Disorders, that are a class of neurological syndromes, which produce particularly impairing conditions especially in the developmental age. Many different solutions have been developed and tested during the years in order to offer the best relief to these children. The lack of efficacy of pharmacological regimes, sometimes the high invasiveness of the surgical procedures, associated with the continuous changing of the clinical pictures, revealed the necessity to develop alternative solutions.

In this respect, the present thesis finds its rationale. Exploiting the knowledge coming from many different disciplines and research fields, a multi-modal strategy has been devised and is here presented. The work suggests a new approach for an adjunct neurorehabilitation treatment of children affected by a particular Movement Disorder: (secondary) Childhood Dyskinesia. This disease affects posture, and the child's manual skills, which are essential to develop and conduct an autonomous life. Considering the upper limb, it is evident that it is of paramount importance to find solutions that offer the dyskinetic children new opportunities to regain or at least maintain sufficient abilities to play, feed themselves, study and train in manual daily-life activities. Studying better these diseases and highlighting the pros and cons of the available treatments, inspired the general hypothesis of the present thesis: a new functional wearable dynamic orthosis, designed according to neurophysiological principles, can be of greater help with respect the present solutions, in supporting a more functional recovery of dyskinetic children. So, the main hypothesis took us to verifying a

whole set of collateral ones, necessary to complete the picture of the present work and in particular: what are the characteristics this device should display in order to achieve its goal? once the aim and the device characteristics are defined, how can it be fabricated? Furthermore, if the device is defined in terms of concept and also in terms of detailed characteristics and it is possible to construct it, how can it be properly evaluated?

This thesis, tries to demonstrate the hypothesis passing through every fundamental milestone of the process that leads from the conceptual design and the necessity to test it on patients to evaluating it in real-life conditions. Therefore it explains how to build a device thought-out in terms of its neurophysiological bases, and customised, on the one hand, on the specific clinical requirements, and on the other hand, on the patient's needs, for the improvement of an individual rehabilitation treatment. In parallel, the work comprises all the aspects necessary to test and evaluate the orthosis from a technical and medical point of view: materials have been optimised and characterised, comfort has been evaluated and then we have prepared all the files necessary for the clinical trials, including the experimental protocol to collect kinematic data from the patients, and those needed to obtain approval from an Ethical Committee and the Ministry of Health. In addition, we developed a suite of *ad-hoc* home-written software subroutines to analyse quantitatively the kinematics of the patients, and extract trends from the tracings collected. In doing this, we also enrolled a cohort of healthy subjects to check that the entire process was *a priori* reliable and harmless for the children, and also to obtain a baseline of comparison for a better understanding of the patients' trends.

Chapter 1

Nature and management of childhood dyskinesia: neurophysiological bases for a new orthotic approach

The chapter presents an analysis of the solutions already implemented and in use to treat Movement Disorders, investigating more deeply the neurophysiological basis of these kinds of diseases, hypothesising a new approach to offer a valid relief, and giving some hints to design and implement a new solution.

1.1 Introduction

Movement Disorders are a class of diseases that impair the daily activities of patients in quite a severe way, conditioning their sensorimotor, cognitive, behavioural capabilities. In particular, Childhood Dyskinesia hinders the motor abilities of the subjects causing difficulties in movement control and the insurgence of unwanted gestures or postures. This kind of movement disorder affects posture, gait and the child's manual skills, which are essential to develop and conduct an autonomous life. Considering the upper limb, it is evident that it would be of paramount importance to find solutions that offer a valid relief and make it possible for the dyskinetic children to regain or at least maintain sufficient abilities to play, feed themselves, study and train in manual activities. Solutions adopted over the years, such as pharmacological, physical and manual treatments, surgical interventions, together with mostly traditional orthotic devices, helped improve the rehabilitation quality and the overall conditions of the patients. Those same methods often fail to restore functional abilities though, due to the complexity of the pathophysiological substrates, so, looking at improving even more the life-quality of those paediatric patients, granting them also a greater independence, which is fundamental during their developmental age, it is evident that there are still many points to be addressed. The preferred scenarios include the introduction of new *non-invasive* therapies. In this respect, the chapter presents several considerations aimed towards the implementation of a possible wearable orthotic solution for Childhood upper-limb Dyskinesia, i.e. in terms of clinical efficacy, functional usability, pain reduction, and better comfort. This new orthosis, besides building upon what has already been done and proposed in the field, will also try to integrate the available knowledge about the neurophysiological bases of dystonia and hyperkinesia, in order to exploit inherent mechanisms such as the sensory and proprioceptive information to recondition dynamic postural

and motor control. The rationale of those principles is exposed in the Discussion to this chapter.

1.2 Definitions and Classifications

1.2.1 Movement Disorders

Movement Disorders can be defined as neurologic syndromes in which either an excess of movement or a paucity of voluntary and automatic movements, unrelated to weakness or spasticity (Fahn et al. 2011). The term Movement Disorders is used synonymously with basal ganglia or extrapyramidal diseases (Bradley, 2004).
Conventionally Movement Disorders are divided into two major categories:

i. Hyperkinetic Movement Disorders also called dyskinesias refers to excessive, often repetitive, involuntary movements that intrude into the normal flow of motor activity.
ii. Hypokinetic Movement Disorders refers to akinesia (lack of movement), hypokinesia (reduced amplitude of movements), bradykinesia (slow movement) and rigidity.

In primary Movement Disorders the abnormal movement is the primary manifestation of the disorder. In secondary Movement Disorders it is an manifestation of other systemic or neurological disorder (Flemming et al. 2015).
Movement Disorders in childhood are more likely to be secondary symptoms of other diseases, rather than primary (Sanger 2003; Sanger et al. 2003; Schlaggar et al. 2003). In addition, whereas adult neurological disorders are often linked to anatomically localised pathology, childhood disorders are frequently due to global or multifocal injury and manifest across multiple areas of function, including sensorimotor and cognitive ones (Bertucco et al. 2016; Hallet 2008).

In this thesis, the focus will be on one type of Movement Disorder of the young, i.e. Childhood Dyskinesia, which will be described in general and in its components in the following sections.

1.2.2 Childhood dyskinesia

Childhood dyskinesia is a complex and impairing motor disease that affects paediatric patients and presents different symptoms that are common to various Movement Disorders (Koy et al. 2016). Practically, these patients are often classified by the predominant movement disorder with listing of secondary disorders. (Sanger et al. 2010), and (Butler et al. 2012). There are different possible neurological classifications in childhood dyskinesia. Generally, authors recognise two main sub-groups, one more static (*dystonic*, *hypertonic*) and one more dynamic (*hyperkinetic*) (Hou et al. 2006). It is generally difficult to identify childhood dyskinesia in a precise manner ascribing the syndrome to a specific sub-form. Most often dyskinetic children show a mixed hypertonia, with components of spasticity and dystonia (Sanger et al. 2003). Despite the formal separation between "more dystonic" and "more hyperkinetic" types, it appears that dystonia is a very relevant component in all forms of childhood dyskinesia. In fact, common observation of dystonia suggests that it can cause hyperkinetic movements as well as hypertonic movements (Sanger 2004).

Dystonia is characterised by sustained or intermittent muscle contractions that cause abnormal, often repetitive movements, postures, or both (Albanese et al. 2013; Sanger 2004). It is possible that dystonia itself has a role in causing hyperkinetic movements (Figure 1.1), i.e. by inserting dystonic postures that interfere with the voluntary movements. If multiple brief dystonic postures are inserted, variable, jerky, and tremulous movements may arise. On the other hand, if the inserted dystonic postures are sustained, movement can become hindered and slower than expected (Bertucco et al. 2016 and refs therein).

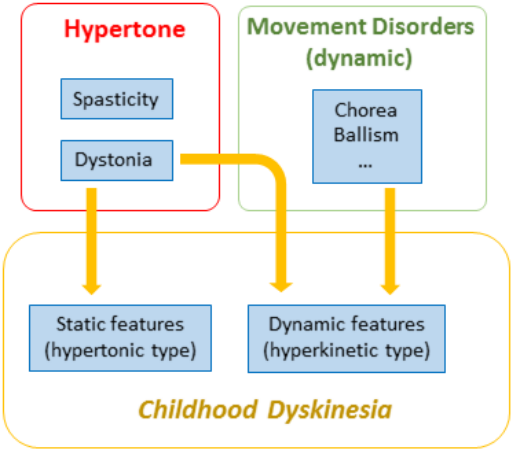

Figure 1.1 The scheme illustrates the fundamental role of Dystonia in determining hypertone and also the static and dynamic features of Childhood Dyskinesia (inspired by Bertucco et al. 2016).

Other components of the hyperkinetic type of childhood dyskinesia include more dynamic Movement Disorders, and in practice, many children with hyperkinetic Movement Disorders have a combination of chorea, athetosis, or ballism; dystonia, tics, or myoclonus may also be present (Singer et al. 2015).

Childhood dyskinesia is mainly seen in cerebral palsy syndromes correlated with extrapyramidal lesions showing increased involuntary movements including dystonia, chorea, athetosis, and tremor (Singer et al. 2015).

Cerebral palsy (CP) is the commonly used name for a group of conditions characterised by motor dysfunction due to non-progressive brain damage early in life (Leavitt 2010). It can be classified as spastic, athetoid (dyskinetic, dystonic) or ataxic (rare) (Leavitt 2010). As widely reported in the literature, the causes of dyskinetic CP are many, including abnormal development of the brain, anoxia, intracranial bleeding,

excessive neonatal asphyxia (hypoxic ischaemic neonatal encephalopathy), trauma, hypoglycaemia, anoxia as in near drowning, choking, neurotrophic virus and from various infections (Rosenbloom 1995; Hagberg et al. 1996; Stanley et al. 2000; Himmelmann et al. 2005). According to the recent data, dyskinetic cerebral palsy (CP), a type of CP primarily associated with damage to the basal ganglia, is the most common cause of dystonia in children. It accounts for approximately 10-15% of cases of cerebral palsy. It has a total incidence of 0.15-0.25 per 1000 in Western countries with an expected prevalence in the US of 50000-75000 (Bertucco et al. 2016; Singer et al. 2015). Some of the main features of dyskinetic CP, which consequently can be generalised as the main traits of Childhood Dyskinesia are the following (Leavitt 2010):

Involuntary movements. These patients produce bizarre, purposeless movements which may be uncontrollable, slow or fast, with different patterns and amplitudes, or unpatterned. Dyskinesia may appear only in the hands or feet, or in proximal joints; or in both distal and proximal joints. Generally, the child finds it very difficult to remain still.
Poor postural control. The involuntary movements or dystonic spasms can be the cause of postural imbalance.
Impaired voluntary movements. Intentional motion is possible but there may be an initial delay before the movement is actually started. The involuntary movements may partially or totally disrupt the voluntary one, making it uncoordinated. There is often a lack of finer movements, and grasping or releasing objects is often very difficult.
Hypertonia. There is often hypertonia or fluctuations of the tone. The hypertone or dystonia produce a continuous resistance to passive stretch throughout the full range-of-motion. Abnormal patterns of muscle activation occur, including excessive co-contractions of antagonist muscles and overflow of activation to muscles other than the task-related ones. Dystonia can be particularly disabling, especially if combined with spasticity.

Changing dyskinetic types. A floppiness in babyhood can change to a picture of sheer involuntary movements when children reach 2 or 3 years of age. Adults do not appear hypotonic but have muscle tension possibly increased by the effort to control involuntary movements.

The lack of movement can affect the general behaviour of the child. Thus, some abnormal behaviour may be due to the lack of satisfying emotional and social experiences for which movement is necessary. Motor dysfunction may therefore interact with emotional and social development of a child (Leavitt 2010). Childhood dystonia can lead to lifelong disability, thus it represents a significant healthcare and rehabilitation challenge (Bertucco et al. 2016).

1.3 Present treatments and solutions

1.3.1 General Management

As presented above, Childhood Dyskinesia is generally a symptom of some major disease (like CP), which comprises many different facets, such as sensorimotor, cognitive, behavioural etc. (Thylefors et al. 2000; Leavitt 2010). As already reported by different authors the earlier the treatment is started, the more opportunity is given for whatever potential there may be for developing any normal abilities and for decreasing the abnormal movement patterns and postural difficulties (Kong 1987; de Groot et al. 1993). A total rehabilitation programme is necessary and should be planned to deal with the whole development of each child. Whilst aiming at the maximum function possible, it is important to take account of the *damaged* nervous system and adjust the expectations of achievements by the child (Leavitt 2010). Treating of the sensorimotor aspects of Childhood Dyskinesia is essential for the general improvement of the patients, and not only for the aspects strictly related to the motor domain, and can therefore be considered of paramount importance. It is clear, in fact, that an abnormal motor

behaviour interacts with other functions. Each area of development, such as gross motor, manipulation, speech and language, perception, social and emotional adjustments, and cognition, interacts as well as has its own pattern or avenue of development (Leavitt 2010).

The principal targets of sensorimotor rehabilitation in this kind of Movement Disorders are to improve or restrict the effect of abnormal movements on the growing musculoskeletal system, to reduce pain, and to increase quality of life (Koy et al. 2016). To achieve this, the management strategy requires a multidisciplinary approach (Koy et al. 2016). As some of the present solutions (such as major surgical interventions or strong pharmacological treatments) still have possible negative counter effects, in some cases better results can be obtained from the combination of different methods and treatments. The rehabilitation process carried out in this way should aim to reinforce life autonomies, but should also avoid as much as possible the patient's dependence on tools or systems that are too cumbersome, and could turn out as a limit in their daily-life activities or social integration.

1.3.2 Sensorimotor rehabilitation in Childhood Dyskinesia

There is little evidence from randomised controlled trials on the best therapeutic strategies for the management of Movement Disorders in children; evidence to determine best practice for the management of abnormalities of tone and movements are particularly lacking. Present management options for paediatric Movement Disorders are primarily based on the personal experience of the treating physician and recommendations inferred from the results of randomised trials in adult patients, with only few exceptions (Koy et al. 2016). Nowadays some different kinds of treatments are employed by clinicians to correct dystonic postures and control dyskinetic movements, such as pharmacological treatments, surgery, physical and manual treatments and orthotics (Sanger 2004; Jankovic 2006; Jankovic 2009). The management of complex paediatric movement disorders requires a

multidisciplinary approach; physiotherapy and pharmacotherapy are the cornerstones of management, and although there are exceptions, most treatment is symptomatic (Koy et al. 2016). In almost all countries, the major pharmacological as well as non-pharmacological treatments that are used in these patients are classified as off-label (Koy et al. 2016).

Drugs

According to the relevant amount of literature written in the last few years, the standard approach starts with pharmacological treatment (Fig. 1.2).

Several different classes of drugs have been used to treat dyskinetic patients, mostly off-label. We just mention the most important ones. Among those working or on the central nervous system, i.e. influencing the neurotransmission include dopaminergic, GABAergic, anticholinergic, antidopaminergic and adrenergic drugs, which are used to modulate the action of inhibitory and excitatory pathways. In addition, antiepilectic drugs are often prescribed to these patients.

A myorelaxant with central action like Baclofen ($GABA_B$ receptor agonist) can be used orally or, often intrathecally.

There are also drugs that act at a peripheral level, including powerful chemodenervation agents such as Botulinum toxin A, which is employed to provoke a temporary paralysis on the muscles affected by dystonia and reduce the negative symptoms.

Pharmacotherapy is marked by variable efficacy and limited by side-effects (Koy et al. 2016). There are some standardised guidelines for their choice (Fig. 1.2).

Surgery

If drugs are inefficient, even changing the types and dose, the following option is surgery that is avoided only in cases where inapplicable due to the high invasiveness, especially in children (Albanese 2007; Jankovic 2009).

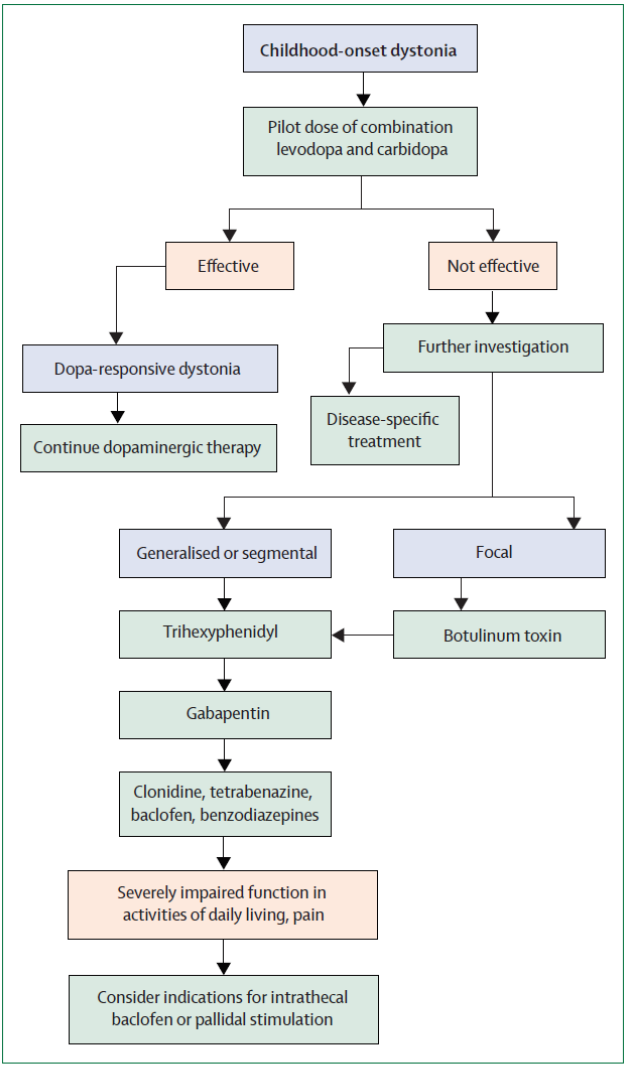

Figure 1.2 The flowchart presents an attempt to standardise the protocol for the selection of pharmacological regimes for childhood-onset dystonia (courtesy of Koy et al. 2016).

Particularly GPi DBS (Deep Brain Stimulation of the Globus Pallidum pars Interna), is considered as a valuable treatment for patients with disabling dystonia; it is used for the correction of symptoms of some forms of dystonia, like primary generalised dystonia, which seems to respond better than secondary dystonia. Those procedures have been mostly abandoned since the botulinum toxin became available, (Jankovic 2006) but now, thanks mainly to the improved understanding of the functional anatomy of the basal ganglia and physiological mechanisms underlying Movement Disorders, coupled with refinements in imaging and surgical techniques a resurgence of their use has been observed (Jankovic 2009 and references therein).

Physiotherapy

Besides pharmacotherapy and surgery, there are various non-pharmacological options, used in combination with or instead of pharmacotherapy, that can be offered to children with motor dysfunction to preserve or restore function, relieve abnormal posturing, and minimise pain.

Supportive therapy (e.g., physiotherapy, occupational therapy, etc.) is central to the clinical treatment of most children with disabling Movement Disorders (Koy et al. 2016).

Some experiences showed the importance of specific and well thought-out manual therapies; in particular the role of sensory stimulation has been stressed in many different physiotherapeutic approaches (Rood 1962; Stockmeyer 1967; Stockmeyer 1972). Herman Kabat, a neurophysiologist and psychiatrist in the United States, has discussed various neurophysiological mechanisms, which could be used in therapeutic exercises. Together with his team, he developed a system of movement facilitation techniques and methods for the decrease of hypertone, for strengthening, coordination and improving joint range (Kabat et al. 1959; Knott & Voss 1968; Voss 1972; Voss et al. 1985). The

main features of these methods include movement patterns, sensory stimuli, resistance, 'special techniques' and functional works. In particular, sensory (afferent) stimuli are skilfully applied to facilitate movements. Stimuli used are touch and pressure, traction and compression, stretch or limb elongation and the proprioceptive effect of muscles contracting against resistance (Leavitt 2010).

Orthotics

Even if nowadays many steps further in the support and treatment of the Childhood Dystonia have been done, current intervention options, including physical and occupational therapies, pharmacological approaches, and deep brain stimulation, are often not successful or only partially successful in controlling symptoms. As a result, there is a need to investigate new non-invasive options for treating dystonia in children (Bertucco et al. 2016). In this respect, orthotic devices have been developed and positively used to support the rehabilitation of patients affected by Movement Disorders.

Physical therapy and well-fitted braces are designed primarily to improve posture and to prevent contractures in dystonia (Jankovic 2006; Jankovic 2009 and refs therein; Rodrígues & Gajardo 2012). Correspondingly, most emphasis in the use of the orthotics for cerebral palsy has often been placed on avoiding deformities rather than favouring functional rehabilitation (Morris et al. 2011). On the other hand, it has been suggested that in childhood dystonia, soft or semi-rigid braces in particular could help the functional positioning during movement, containing the joint and giving proprioceptive information (Rodrígues & Gajardo 2012).

While there is substantial evidence that ankle foot orthoses can improve gait efficiency in ambulant children, little high quality evidence exists to support the use of orthoses for the hip, spine or upper limb. Where the evidence for orthosis use was not compelling, consensus was anyway

reached on recommendations for orthotic intervention (Morris et al. 2011).
Here will be presented a number of wearable devices found in the literature, which have been divided, for our purposes, in the following categories: *casting*, *rigid orthoses*, *soft orthoses* and *devices providing stimulation*.

Casting
Casting is reported as a technique to reduce hypertone. Two studies by the same group (Law et al. 1991; Law et al. 1997) considered the use of casting in connection with neuro-developmental therapy (NDT). The study compared two different intensities of NDT provided by occupational therapists with and without the association of bivalve casts. The studies report discordant results in populations of similar age (18 months – 4 years and 18 months – 8 years old) with different conclusions about the effects on hand function and upper extremity movements.

Rigid orthoses
In general rigid orthoses are made of relatively thick thermoplastic in order to provide rigidity, position and stretch the muscles in patients with increased muscle tone. These devices are therefore employed especially to avoid deformities, but they tend to block the function, and prevent the beginning of the chain of disuse, atrophy, malfunctioning, created as a functional pattern (Rodrígues & Gajardo 2012). Besides the traditional splints, which only provide stretch and position (e.g. Figure 1.3), the literature reports applications of rigid orthoses that could influence the control of movement in dystonia based on different rationales.
The possible approaches are (1) that immobilisation of some degrees of freedom in the kinematic chain can help control the others; (2) that

Figure 1.3 The picture shows a traditional rigid resting splint nowadays used to stretch and position the upper limb extremities (adapted from Rodrígues & Gajardo 2012).

immobilising the unaffected limb can help exercise more the impaired limb (cf. constraint-induced therapy); or (3) that immobilising the affected limb could bring a beneficial effect through sensory deprivation. An example of the first approach is from Taş (Taş et al. 2001). In this case, improvements in the writing ability of dystonic patients was obtained by using a static hand orthosis, that supported and immobilised the segments of the hand interfering with writing (thumb, fingers, or wrist), and allowing the proximal large muscles to control the writing movements (Fig. 1.4). A second example of the same approach was given by the study of the Egyptian researchers El-Maksoud et al. who concluded that wearing an elbow immobiliser during the application of an occupational therapy programme has a potential benefits to improve the hand function in children with athetoid CP. That device restricted the unwanted movement around the proximal joints (shoulder and elbow joints), which made it easier for the child to control distal joint (wrist joint) and produce smooth movements. In particular, the elbow immobiliser allowed the children to sustain their training for longer time

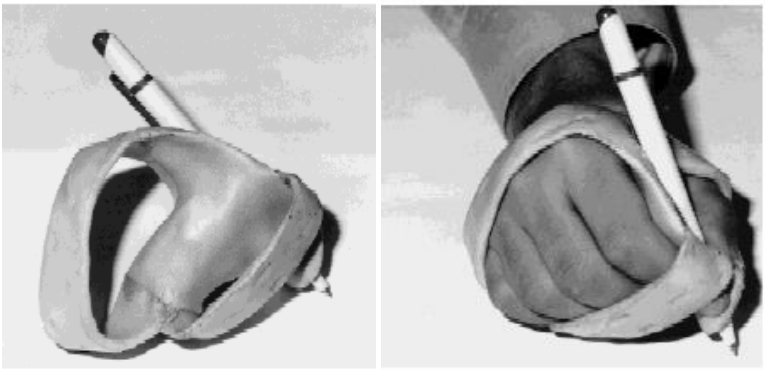

Figure 1.4 Figure 4 The pictures show a rigid hand orthosis worn (right) by a subject affected by writer's cramp (courtesy of Taş et al. 2001).

and in an effective way. The significant improvement noticed in hand function in the study group vs controls (that only did the occupational routine) may be due to reduced distal involuntary movement by wearing the elbow immobiliser during training of fine motor skills (El-Maksoud et al. 2009).

Constraint-induced movement therapy (2) has been widely and successfully used in the rehabilitation of patients with spasticity after stroke (attributed in part to cortical reorganisation), to constrain non-dystonic segments to exercise the affected ones (Candia et al. 1999), but whether this approach will have any use in the treatment of dystonia is unclear (Jankovic 2009 and refs therein; Crocker et al. 1997). Looking at the third possible approach (3), casting or immobilisation by an orthosis has been suggested also as a treatment aiming to deprive the dystonic segments of motion and sensation, which, according to the authors, could help patients reset lost motor schemes (Priori et al. 2001).

Regardless the rationale, it must be considered that immobilisation can actually exacerbate or even precipitate dystonia, as is the case in peripherally induced dystonia (Jankovic 2009 and refs therein).

Figure 1.5 Figure 5 The pictures show a dystonic CP young girl before and after wearing TheraTogs® vest for the hip repositioning. (from the TheraTogs® website: theratogs.com/sma/)

Soft orthoses

In general, soft orthoses are made of relatively thinner thermoplastic structures or other soft and compliant materials, which help the technicians to build devices, specially designed to allow some voluntary movements or at least preserve and favour residual motion. Their design in the last few years has been done in the respect to offer not only a repositioning action in controlling the worsening of the deformities, but also in trying to add a sensory action useful in increasing the functional recovery of the patient or at least their limb perception, in order to use it better.

Amongst the flexible wearable splints for CP, there have been studies on several garments made of Lycra®. Results regarding their efficacy are not conclusive and they appeared to be very difficult to don and doff (Nicholson et al. 2001; Coghill et al. 2010; Morris et al. 2011). Also TheraTogs® has been employed in the rehabilitation support of dystonic patients. This system is generally applied only to lower limbs and trunk, to sustain walking or steady standing, acting on the hips and pelvis (Fig. 1.5).

Another solution was developed (originally as a countermeasure for microgravity in space missions), and used especially in the countries of

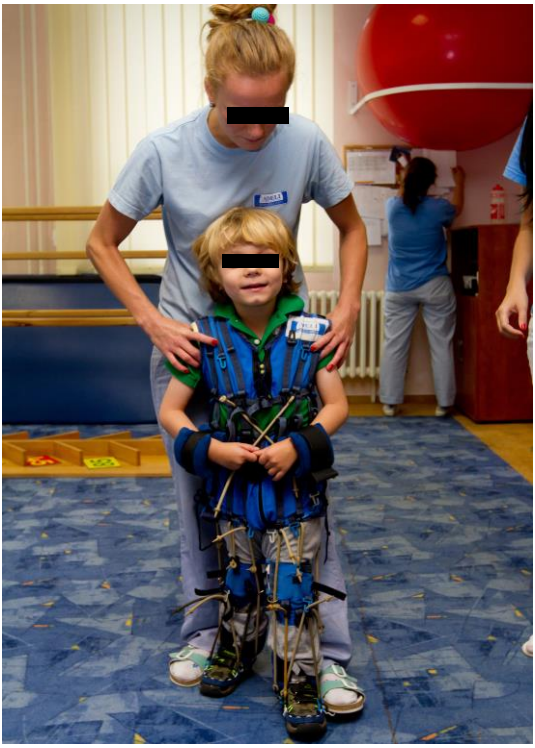

Figure 1.6 Figure 6 Adeli suit for a CP children (from the Wikipedia website: en.wikipedia.org/wiki/Adeli_suit)

Eastern Europe. This is the Adeli suit (various versions), which concentrates the corrective elastic elements in specific parts of the vests (Fig. 1.6). Muscle strengthening with the Adeli suit, which provides resistance to some movements, is claimed to improve also sensory feedback during movement and subsequent mechanical efficiency in the lower limbs and trunk (Semenova et al. 1997; Shvarkov et al. 1997; Bar-Haim et al. 2006).

As a further tool, the Ukrainian Kozyavkin method introduced the Spiral suit, which consists of a system of elastics straps which are wrapped in a

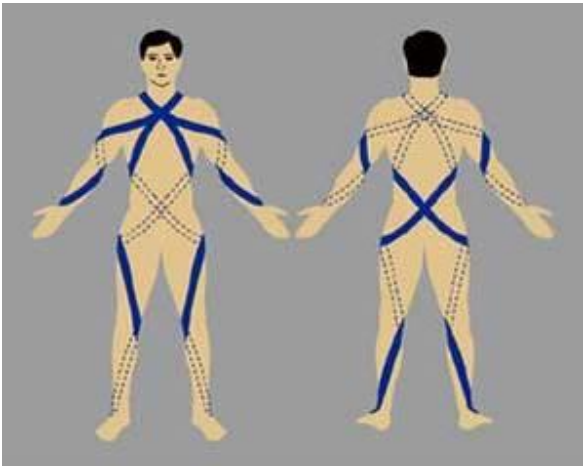

Figure 1.7 Figure 7 The Ukrainian 'Spiral suit' for lower limbs, trunk and upper limbs used for the Kozyavkin method (from the website: reha.lviv.ua/spiral.98.html?&no_cache=1).

spiral across the body and extremities and attached to supportive elements on the trunk and extremities (vest, shorts, knee, elbow, foot and wrist pieces), and consequently also the upper limb can be treated by wearing this device (Fig. 1.7). Elastic straps, by imitating the positions of the main muscle groups, provide the necessary corrective force. Velcro attachments on the straps allow for various adjustments to be made optimising the corrective action desired. The absence of the rigid parts in the suit significantly broadens the range of possible physical therapy exercises. The system consists of an axial spiral, main extremity spirals and supplemental correction bands (straps) (reference in http://reha.lviv.ua/spiral.98.html?&no_cache=1&L=quymchwfustk).

Devices providing stimulation

Amongst the devices found in the literature, which have been used in the last decade to support the rehabilitation of patients affected (by dystonia mainly) there are system inducing sensory stimulation on the

limbs, i.e. peripherally, or directly on the central nervous system, such as non-invasive brain stimulation (NIBS).
In particular, some authors have reported how providing a sensory stimulation (peripherally) on the affected limb, i.e. additional proprioceptive feedback, could help facilitate its control. For instance, it was reported that in children with dystonia, the ability to voluntarily and selectively control the activation of a target muscle at different levels of the upper limb kinematic chain could be improved by means of a EMG-based vibro-tactile biofeedback device placed on the skin over that muscle (Bloom et al. 2010).
Other researchers investigated the possibility to impart a stimulation directly on the motor cortex to drive the motor action from the source. Some interesting results in the treatment of dystonia have been obtained in adults using NIBS (Non-Invasive Brain Stimulation), and in particular rTMS (repetitive Transcranial Magnetic Stimulation), (Siebner et al. 1999; Kimberley et al. 2013; Matsumoto et al. 2016). Other experiments have been done by different groups, to treat cerebral palsy, including cases of dystonia especially using rTMS and tDCS (transcranial Direct Current Stimulation), (Kirton et al. 2016; Bertucco et al. 2016). Most of the results reported by Kirton are quite encouraging. The stimulation targets and parameters used by the cited groups tend to be different, so more experimentation is probably necessary to define consensus procedures.

1.4 Neurophysiological considerations on the development of a new orthosis for Childhood Dyskinesia

1.4.1 Movement control and the role of extrapyramidal circuitry (Basal Ganglia)

The movement is the final manifestation of a complex series of interactions of different structures, in particular cortical structures, deep

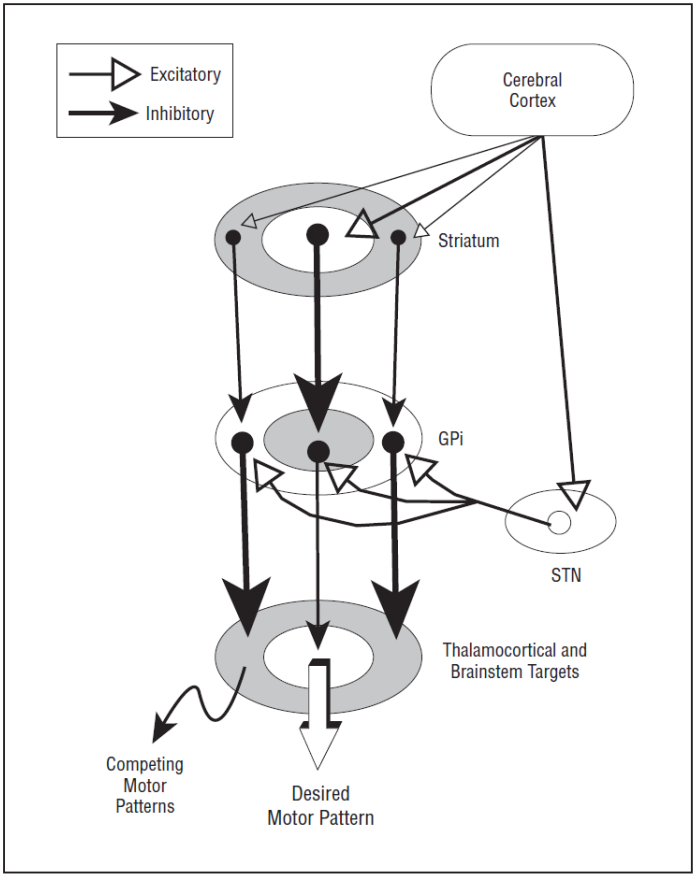

Figure 1.8 Figure 8 The pictures reports the functional organisation of the Basal Ganglia output for selective facilitation and surround inhibition of competing motor patterns. Open arrows indicate excitatory projections; filled arrows, inhibitory projections. Relative magnitude of activity is represented by line thickness. GPi indicates globus pallidus pars interna; STN, subthalamic nucleus (courtesy of Mink 2003).

brain and spinal cord structures, sensorimotor receptors, muscles and the skeletal system. All these parts work together at different levels in

order to generate, transmit, actuate and evaluate in feedback, the brain input signals. In case of malfunctioning or damage to one of the actors in this complex network bring to a motor dysfunction that could affect and impair the subject at different severity. Due to the dimension of this network and the related complexity, the present section will not try to cover all aspects of its functioning, but it will present briefly the role and the general function of the Basal Ganglia, because of their central role in the extrapyramidal syndromes that are in the focus of this thesis (for the general and detailed aspects of the overall system the reader is referred to a good textbook of neurophysiology e.g. Bloom et al. 2008 or Kandel et al. 2012).

It is known from abundant observations, that a malfunctioning of the Basal Ganglia produces severe movement impairment, such as affects patients with Childhood Dyskinesia. This is due to the role that these structures have in binding the motor execution to a desired voluntary action, rather than allowing the execution of competing (unwanted) patterns.

A very well-recognised model devised in 1996 by Mink explains this mechanism:

"*Basal ganglia output neurons inhibit the motor thalamus and the midbrain extrapyramidal area; their role has been proposed to be analogous to a braking mechanism such that increased activity inhibits and decreased activity facilitates motor pattern generators in the cerebral cortex and brainstem. The inputs to the GPi and SNpr from the striatum and subthalamic nucleus (STN) are organised anatomically and physiologically such that the striatum provides a specific, focused, context-dependent inhibition, while the STN provides a less specific, divergent excitation. Because the output from the GPi and SNpr is inhibitory, this organisation translates to a focused facilitation and surround inhibition of motor mechanism in thalamocortical and brainstem circuits (Fig. 1.8). The function of this organisation is to*

selectively facilitate desired movements and to inhibit potentially competing movements" (Mink 1996; Mink 2003).

Although the basal ganglia do not directly receive sensory information, processing of indirect information by the basal ganglia has a distinct effect on movement. Several neurophysiological studies provide support for the idea that the basal ganglia serve as a *gate-keeper for sensory inputs* at various levels along the CNS, and that abnormal sensorimotor integration is a key feature in the pathogenesis of many movement disorders (Patel et al. 2014 and refs therein). Abnormal sensorimotor processing could lead not only to sensory symptoms but also to sensory and motor abnormalities. Increasing evidence suggests that proprioceptive sensory input plays a crucial part in the generation and coordination of movements (Patel et al. 2014 and refs therein). For all those reasons, if a damage or a malfunctioning occurs to Basal Ganglia structures, the resulting picture will be of severe and disabling Movement Disorders. Extrapyramidal primary lesions in the basal ganglia may result in voluntary motion disorders with increased involuntary movements, showing torsion, spasm, dystonia, chorea, athetosis and others. How these symptoms are combined in children with dyskinetic cerebral palsy depends on the period, aetiology, and spot of the brain lesions (Hou et al. 2006). More in specific, some authors reported that *dystonia* has been associated with injury to the basal ganglia, and in particular, dystonia arises from a net decrease in firing of inhibitory neurons projecting from the internal segment of globus pallidus to the ventral thalamus, causing an increase in the activity of excitatory thalamo-cortical projections to motor and premotor regions of the frontal cortex (Bertucco et al. 2016). Many observation pointed out that sensorimotor integration is extremely important in the planning and execution of movements. The principal manifestations, observed in patients affected by Dyskinesia, and derived from the dysfunction to this extremely complicated circuitry, bring to variability in motor commands,

overflow, hypertone, changes in sensorimotor integration; all these alterations from the physiological pathway will be exposed in the following section.

1.4.2 Observations and models concerning the phenomenology of Childhood Dyskinesia

This section tries to analyse Childhood Dyskinesia in terms of its symptoms, phenomena and their neurophysiological bases in order to extract useful knowledge about specific mechanisms that can be seen and used as design constraints or an exploitable help in conceiving a new orthosis to treat this disease. Variability in motor command, overflow, hypertone, changes in sensorimotor integration, will be presented to this end.

Variability

The higher than normal variability in the repeated execution of a motor task in dyskinetic cerebral palsy supports the interpretation of basal ganglia dysfunction as the lack of appropriate filtering of random motor schemes (Sanger 2006). It has been shown that hyperkinetic and unwanted movements in upper extremities in children with dyskinetic CP are characterised by increased signal-dependent noise (SDN) of the motor system. The SDN theory states that noise in motor commands (e.g. spatial variability) tends to increase with the motor command's magnitude (e.g. force, velocity). This means that children with dystonia require significantly slower movements to contain the increased motor variability if they want to achieve comparable precision to typically developing children. Even if the relationship between basal ganglia injury and increased signal dependent noise is not known, it could be inferred that, based on the model reported in the above section 1.4.1 of this chapter, the Basal Ganglia disease might lead to decreased inhibition or perhaps even excitation of unwanted patterns, resulting in increased motor variability (Bertucco et al. 2016 and refs therein)**.** An increased

sensitivity to the accuracy requirements of the task arises from an increase in the variability of movement with increasing movement speed. According to Sanger, the hypothesis of increased signal-dependent noise in dystonia, and a simple computational model provides a possible explanation for such noise on the basis of decreased specificity in the selection of movements by the basal ganglia (Sanger et al. 2005).

Lesson learnt

The noise superimposed on the movement affects the outcome of motor task execution and causes variability and imprecision. The fact that there is a direct dependency between the noise, the movement amplitude and speed suggests that a solution that reduces or at least contains the positioning inaccuracy could help patients achieve higher velocities and broader movement spans for a given precision.

Overflow

Amongst the disabling features characteristic of dystonia, there is *overflow*, which is the close temporal association of unwanted muscle contractions with an intended movement. In many circumstances it is the apparent spread of motor activation to surrounding or distant muscles different from those typically recruited for the goal-directed action. Overflow may also trigger a dystonic posture during voluntary movement (Bertucco et al. 2016). The current hypothesis, expressed in the Mink model (Mink 2003), is that dystonia results from incomplete suppression of competing motor patterns due to insufficient surround inhibition of competing motor patterns generators. This deficient surround inhibition may also lead to expansion of the facilitatory centre, which would lead to “overflow” contraction of adjacent muscles. Decreased efficacy of the surround with or without expansion of the centre causes inappropriate disinhibition of unwanted muscle activity.

Lesson learnt

A contraction of unwanted muscles accompanying the activation of the specific muscles required for the execution of some task is the principal external expression of the dyskinetic overflow. This observation brings to different possible management approaches: (1) avoid to contract a muscle to prevent the undesired activation of adjacent muscles, (2) provide adequate forces to support the muscles involved in the execution of the desired motor task; in doing this it is expected that a burden of voluntary control could be partially shifted to limiting the unwanted contractions, i.e. the overflow; (3) offer a direct constraint to control the movements not specifically involved for the execution of the action. While option (1) is inapplicable, lest the voluntary action is not achieved, options (2) and (3) could be implemented with different devices.

Hypertone

Hypertonia is defined as abnormally increased resistance to externally imposed movement about a joint. There is still a debate about the machanisms by which hypertonia occurs in dystonia. It was previously thought to be the result of tonically co-contracting muscles that contribute to passive joint stiffness. This model is coherent with what is known about joint stiffening in normal posture. More recent studies suggest that reflexes may play an important role (Bertucco et al. 2016).

Co-contraction (the simultaneous contraction of antagonist muscles) is known to stabilise limb movements (Bizzi et al. 1978; Milner et al. 1995; Milner 2002). Co-contraction alters the biomechanical operating ranges of muscle and tendon by increasing both muscle-tendon stiffness (elasticity) and muscle damping (viscosity) (Winters et al. 1988; Milner et al. 1998; Heitmann et al. 2012). The hypothesis that excessive tonic co-contraction is the main mechanism of stiffening in dystonia rests upon the above observations and is supported by the fact that co-

contraction is present in adult focal dystonias (van Doornick et al. 2009). On the other hand, this has not been tested in childhood generalised secondary dystonias. Furthermore, adult focal dystonia is often not associated with hypertonia at rest (van Doornick et al. 2009).

Looking at the considerations leading to hypertonia being linked to reflexes there are several interesting results. One prominent feature of hypertonic dystonia is that a fixed posture may be maintained at a non-extreme joint angle. This is different from spasticity, in which fixed postures tend to occur at joint limits (maximal ankle or knee extension, or wrist flexion, for example). In the literature different theories have been suggested about the possible causes of hypertone and its manifestations. For example Kats et al. reported that a hypertonic limb with dystonia may not necessarily have involuntary muscle activation prior to movement. Since the characteristic activation does not exhibit a threshold velocity or angle leading to a “catch”, and since spinal mechanisms are presumably normal, it is likely that, if such dystonic reflex activation occurs, it occurs through a different mechanism from that of the monosynaptic stretch reflex (Kats et al. 1989; Kats et al. 1992). On the other hand, van Doornik observed that during passive flexion and extension movements of the elbow in 8 children with hypertonic arm dystonia, due to dyskinetic cerebral palsy, there was always significant phasic electromyographic activity in the lengthening muscle, consistent with reflex activity. Based on the evidence that some children exhibit position-dependent activation, some exhibit velocity-dependent activation, and some exhibit a mixed pattern of activation, the same authors conclude that, the involuntary or reflex muscle activation in response to stretch, may also be a significant contributor to increased tone in hypertonic dystonia. Most of the subjects (7 out of 8) had little or no triceps activity at rest, which means that their biceps activity at rest was not a component of involuntary co-contraction of agonist and antagonist (van Doornick et al. 2009). There have been attempts (Gordon et al. 2006) to separate dystonic contributions from spastic ones

in children affected by cerebral palsy. That was done utilising measures of overflow to other muscles (dystonic features) and force-velocity relationship (spastic features). The results showed that in spite of a "spastic" or "extrapyramidal" diagnosis, most children had a combination of both spasticity and dystonia. As demonstrated by the different, and not completely in accordance, opinions stated by researchers over the years, and considering that, many of them suggested further investigations to shed more light on the nature of hypertone, a wise approach looking at the hypertone symptom in Childhood Dyskinesia is to point out the main features of this problem and a possible way to face with it.

Lesson learnt

The hypertone, which is thought to be a cause of joint stiffness during normal posture could be described both as co-contraction of opposing muscles, agonists and antagonists, or as a stiffness reflex-dependent response of a muscle. In the first case, there is no dependency from position and speed, there can be a stable dystonic (ill-)posture but the hyperactivation occurs along the entire range of motion: this picture leads to the necessity to favour in general a repositioning therapy where the intensity may not impact on the level of response. The reflex-dependent response, on the other hand, leads to a type of stiffness more similar to the spastic picture: it depends on spatial and/or temporal parameter (albeit without thresholds); this model would suggest an approach, which tends to obtain a more physiological posture, imparting forces without activating the stretch-reflex response, i.e. mild ones, producing gradual and slow postural evolution.

Proprioception and sensorimotor integration

In this respect, sensory information has two roles: first to inform consciousness about the state of the world (exteroceptive) and the state

of the body (interoceptive), and second to guide the driving of the motor system (Patel et al. 2014; Franco et al. 2015). Proprioception, in particular, is the sense which allows perception of the location, movement, and action of parts of the body relative to each other and is also essential for motor learning (Taylor 2009). Proprioception is so closely tied to the control of voluntary movement that impairments are more likely to be noticed as deficits in the performance of motor tasks than as impaired sensations (Taylor, 2009). Abnormalities in this sensorimotor integration underlie many hypokinetic and hyperkinetic movement disorders (Patel et al. 2014 and references therein). Increasing evidence of sensory system involvement in the pathophysiology of certain Movement Disorders makes it essential to consider the possible contribution of changes in sensorimotor integration, that is to say, the ability to use sensory information properly for assisting motor program execution (Abruzzese et al. 2003 and references therein). Sensorimotor integration seems to play an important role in the disturbances of motor control (movement guide, muscle activation) typically seen in patients with Parkinson's disease, Huntington's disease, and dystonia. Defective elaboration of sensory inputs is likely to be of particular clinical relevance to the development of focal forms of dystonia, where there are also deficits in visual-tactile-proprioceptive integration (Patel et al. 2014; Abruzzese et al. 2003). It is known that for some specific forms of dystonia, such as cervical dystonias, writers' cramp and focal dystonias, there are some specific actions that can be voluntarily done to reduce the symptoms connected to dystonia such as ill postures, tremors etc. These actions, generally involving light-touch (not forceful constraining), are called alleviating manoeuvres (AM) or sensory tricks (Wissel et al. 1999). Such effects can be considered in the broader respect that sensory inputs can modify dystonia and they may influence dystonic contractions by changing the level of excitability in all the pathways, so as to alter the motor "focus" (Berardelli et al. 1998). In the last years, new insights suggest that

dystonia could originate from a lack of reliable sensory feedback regarding motor actions. In particular, dystonia could stem from distorted and excessive afferent inputs linked via reflexes to create abnormal motor outputs (Bertucco et al. 2016).

Even if the AM as such are specific for focal dystonias, the phenomena that rule this kind of effects (touch, sensory stimulation, proprioception) could be useful in the management of dystonic syndromes in general. In cervical dystonia sensory tricks seem to improve dystonia through an inhibitory effect on motor cortex excitability (Amadio et al. 2014). Proprioceptive stimulation could elicit AM (Muller et al. 2001), and their effectiveness is strongly dependent on the initial district position (e.g. head rotation angle) (Deusch et al. 1992). Furthermore the phenomenon of the sensory trick can take effect through a change in the level of fusimotor drive (Berardelli et al. 1998). Actually, it has been shown that abnormal spindle function is present in focal dystonia (Grünewald et al. 1997; Trompetto et al. 2006; Grünewald 2012). This is consistent with Grünewald's experiments of passive mobilisation and vibrotactile stimulation of the forearm. His results suggest that patients with focal dystonia can display abnormal perception, with an involvement of impaired muscle spindle function and in particular that there is an abnormal perception of motion, but not position (Grünewald et al. 1997). These observations could be taken as a source of inspiration in designing approaches including sensory enhancement.

Lesson learnt

Proprioceptive sensory input plays a crucial part in the generation and coordination of movements; peripheral sensory afferences are fundamental in planning and executing of the movement. Disruptions of sensory input integration are considered to be of clinical relevance to the development of focal forms of dystonia, and they are addressed more as linked to deficits in the performance of motor tasks than as merely

sensory impairments (Taylor 2009). In this respect, it could be a clever option to take these aspects into account, conceiving devices, that try to fulfil not only the biomechanical aims, but also offer proprioceptive and sensory inputs in general.

1.4.3 Discussion of the available physical and orthotic treatments

As discussed in the previous section, in response to the many different problems, which draw the picture of Childhood Dyskinesia, some solutions, like the ones reported in the section 1.3.2, have been implemented to offer a relief, acting on one or more of the impairing manifestations of the disease.

It is evident from the above presentation that non-invasive and non-pharmacological tools could be of particular interest as adjuncts in the multimodal management of this movement disorder. We believe that further effort should be put in establishing validated combined uses of rehabilitation treatments, like physiotherapy, robotics, and especially orthotics with pharmacological treatments (both peripherally acting ones, like botulinum toxin, and centrally-acting ones, such as neurotransmitter-like molecules or new drugs enhancing neural plasticity). For the purpose of this chapter we will not enter that topic, but will stay focussed on discussing the orthotic solutions implemented in the past in the light of the lessons learnt about neurophysiological mechanisms (cf. section 1.4.2, above). This will be useful to pursue the aim of the present thesis, which is to develop a passive wearable device to support the functional activities of patients affected by Childhood Dyskinesia and their rehabilitation.

The *rigid orthoses* for Childhood Dyskinesia (or dystonia in general), exploiting the rigidity provided by the materials employed, were designed based on the idea to block, to prevent the motion of the joints involved in either the residual voluntary movements, or the involuntary ones, i.e. the dyskinetic actions. Although the mechanisms of action of

immobilisation are largely unknown, the paper by Priori et al. has postulated that removing all motor and sensory input to a limb, this could allow the cortical map to reset to the previous normal topography (Priori et al. 2001). Although the study is interesting for occupational focal upper-limb dystonia, it is not clear to us, how this could work for dyskinetic subjects in the developmental age, who were born without a normal topography. Furthermore, the idea to provoke sensory deprivation clashes with more abundant evidence that *appropriate* sensory input can alleviate many forms of dystonia (cf. section 1.4.2 above). The different approach, implemented in the Egyptian research by El-Maksoud (El-Maksoud et al. 2009), shows how blocking one of the joints in the affected limb, it becomes easier for the dyskinetic children to control the other joints better. This method is interesting, because it suggests that, at least for the observed cases, *limiting the degrees of freedom to be governed, the system can re-distribute more effectively the control resources to carry out upper-limb motor tasks*.

Another observation regarding rigid orthoses and joint immobilisation has to do with the development of interface forces. On the one hand, limiting involuntary movements with fixed constraints produces discomfort due to the resulting pressures on the skin; on the other, the continuous isometric contraction of the muscles affected by hyperkinesia or overflow could generate hypertrophy and exacerbate the dominating presence of those muscles in determining posture. Furthermore, if the reflex-mediated interpretation of hypertonic dystonia is true (cf. section 1.4.2), the unyielding stretch produced by the rigid orthoses could directly worsen limb stiffness.

Discussing more in detail the results in the field of soft orthoses it could be inferred that, despite their higher material compliance and thus adaptability of use, from a functional point of view some of them do not provide well defined forces (Lycra vest), or the elastic strings (Adeli suit) or bands (Spiral suit) impart a forces that are quasi–linear: the more the

elastic element is stretched, the higher will be the force. This shows how much this solutions could become ineffective for little elongations, i.e. around the rest position (non-stretched) or quite uncomfortable on the opposite side, i.e. end-range maximum stretching. Furthermore even if these soft orthoses are tailored on the size of the patients, they are often reported to be uncomfortable to wear, especially the Lycra garment because of the donning and doffing problems. Bearing in mind all these aspects it is evident that a wiser *customisation of both shape and function* would be necessary to solve the negative aspects of these devices. On the other hand, what is interesting about the soft technologies is that (1) *they allow for residual movements to be initiated and carried out by the patients*; (2) *they can provide some sensory stimulation that could be achieved through a general wrapping stimulus or designing some parts in the orthosis ad hoc to achieve this aim*.

Amongst the systems, which can enhance stimulation, there are the wearable solutions that provide biofeedback. Findings that come from the literature show how biofeedback can help some patients eliminate the co-contraction of the flexors and extensors and to quiet unnecessary motor contraction (Kanovsky et al. 2015). Some studies showed that muscle vibration may trigger focal hand dystonia, that can be partially relieved by muscle afferent block with lidocaine (Abruzzese et al. 2003 and refs therein). In contrast to that observation, vibrotactile systems for the proprioceptive enhancement are being tested for the rehabilitation support of dystonic pictures, especially in clinical pictures of focal dystonia (Leis et al. 1992), and in children with primary or secondary dystonia (Casellato et al. 2014; Lunardini et al. 2015; Casellato et al. 2016). The principle of action of biofeedback is that it provides the subjects with instant, reliable information on their performance, making covert physiological processes more manifest. The aim of biofeedback is to improve the efficacy of the rehabilitation treatment by allowing patients to adjust their movements. Additionally, biofeedback training is able to capture and maintain the subject's attention and to allow the

participant to exercise in immersive settings (Casellato et al. 2016). Electromyography-based biofeedback in particular has been reported for children with cerebral palsy (Bloom et al. 2010). Further research is warranted to determine the effectiveness of multiple simultaneous feedback modalities, such as tactile, visual, haptic and auditory, and to determine which particular motor deficits and types of dystonia are most influenced by these interventions (Bertucco et al. 2016). While cognitively-intense definitions of biofeedback can be certainly useful in the framework of rehabilitation sessions, they may be less applicable in mixed rehabilitative-assistive treatments. In fact it is hard and tiring to maintain attention and focus for longer periods, and fatigue may arise; patients should be very collaborative and this is not always the case, especially dealing with children, in particular if they are very young or their conditions are severe, possibly including cognitive or behavioural deficits: they can even fail to completely understand the requests, or be frankly unable to try and control specific muscles due to excessive functional deficits in the neuromusculoskeletal system.

In this respect, a different less-cognitively-mediated definition of biofeedback could be more broadly applicable, i.e. one based on interoceptive sensation and proprioceptive feedback. For example, some patients with cervical dystonia were shown to benefit from specially-designed neck and head braces that provide a sensory input, by touching certain portions of the neck or head, in a fashion similar to a patient's own sensory trick; they enable patients to maintain a desired head position (Jankovic 2006). Apart from this example referring to alleviating manoeuvres, also other *sensory (afferent) stimuli*, skilfully applied by people or objects are useful to facilitate movement: e.g. touch and pressure, traction and compression, stretch or limb elongation. In particular *the proprioceptive effect of muscles, contracting against a resistance* (Kabat et al. 1959; Knott & Voss 1968; Voss 1972; Voss et al. 1985), could be exploited to control the motor symptoms or at least enhance the afferent pathways in a way as to provide from the "outside"

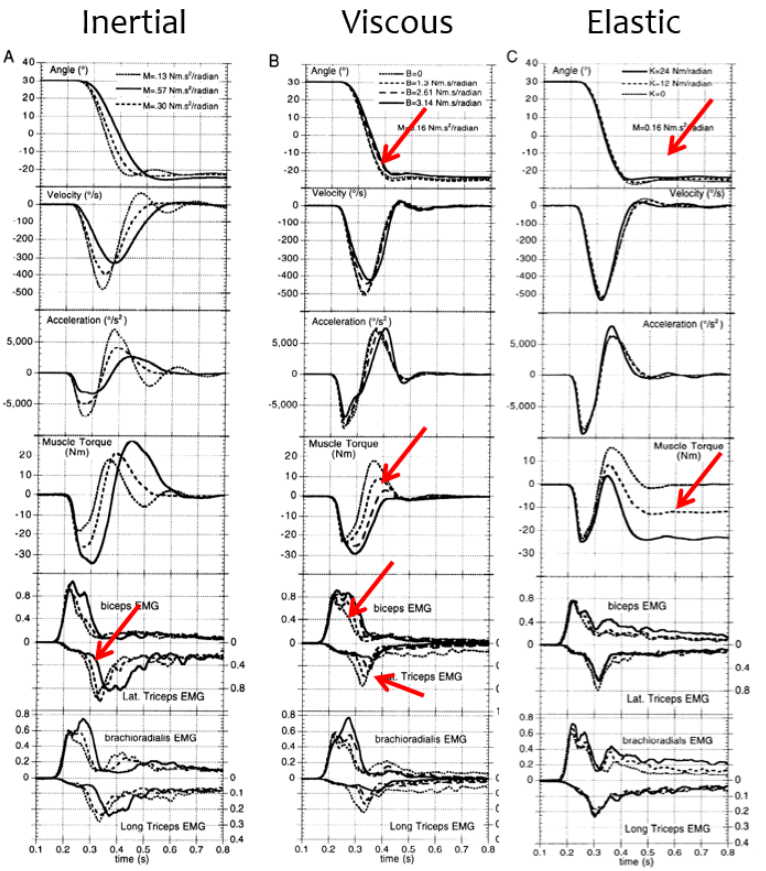

Figure 1.9 Figure 9 The pictures reports the electrical activation of the muscles in response to the application of different types of external forces. The *red arrows* highlight the muscles mainly affected by increase or decrease in the burst intensity. The area of the antagonist bursts increases for inertial loads (*left column*), decreases with viscous loads (*middle column*), and decreases slightly with elastic loads (*right column*) (adapted from Gottlieb 1996).

(non-invasively) a help for the central nervous system in managing the disabling disorder and thus modifying the response based on an

automatic sensorimotor feedback from the end effectors. To achieve this target orthoses could be designed to respond to movement with appropriate force fields acting as sources of enhanced proprioceptive feedback to reduce or at least contain the symptoms. In fact, even if it is known that light forces can be used to counteract dystonia (Fructh et al. 1999), it is very important to know, *which types of forces* are the best to control the variability, overflow, hypertone and enhance peripheral sensations. Some studies in the literature have investigated the relationship between the types of forces applied to a muscle and the electrical response of the muscle (Stoeckmann 2009). In particular, inertial loads prolong the durations of both agonist and antagonist pulses, increasing the areas of the rectified EMG bursts (Angel 1975) and delaying the antagonist burst (Gottlieb 1993; Gottlieb et al. 1989; Smeets et al. 1990). External viscous loads reduce the antagonist burst (Sanes 1986; Stein et al. 1988), similar to the effect of intrinsic limb viscosity (Lestienne 1979). Elastic loads demand static torques to be maintained to hold some posture (Richardson et al. 1985; Stein et al. 1988). Viscous loads also demonstrate the unusual property of causing changes in peak velocity without corresponding changes in movement time. Agonist EMG bursts rise at a rate that is independent of the type or magnitude of the load. The area of the antagonist bursts increase for inertial loads, decreased with viscous loads, and decreased slightly with elastic loads. The areas of the two bursts can be independently controlled by the subject, based on the torque requirements of an external load (Gottlieb 1996 – Fig. 1.9). All these findings suggest that a *personalised visco-elastic force field could be the best solution meeting the requirements connected to the orthotic management of Childhood Dyskinesia*, by offering a suitable tool for the rehabilitation and the support of daily activities.

1.5 Conclusions: Design principles for the development of a new wearable orthotic system

The conclusions of the present chapter arise from the sum of the knowledge and experiences we found in the literature, and the discussions made above, about the possible alternative management of paediatric patients affected by Childhood Dyskinesia. These final considerations are the practical basis to define the requirements that we feel the orthotic wearable device we shall design should have in order to fulfil the clinical requests and the patients-specific needs that we shall encounter.

Firstly, we choose a ***dynamic postural control***: from a functional point of view, in our opinion, this solution is better than static and fixed ones, because the neutral position is allowed to vary in dependence to the fluctuations of the daily conditions of the subjects and is compliant towards involuntary movements. This choice is therefore expected to improve comfort, tolerability and treatment times. When manufacturing the orthotic device the therapists together with the technicians and the bioengineers should re-define the positions and angulations of the limb joints, in order to facilitate the initiation of the movement chain. Since the posturing will be dynamic, this corresponds to imposing a suitable *reference* (neutral) posture. It is worth to notice that in some cases the reference posture will not correspond to established biomechanically functional positions, but may take into account the necessity to recondition *patient-specific* ill-postures, possibly in connection to specific motor tasks. We think that a dynamic and compliant device is a better choice also because the potential voluntary actions are allowed. Consequently, the device, exploiting the positive aspects of soft orthoses, results to be a balance between a rehabilitative and an assistive one.

Furthermore the solution we are set to devise will not only be an orthotic device designed from a biomechanical point of view, but will also try to provide ***proprioceptive stimulation***. As it has emerged from the literature review, it is important to have sensory information available to support motion, and in particular, afferent stimuli from the outside could help improve, strengthen or at least support the feedback control, and thence motor performance.

In implementing a proprioceptive stimulation, we are going to use force fields that are generated by the orthosis in response to movement by the patient. We understood that a paramount importance must be given to the choice of the *type of forces imparted*. We shall construct an orthosis, which exploits the characteristics of materials able to impart ***visco-elastic damping forces***, to stabilise better the motion and the control of voluntary actions, because they act similarly to muscles, which are visco-elastic structures. Mimicking their action, the materials will generate forces that do not stimulate an overshooting in the activation of the impaired muscular system, but are rather expected to reduce co-contractions, decrease tonic activities and thus contain hypertone and the negative phenomena of variability and overflow.

Another aspect we have to take into account in designing our device is *the level of the forces* imparted: we decided to keep ***forces as low as possible*** to prevent the stretch-reflex response and to reduce hypertone in order to decrease the phasic and tonic responses of the muscles affected by the syndrome. The use of mild forces is also appropriate in that it may help safeguard the capability to carry out the voluntary actions.

While utilising this less-cognitively-mediated approach to proprioceptive enhancement, we decide not to implement any *cognitively-intense biofeedback tools*; considering the target of the present research, that is to deal with often very severe children, we deemed too difficult for our

patients to make the most of those features. In addition, we decided to construct a *passive orthosis* because of lightness and independence from a power supply in order to increment comfort and usability by the children, also during their daily activities.

The solution we wish to construct tries to optimise the fit to improve comfort and function at the same time; ***a light, comfortable and wearable device, that can be donned and doffed quite easily*** is considered to be fundamental, especially for children in their developmental age.

Bearing in mind all the above, we believe that the *customisation aspects* are key: a customised posture for every different clinical picture (mainly hypertonic or mainly hyperkinetic, degrees of freedom mostly affected, degree and type of overflow, etc.), personalised viscoelastic forces, together with the fine design of contact surfaces anatomically adherent to the patient's upper-limb shape, converge towards light, wearable and functional passive orthoses.

The overall objective is to offer patients the possibility to improve both rehabilitation and daily-life autonomy, such as in playing, drawing, feeding themselves, and carrying out different actions at school with other children or at home. All these aspects should also bring to a social recovery, which is of paramount importance to decrease or at least contain not only the motor impairments, but also the cognitive and behavioural ones, leading towards an overall quality of life.

1.6 References

Abbruzzese, G., & Berardelli, A. (2003). Sensorimotor integration in movement disorders. *Movement disorders*, *18*(3), 231-240.

Albanese, A. (2007). Dystonia: clinical approach. *Parkinsonism & related disorders*, *13*, S356-S361.

Albanese, A., Bhatia, K., Bressman, S. B., DeLong, M. R., Fahn, S., Fung, V. S., ... & Lang, A. E. (2013). Phenomenology and classification of dystonia: a consensus update. *Movement Disorders*, *28*(7), 863-873.

Amadio, S., Houdayer, E., Bianchi, F., Tesfaghebriel Tekle, H., Urban, I. P., Butera, C., ... & Del Carro, U. (2014). Sensory tricks and brain excitability in cervical dystonia: a transcranial magnetic stimulation study. *Movement Disorders*, *29*(9), 1185-1188.

Angel, R. W. (1975). Electromyographic patterns during ballistic movement of normal and spastic limbs. *Brain research*, *99*(2), 387-392.

Bar-Haim, S., Harries, N., Belokopytov, M., et al. (2006). Comparison of efficacy of Adeli suit and neurodevelopmental treatments in children with cerebral palsy, *Dev Med Child Neurol* 48(5), 325–330.

Berardelli, A., Rothwell, J. C., Hallett, M., Thompson, P. D., Manfredi, M., & Marsden, C. D. (1998). The pathophysiology of primary dystonia. *Brain*, *121*(7), 1195-1212.

Bertucco, M., & Sanger, T. D. (2015). Current and emerging strategies for treatment of childhood dystonia. *Journal of Hand Therapy*, *28*(2), 185-194.

Bizzi, E., Dev, P., Morasso, P., & Polit, A. (1978). Effect of load disturbances during centrally initiated movements. *Journal of Neurophysiology*, *41*(3), 542-556.

Bloom, R., Przekop, A., & Sanger, T. D. (2010). Prolonged electromyogram biofeedback improves upper extremity function in children with cerebral palsy. *Journal of child neurology*, *25*(12), 1480-1484.

Bloom, F., Squire, L. R., Lac, S. D., & Berg, D. (2008). Fundamental neuroscience. 5th Ed.

Bradley, W. G. (Ed.). (2004). Neurology in clinical practice: principles of diagnosis and management (Vol. 1). Taylor & Francis.

Butler, E. E., & Rose, J. (2012). The Pediatric Upper Limb Motion Index and a temporal–spatial logistic regression: Quantitative analysis of upper limb movement disorders during the Reach & Grasp Cycle. *Journal of biomechanics*, *45*(6), 945-951.

Candia, V., Elbert, T., Altenmüller, E., Rau, H., Schäfer, T., & Taub, E. (1999). Constraint-induced movement therapy for focal hand dystonia in musicians. *The Lancet*, *353*(9146), 42.

Casellato, C., Maggioni, S., Lunardini, F., Bertucco, M., Pedrocchi, A., & Sanger, T. D. (2014). Dystonia: altered sensorimotor control and vibro-tactile EMG-based biofeedback effects. In *XIII Mediterranean Conference on Medical and Biological Engineering and Computing 2013* (pp. 1742-1746). Springer International Publishing.

Casellato, C., Lunardini, F., & Pedrocchi, A. (2016). EMG-Based Biofeedback to Improve Motor Control in Children with Dystonia. *Computer Engineering & Information Technology*, *2016*.

Coghill, J. E., & Simkiss, D. E. (2010). Do lycra garments improve function and movement in children with cerebral palsy?. *Archives of disease in childhood*, *95*(5), 393-395.

Crocker, M. D., MacKay-Lyons, M., & McDonnell, E. (1997). Forced use of the upper extremity in cerebral palsy: a single-case design. *American Journal of Occupational Therapy*, *51*(10), 824-833.

de Groot, L., vd Hoek, A. M., Hopkins, B., & Touwen, B. C. L. (1993). Development of muscle power in preterm infants: individual trajectories after term age. *Neuropediatrics*, *24*(02), 68-73.

Deuschl, G., Heinen, F., Kleedorfer, B., Wagner, M., Lücking, C.H., Poewe, W. (1992). Clinical and polymyographic investigation of spasmodic torticollis. *J Neurol,* 239:9–15.

El-Maksoud, G. M. A., Gharib, N. M., & El-Shemy, S. A. (2009). Influence of Elbow Immobilizer on Hand Function in Children with Athetoid Cerebral Palsy. *Bull. Fac. Ph. Th. Cairo Univ*, *14*(2), 75.

Fahn, S., Jankovic, J., & Hallett, M. (2011). *Principles and practice of movement disorders*. Elsevier Health Sciences.

Flemming, K. D., & Jones, L. K. (Eds.). (2015). Mayo Clinic Neurology Board Review: Clinical Neurology for Initial Certification and MOC. Oxford University Press.

Franco, J. H., & Rosales, R. L. (2015). Neurorehabilitation in Dystonia. In *Dystonia and Dystonic Syndromes* (pp. 209-226). Springer Vienna.

Frucht, S., Fahn, S., Ford, B., & Gelb, M. (1999). A geste antagoniste device to treat jaw-closing dystonia. *Movement disorders*, *14*(5), 883-886.

Gordon, L. M., Keller, J. L., Stashinko, E. E., Hoon, A. H., & Bastian, A. J. (2006). Can spasticity and dystonia be independently measured in cerebral palsy?. *Pediatric neurology*, *35*(6), 375-381.

Gottlieb, G. L. (1993). A computational model of the simplest motor program. *Journal of motor behavior*, *25*(3), 153-161.

Gottlieb, G. L. (1996). On the voluntary movement of compliant (inertial-viscoelastic) loads by parcellated control mechanisms. *Journal of neurophysiology*, *76*(5), 3207-3229.

Gottlieb, G. L., Corcos, D. M., & Agarwal, G. C. (1989). Strategies for the control of voluntary movements with one mechanical degree of freedom. *Behavioral and brain sciences*, *12*(02), 189-210.

Grünewald, R. A., Yoneda, Y., Shipman, J. M., & Sagar, H. J. (1997). Idiopathic focal dystonia: a disorder of muscle spindle afferent processing?. *Brain*, *120*(12), 2179-2185.

Grünewald, R. (2012). Dystonia and Muscle Spindles: The Link in Idiopathic Focal Dystonias. In R. L. Rosales (Ed.), *Dystonia – The Many Facets*, Rijeka: INTECH.

Hagberg, B., Hagberg, G., Olow, I. & von Wendt, L. (1996). The changing panorama of cerebral palsy in Sweden. The birth year period 1987–90. *Acta Paediatr. Scand.*, 85, 954–960.

Hallett, M., & Poewe, W. (Eds.). (2008). Therapeutics of Parkinson's Disease and Other Movement Disorders. John Wiley & Sons.

Heitmann, S., Breakspear, M., & Ferns, N. (2012). Muscle co-contraction modulates damping and joint stability in a three-link biomechanical limb. *Frontiers in neurorobotics*, *5*, 5.

Himmelmann, K., Hagberg, G., Beckung, E., Hagberg, B. & Uvebrant, P. (2005). The changing panorama of cerebral palsy in Sweden. IX. Prevalence and origin in the birth-year period 1995–1998. *Acta Paediatr.* 94, 287–294.

Hou, M., Zhao, J. H., & Yu, R. (2006). Recent advances in dyskinetic cerebral palsy. *World J Pediatr*, *1*, 23-28.

Jankovic, J. (2006). Treatment of dystonia. *The Lancet Neurology*, *5*(10), 864-872.

Jankovic, J. (2009). Treatment of hyperkinetic movement disorders. *The Lancet Neurology*, *8*(9), 844-856.

Kabat, H., McLeod, M. & Holt, C. (1959). The practical application of proprioceptive neuromuscular facilitation. *Physiotherapy*, 45, 87.

Kandel, E. R., Schwartz, J. H., Jessell, T. M., Siegelbaum, S. A., Hudspeth, A. J. (2012). *Principles of neural science* (5th ed.). New York: McGraw-hill.

Kanovsky, P., Bhatia, K. P., & Rosales, R. L. (Eds.). (2015). *Dystonia and Dystonic Syndromes*. Springer Vienna.

Katz, R. T., & Rymer, W. Z. (1989). Spastic hypertonia: mechanisms and measurement. *Arch Phys Med Rehabil*, *70*(2), 144-55.

Katz, R. T., Rovai, G. P., Brait, C., & Rymer, W. Z. (1992). Objective quantification of spastic hypertonia: correlation with clinical findings. *Arch Phys Med Rehabil*, *73*(4), 339-47.

Kimberley, T. J., Borich, M. R., Arora, S., & Siebner, H. R. (2013). Multiple sessions of low-frequency repetitive transcranial magnetic stimulation in focal hand dystonia: clinical and physiological effects. *Restorative neurology and neuroscience,* 31(5), 533-542.

Kirton, A., & Gilbert, D. L. (Eds.). (2016). Pediatric Brain Stimulation: Mapping and Modulating the Developing Brain. Academic Press.

Koy, A., Lin, J. P., Sanger, T. D., Marks, W. A., Mink, J. W., & Timmermann, L. (2016). Advances in management of movement disorders in children. *The Lancet Neurology*, *15*(7), 719-735.

Kong, E. (1987). The importance of early treatment. In *Early Detection and Management of Cerebral Palsy* (eds H. Galjaard, H.F.R. Prechtl & M. Velickovic), p. 107. Martinus Nijhoff, Dordrecht.

Knott, M. & Voss, D.E. (1968). Proprioceptive Neuromuscular Facilitation. Patterns and Techniques, 2nd edn. Harper & Row, New York.

Law, M., Cadman, D., Rosenbaum, P., Walter, S., Russell, D., & De Matteo, C. (1991). Neurodevelopmental therapy and upper-extremity inhibitive casting for children with cerebral palsy. *Developmental Medicine & Child Neurology*, *33*(5), 379-387.

Law, M., Russell, D., Pollock, N., Rosenbaum, P., Walter, S., & King, G. (1997). A comparison of intensive neurodevelopmental therapy plus casting and a regular occupational therapy program for children with cerebral palsy. *Developmental Medicine & Child Neurology*, *39*(10), 664-670.

Leis, A. A., Dimitrijevic, M. R., Delapasse, J. S., & Sharkey, P. C. (1992). Modification of cervical dystonia by selective sensory stimulation. *Journal of the neurological sciences*, *110*(1), 79-89.

Lestienne, F. (1979). Effects of inertial load and velocity on the braking process of voluntary limb movements. *Experimental Brain Research*, *35*(3), 407-418.

Levitt, S. (2010). *Treatment of cerebral palsy and motor delay*. John Wiley & Sons. 5th Ed.

Lunardini, F., Casellato, C., Bertucco, M., Sanger, T. D., & Pedrocchi, A. (2015, August). Muscle synergies in children with dystonia capture "healthy" patterns regardless the altered motor performance. In *Engineering in Medicine and Biology Society (EMBC), 2015 37th Annual International Conference of the IEEE* (pp. 2099-2102). IEEE.

Matsumoto, H., Ugawa, Y. (2016). Therapeutic effects of non-invasive brain stimulation for dystonia. *Basal Ganglia*, 6(2), 101-105.

Milner, T. E., & Cloutier, C. (1995, September). The effect of antagonist muscle co-contraction on damping of the wrist joint during voluntary movement. In *Engineering in Medicine and Biology Society, 1995., IEEE 17th Annual Conference* (Vol. 2, pp. 1247-1248). IEEE.

Milner, T. E. (2002). Adaptation to destabilizing dynamics by means of muscle cocontraction. *Experimental brain research*, *143*(4), 406-416.

Milner, T. E., & Cloutier, C. (1998). Damping of the wrist joint during voluntary movement. *Experimental brain research*, *122*(3), 309-317.

Mink, J. W. (1996). The basal ganglia: focused selection and inhibition of competing motor programs. *Progress in neurobiology*, *50*(4), 381-425.

Mink, J. W. (2003). The basal ganglia and involuntary movements: impaired inhibition of competing motor patterns. *Archives of neurology*, *60*(10), 1365-1368.

Mir, P., Edwards, M. J., Curtis, A. R., Bhatia, K. P., & Quinn, N. P. (2005). Adult-onset generalized dystonia due to a mutation in the neuroferritinopathy gene. *Movement disorders*, *20*(2), 243-245.

Morris, C., Bowers, R., Ross, K., Stevens, P., & Phillips, D. (2011). Orthotic management of cerebral palsy: recommendations from a consensus conference. *NeuroRehabilitation*, *28*(1), 37-46.

Müller, J., Wissel, J., Masuhr, F., Ebersbach, G., Wenning, G. K., & Poewe, W. (2001). Clinical characteristics of the geste antagoniste in cervical dystonia. *Journal of neurology*, *248*(6), 478-482.

Nicholson, J. H., Morton, R. E., Attfield, S., & Rennie, D. (2001). Assessment of upper-limb function and movement in children with cerebral palsy wearing lycra garments. *Developmental Medicine & Child Neurology*, *43*(6), 384-391.

Patel, N., Jankovic, J., & Hallett, M. (2014). Sensory aspects of movement disorders. *The Lancet Neurology*, *13*(1), 100-112.

Priori, A., Pesenti, A., Cappellari, A., Scarlato, G., & Barbieri, S. (2001). Limb immobilization for the treatment of focal occupational dystonia. *Neurology*, *57*(3), 405-409.

Richardson, C. And Simmons, R. W. (1985). Electromyographic and neuromuscular force patterns associated with unexpectedly loaded rapid movements. *Brain Res.* 343: 246-251.

Rodríguez, M. I., & Gajardo, C. (2012). Dystonia and Rehabilitation in Children. In R. L. Rosales (Ed.), *Dystonia – The Many Facets*, Rijeka: INTECH.

Rood, M.S. (1962) Use of sensory receptors tointestazioni di activate, facilitate and inhibit motor response, automatic and somatic, in developmental sequence. In *Approaches to the Treatment of Patients with Neuromuscular Dysfunction* (Ed. C. Sattely). Third International Congress of World Federation of Occupational Therapists, pp. 26–37.

Rosenbloom, L. (1995). Diagnosis and management of cerebral palsy. *Archives of disease in childhood*, *72*(4), 350-354.

Sanes, J. N. (1986). Kinematics and end-point control of arm movements are modified by unexpected changes in viscous loading. *Journal of Neuroscience*, *6*(11), 3120-3127.

Sanger, T. D., Delgado, M. R., Gaebler-Spira, D., Hallett, M., & Mink, J. W. (2003). Classification and definition of disorders causing hypertonia in childhood. *Pediatrics*, *111*(1), e89-e97.

Sanger, T. D. (2003). Pathophysiology of pediatric movement disorders. *Journal of child neurology*, *18* (1 suppl), S9-S24.

Sanger, T. D. (2004). Toward a definition of childhood dystonia. *Current opinion in pediatrics*, *16*(6), 623-627.

Sanger, T. D., Kaiser, J., & Placek, B. (2005). Reaching movements in childhood dystonia contain signal-dependent noise. *Journal of child neurology*, *20*(6), 489-496.

Sanger, T. D. (2006). Arm trajectories in dyskinetic cerebral palsy have increased random variability. *Journal of Child Neurology*, *21*(7), 551-557.

Sanger, T. D., Chen, D., Fehlings, D. L., Hallett, M., Lang, A. E., Mink, J. W., ... & Chen, R. (2010). Definition and classification of hyperkinetic movements in childhood. *Movement Disorders*, *25*(11), 1538-1549.

Schlaggar, B. L., & Mink, J. W. (2003). Movement disorders in children. *Pediatrics in Review*, *24*(2), 39-51.

Semenova, K.A. (1997). Basis for a method of dynamic proprioceptive correction in the restorative treatment of patients with residual-stage infantile cerebral palsy. *Neurosci Behav Physiol,* 27.

Shvarkov, S.B., Davydov, O.S., Kuus, R.A., Aipova, T.R., Vein, A.M. (1997). New approaches to the rehabilitation of patients with neurological movement defects. *Neurosci Behav Physiol,* 27, 644–647.

Siebner, H. R., Tormos, J. M., Ceballos-Baumann, A. O., Auer, C., Catala, M. D., Conrad, B., & Pascual-Leone, A. (1999). Low-frequency repetitive transcranial magnetic stimulation of the motor cortex in writer's cramp. *Neurology*, *52*(3), 529-529.

Singer, H. S., Mink, J., Gilbert, D. L., & Jankovic, J. (2015). *Movement disorders in childhood*. Academic Press.

Smeets, J. B. J., Erkelens, C. J., And Denier Van Der Gon, J. J. (1990). Adjustments of fast goal-directed movements in response to an unexpected inertial load. *Exp. Brain Res*. 81: 303 -3 12.

Stanley, F.J., Blair, E. & Alberman, E. (2000). Cerebral Palsies: Epidemiology and Causal Pathways. *Clinics in Developmental Medicine*. No. 151. Mac Keith Press, London.

Stein, R. B., Cody, F. W. J., & Capaday, C. (1988). The trajectory of human wrist movements. *J. Neurophysiol*. 59: 18 14- 1830.

Stockmeyer, S.A. (1967). The Rood approach. *Am. J. Phys. Med.*, 46 (1), 900.

Stockmeyer, S.A. (1972). A sensorimotor approach to treatment. In *Physical Therapy Services in the Developmental Disabilities* (Eds. P.H. Pearson & C.E. Williams), Chapter 4. Thomas, Springfield, Illinois.

Stoeckmann, T. M., Sullivan, K. J., & Scheidt, R. A. (2009). Elastic, viscous, and mass load effects on poststroke muscle recruitment and co-contraction during reaching: a pilot study. *Physical therapy*.

Taylor, J.L. (2009). Proprioception. In *Encyclopedia of Neuroscience*, (Ed.) L. R. Squire, Oxford: Academic Press.

Taş, N., Karataş, G. K., & Sepici, V. (2001). Hand orthosis as a writing aid in writer's cramp. *Movement disorders*, *16*(6), 1185-1189.

Thylefors, I., Price, E., Persson, T.O. & von Wendt, L. (2000). Teamwork in Swedish neuropaediatric habilitation. *Child Care Health Dev.*, 26, 515–532.

Trompetto, C., Currà, A., Buccolieri, A., Suppa, A., Abbruzzese, G., & Berardelli, A. (2006). Botulinum toxin changes intrafusal feedback in dystonia: a study with the tonic vibration reflex. *Movement disorders*, *21*(6), 777-782.

van Doornik, J., Kukke, S., & Sanger, T. D. (2009). Hypertonia in childhood secondary dystonia due to cerebral palsy is associated with reflex muscle activation. *Movement Disorders*, *24*(7), 965-971.

Voss, D.E. (1972). Proprioceptive neuromuscular facilitation. In *Physical Therapy Services in the Developmental Disabilities* (Eds. P.H. Pearson & C.E. Williams), Chapter 5. Thomas, Springfield, Illinois.

Voss, D.E., Jonta, M. & Meyers, B. (1985). *Proprioceptive Neuromuscular Facilitation Patterns and Techniques*, 3rd eds. Harper & Row, New York.

Winters, J. M., & Stark, L. (1988). Estimated mechanical properties of synergistic muscles involved in movements of a variety of human joints. *Journal of biomechanics*, *21*(12), 1027-1041.

Wissel, J., Heinen, F., Schenkel, A., Doll, B., Ebersbach, G., Müller, J., & Poewe, W. (1999). Botulinum Toxin A in the Management of Spastic Gait Disorders in Children and Young Adults with Cerebral Palsy: A Randomized, Double-Blind Study. *Neuropediatrics*, *30*(03), 120-124.

Chapter 2

Functional materials for the dyskinesia orthotics: considerations and experiences in the use of Shape Memory Alloys

The chapter introduces the specific characteristics that a class of materials should possess in order to be employed for the construction of an orthotic device with the requirements devised in the Chapter 1. Furthermore the work presents the optimisation and the characterisation of the class of metallic materials chosen for the present purpose: the Niti-based alloys. The study concludes discussing the personalisation of the selected material to design and construct the wearable dynamic viscoelastic orthosis for upper limb, in patients affected by Childhood Dyskinesia.

2.1 Introduction

By integrating the knowledge about the neurophysiological bases of dystonia and hyperkinesia, the sensory and proprioceptive information able to condition dynamic postural and motor control, and the characteristics of different solutions devised in the past years, in the previous chapter we tried to define some requirements that a new wearable orthotic device should comply with in order to support the functional rehabilitation of children affected by Childhood Dyskinesia and to control the negative symptoms of this impairing disease. Briefly, it is fundamental that the orthosis be a dynamic device, with a tuneable neutral angle, i.e. a customisable resting position, specific for the patients' needs; it shall impart light visco-elastic forces, and moreover it shall be customised to fulfil clinical and subject-specific necessities, in terms of comfort at the interfaces, lightness, and usability.

An orthotic device is the result of a process that involves many different actions, such as the creation of one or more valves, their fitting on the limb, the construction of the junction elements, the definition of the quantity and the position of the padding, etc. The shapes and roles of all these parts contribute to defining a general concept of the orthosis. In order to create a new device with the above-mentioned characteristics it is necessary to find the right constructive solutions able to match and tune the general concept to the set requirements. In our case, for instance, the aim to build a dynamic device could be achieved by articulating the shells of the orthosis rather than making them one single piece; moreover the dynamic device shall produce light viscoelastic forces, and this could be obtained either with a mechanism like a viscoelastic damper, which connects the valves, or better, by exploiting the inherent properties of some material that behaves like a damper, in response to a mechanical stimulus.

In keeping with these basic ideas, not only will the junction elements connect the shells, but they shall also serve the fundamental function to provide the required force fields around the affected joints, i.e. the therapeutic action. The transmission and the generation of the force fields are the key functions of the new orthotic devices.

The type of forces useful to our purpose, as already mentioned, are passive, i.e. they are generated as a mechanical response to movement, and therefore they have the nature of a spring-back force. Compared to active forces (that are often provided by some motor), passive ones possess the additional advantage that device will generally be lighter and more compact, and will not require either power supply or automatic control features.

As mentioned above, spring-back actions can be obtained as the direct mechanical response of materials to deformation, so the problem of generating appropriate therapeutic force-fields can be transformed into the requirement to find a suitable material for the junctions with the right constitutive law. The relationship between the deformation and the force generated by a given material can be *linear*, i.e. with a proportional dependency of the output force on the displacement (or deformation), or *nonlinear*, if the elastic modulus is itself a function of strain. Furthermore, the relationship can be speed-dependent, if the force produced by the material is a function of the strain-rate, which is one definition of viscous behaviour. Bearing in mind these definitions and the general requirements of the orthosis, the choice of the material shall be in the direction of maximising of these characteristics: nonlinear elasticity and added viscous behaviour.

The purpose of the present chapter is to discuss the selection of a class of materials able to provide the therapeutic action requested. Furthermore it presents the results of property optimisation and mechano-physical characterisation on the selected material. The aspects

concerning the transmission of these forces to the patient's body, which are mainly linked to the forming of the valves, will be covered in the next chapter.

2.2 Background on Shape Memory Alloys (SMA)

A brief introduction of the main properties of SMA can be useful for subsequent considerations. Shape memory alloys are very interesting class of metallic materials that display a number of useful characteristics for many different applications. In particular we shall discuss pseudoelasticity (PE) and damping, and barely touch upon the shape memory effect (SME), which we consider of lesser consequence for our current application. Although there are several different systems, which possess shape memory characteristics, the presentation made here is particularly referred to the binary (or some of the ternary) intermetallic compounds based on the quasi-equiatomic Ni-Ti composition.

2.2.1 Phenomenology of the athermal martensitic transformation in SMA

The martensitic phase transformation is a solid-solid diffusionless transformation between two types of crystallographic lattices, accompanied by both micro- and macroscopic deformation that can be recovered by heating the material (Otsuka et al. 1999). The martensitic formation in binary and ternary alloys is thermoelastic, meaning that upon decreasing and increasing the temperature the amount of martensite increases or decreases with good reversibility, whereby the deformation accompanying the transformation is almost completely elastically accommodated. Also by applying a stress, martensite can be induced and/or already existing martensite plates can be reoriented into another martensite plate variant. These important phenomena are accompanied by a temperature and stress hysteresis.

In binary NiTi, the phase which is stable at higher temperature is based on a B2 (ordered body-centred cubic) lattice and is called *austenite*, while the low temperature one has a twinned B19' (deformed monoclinic) structure and is named *martensite*. Certain process conditions can lead to the existence of a pre-martensitic rhombohedral structure (called the *R phase*), at intermediate temperatures. There are four main characteristic temperatures defining a thermoelastic martensitic transformation between two phases; the martensite start temperature, M_s , at which martensite first appears in the unstressed parent austenitic structure upon cooling. The transformation proceeds with further cooling and is complete at the martensite finish temperature, M_f . Below M_f , the entire body is in the martensitic phase, and a specimen typically consists of many regions each containing a different variant of martensite, which is twinned. The boundaries between the variants are mobile under small applied loads. With heating, the austenite start temperature, A_s , is the temperature at which austenite first appears in the unstressed martensite. With further heating, more and more of the body transforms back into austenite, and this reverse transformation is complete at the austenite finish temperature, A_f . Above A_f , the specimen is in the original non-deformed state. Connected to this the characteristic temperatures of a SMA have a fundamental role to show the range in which the different functional properties will be available. The presence of 4 (and not 2) characteristic temperatures separating the stability ranges of austenite and martensite is an effect of hysteresis (partial irreversibility of the energy flow connected with the transformation). In particular $A_f > A_s > M_s > M_f$. The value of the different temperatures is a function of alloy composition (Ni content in NiTi), thermomechanical history and applied stress (Clausius-Clapeyron relationship).

It is beyond the scope of the present section to give further explanations about the thermodynamics, metallurgy and models of shape memory

alloys; the readers are referred to the literature for more details (Melton et al. 1980, Otuska et al. 1998; Otuska et al. 2005; Liu et al. 2007; Lagoudas et al. 2012).

Shape memory effect

The best-known property of shape memory alloys is the shape memory effect, i.e. the capacity to induce the recovery of the original shape of a part that was deformed at a temperature below M_f, by simply heating the sample above the A_f temperature. The process can be repeated many times. This property can be exploited to obtain solid-state actuators that convert (with rather low efficiency) heat into mechanical work.

Pseudoelasticity

Pseudoelasticity is the ability to sustain large deformations of up to 6% with a very little increase in stress beyond the elastic domain. Upon unloading, strains are recovered. Based on this property, SMA can make useful non-linear devices, such as springs, wires, and bars used in different fields of application. This behaviour is typical for working temperatures T higher than A_f,. In this range, martensite can still be formed in a metastable way by inputting mechanical energy into the system. In particular, strain energy above a certain level determines transformation of austenite into martensite. Variants aligned with developing stress are selected and martensite plates become de-twinned. Figure 2.1 describes the tensile characteristic of a pseudoelastic alloy. Section AB represents purely elastic deformation of the parent phase. At point B, corresponding to a stress level $\sigma_{T1}^{P\rightarrow M}$, the first martensite plates start to form. The transformation is essentially complete when point C is reached. The slope of section BC reflects the ease with which the transformation proceeds to completion. With further straining, the material, which is in the completely transformed

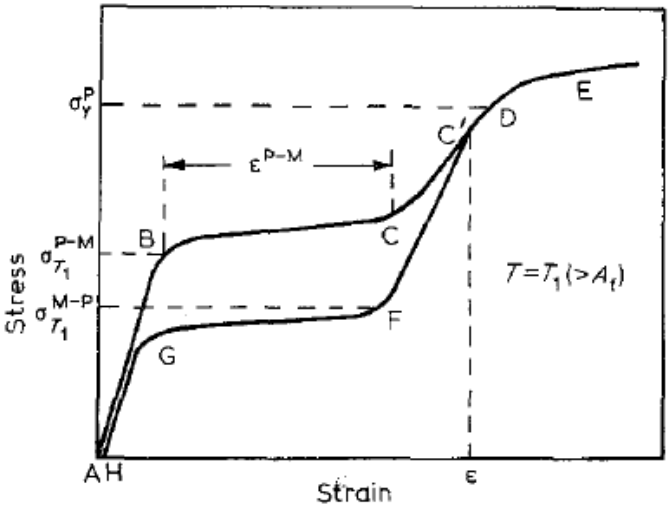

Figure 2.1 Stress-strain characteristic of a pseudoelastic NiTi-based alloy obtained from a tensile test. *Loading curve*: section AB represents pure elastic deformation of the parent phase. In B point, martensite phase start to form and ends in C (BC is the loading plateau). Further straining, brings the material to deform elastically (section CD). After D, the material deforms plastically until fracture. *Unloading curve*: section C'F of the curve corresponds to elastic unloading of the martensite. The reverse martensitic transformation starts in F and the fraction of martensite decreases until the parent phase is completely restored (G). Section GH represents the final elastic unloading of the parent phase.

condition (pure de-twinned martensite), deforms elastically as represented by section CD of the curve. At D, the plastic yield point, σ_Y^P, of martensite is reached and the material deforms plastically until fracture occurs. If the stress is released before reaching the point D, e.g. at point C', the strain is recovered in several stages. Part C'F of the curve corresponds to elastic unloading of the martensite. On reaching a stress $\sigma_{T1}^{M\rightarrow P}$ at F, the reverse martensitic transformation starts and the fraction of martensite decreases until the parent phase is completely

restored (G). Section GH represents the final elastic unloading of the parent phase. The total strain may or may not be completely recovered, the latter being the case if some irreversible deformation has taken place either during loading or during unloading. The magnitudes of $\sigma_{T1}{}^{P\rightarrow M}$ and $\sigma_{T1}{}^{M\rightarrow P}$ with respect to the yield stress, $\sigma_Y{}^P$, of the parent at T_1 determine the actual tensile behaviour. The difference between $\sigma_{T1}{}^{P\rightarrow M}$ and $\sigma_{T1}{}^{M\rightarrow P}$ determines the stress hysteresis. The area enclosed by the loading and unloading curves gives the amount of the dissipated energy. The stress necessary to induce the transformation, $\sigma_T{}^{P\rightarrow M}$ has been found to be a linear function of temperature. A similar relationship exists for $\sigma_T{}^{M\rightarrow P}$. The stresses $\sigma_{T1}{}^{P\rightarrow M}$ and $\sigma_{T1}{}^{M\rightarrow P}$ increase with increasing temperature while the yield stress of the austenitic phase, $\sigma_Y{}^P$, decreases with increasing temperature.

Damping

The high damping capacity is known as one of the important functional properties of shape memory alloys. This functional property has been the least successful of all in applications, so far. It has been investigated especially for civil applications, for which, the damping level obtained related to the payback of financial investments is not completely unfavourable (Van Humbeeck et al. 2005). Indeed, a material damping capacity of 40% is quite high, but in devices, generally only a part of all mechanical energy can be transmitted from the source of vibration to the damping component. If 10% could be transferred to the damping part, the total energy reduction would be only 4%. Thus in order to use optimally the damping capacity, the maximum amount of vibration or noise energy must be transmitted to the damping alloy. A second important reason is that the damping capacity is dependent, among others, on the amplitude. In fact, strain amplitudes of 10^{-5} or higher are needed to obtain reasonable damping values. Such high amplitude vibrations are not very common, which means that successful damping

can be obtained mostly for high-amplitude vibrations (earthquakes) or impact loading, and that is why the few present applications are in the field of civil engineering or seismic controls.

Based on the microstructure (interphase and inter-variant planar interfaces) the origin of this high damping capacity is generally linked to the presence and the (hysteretic) mobility of those interfaces (Van Humbeeck et al. 2005). Recent more detailed and systematic researches have however revealed that the whole defect structure has to be considered—including not only interfaces, but internal defects of martensitic variants as well, each type of defect contributing to a different extent to the observed damping behaviour. An important conclusion from these latest observations is that the damping capacity can be optimised depending on temperature, strain amplitude, frequency, alloy system and thermomechanical treatment (TT).

Hysteresis is a complex phenomenon related to the SMA, and is the macroscopic manifestation of energy dissipation in the system, during a cycles of loading and unloading.

The loss-coefficient η (a dimensionless quantity), measures the degree to which a material dissipates strain energy during a cycle of stress-strain loading and unloading. If a material is loaded to a stress σ, it stores an energy per unit of volume which is:

$$\mathrm{U}=\int_0^{\varepsilon_{max}} \sigma(\varepsilon)\, \mathrm{d}\varepsilon \qquad (2.1)$$

If, after loading, it is unloaded, the material dissipates an energy:

$$\Delta \mathrm{U}=\oint \sigma(\varepsilon)\, \mathrm{d}\varepsilon \qquad (2.2)$$

The loss coefficient is defined as:

$$\eta = \frac{\Delta \mathrm{U}}{2\pi \mathrm{U}}, \qquad (2.3)$$

with the 2π constant, whose origin is in the treatment of harmonic oscillations.

Generally, terms such as loss factor, loss coefficient or internal friction are more commonly used in the scientific research society. This might lead sometimes to confusion since quantitative data may be dependent on the applied expression.

So, the phrase 'damping capacity' will be used here in general (without a reference to a particular formula), while η will be referred to as *loss coefficient*. The expression *specific damping capacity* (SDC), identifies the ratio between the converted energy (mechanical into heat) and the provided energy (Van Humbeek 1999):

$$\mathrm{SDC} = \frac{\Delta \mathrm{U}}{\mathrm{U}} \qquad (2.4)$$

Other important parameters are used to identify and measure damping. In particular, the *phase-lag* (δ) between stress and strain, and the *quality factor* or Q-factor, are related to η and SDC as follows:

$$\tan\delta = 1/\mathrm{Q} = \eta = \mathrm{SDC}/2\pi \qquad (2.5)$$

The internal cycles in Fig. 2.2 demonstrate another interesting property of hysteresis in SMA: the return-point memory (RPM). During cycling a SMA can be subjected to *partial cycles*, and in particular for example, during loading once a certain value of stress is reached, the sample is unloaded until a defined value of stress (that can be different from zero). It is very interesting to see, that subsequent load, drives the sample to values of stress-strains equal to the ones that has been reached in the case of complete loading-unloading cycles. After a cyclic variation of the driving, the system follows exactly the same trajectory that it would have followed if the cyclic variation had not taken place. In this way, a hierarchy of loops within loops is formed, each internal loop being

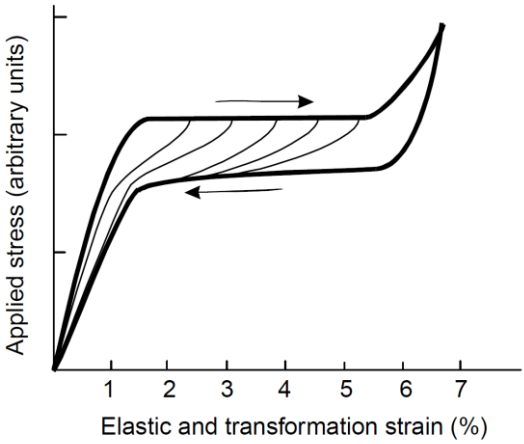

Figure 2.2 Cyclic loading-unloading tensile tests on austenite pseudoelastic wire: influence of strain amplitude: the successive partial loading-unloading cycles drive the sample to values of stress-strains equal to the ones that were reached during the complete loading-unloading cycles. The system follows the same trajectory cycle after cycle while the strain amplitude is increased (courtesy of Ortin et al. 2002).

characterised by the point at which it was initiated (return-point). The RPM in SMA is very well established in policrystals and very often found in single crystals, in both thermally and stress-induced transformations, although differing behaviours have also been reported in the last case. The possibility of transforming to different martensite crystalline structures by uniaxial tension or compression at various temperatures gives rise to a rich variety of hysteresis cycles in both stress–strain and strain–temperature diagrams, such as those reported in Ortin (Ortin et al. 2002).

Another interesting aspect related to the partial cycles in pseudoelastic alloys, and thus to mechanical hysteresis, is shown in figure 2.3. As in temperature-induced transformation, the *trigger line* governs the

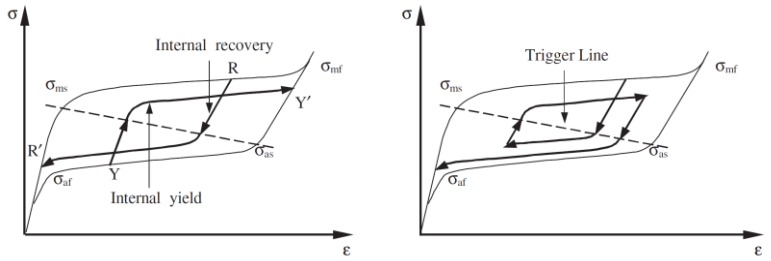

Figure 2.3 Cyclic loading-unloading tensile tests on austenite pseudoelastic wire. The *trigger line* rules the overall behaviour of the alloy when it goes through internal yield and recovery, in particular the stress and the strain at which the martensitic transformation starts and ends (*left*). On the *right*, it is shown how the trigger line controls the area of pseudoelastic hysteresis during partial cycles of loading-unloading (courtesy of Saadat et al. 2002).

overall behaviour of the alloy when it goes through internal transformation and strain recovery. Similar to temperature-induced transformation, the energy requirements for either forward and reverse transformations are functions of the induced martensitic phase. If forward transformation stops at point R in figure 2.3 *left* and unloading starts at this point, the alloy deforms back elastically and the phase composition as well as Young's modulus does not change until the stress level reaches the corresponding transition stress of the *trigger line*. Once that happens, the reverse transformation starts and finishes at point R'. Similarly, if during unloading, the unloading process reverses at point Y, then upon loading the alloy deforms elastically and there is no change in phase composition or Young's modulus until the stress level reaches the transition stress of the trigger line. Similarly, once that happens, forward transformation starts and finishes at point Y'. Pseudoelastic hysteresis, figure 2.3 *right*, occurs when there are successive loading–unloading processes, in the pseudoelastic temperature range. In such cases, the trigger line controls the critical points of transformation and recovery initiation in the alloy. As stated by the definition of SDC, the area of

pseudoelastic hysteresis represents the amount of energy dissipation, even in partial cycles (Saadat et al. 2002).

2.2.2 Viscoelasticity of NiTi

The viscoelastic behaviour of NiTi can be studied under different experimental conditions to characterise the specific roles of the martensitic lattice, the austenitic one, and the transformation phaenomena. In particular, there are many works analysing the martensitic and thermal transformation conditions, which clarify the role of the thermally activated phase transition as one of the main factors giving rise to net damping peaks in connection to the shape memory effect. Suggested reading about this topic includes the following literature items (Xiao 1993; Van Humbeek 1996; Liu et al. 1997). For the sake of the present thesis, the damping capacity displayed under pseudoelastic conditions is far more relevant and will therefore treated in greater detail, next.

While the B2 phase (austenite) by itself shows a very low damping capacity, it becomes interesting during pseudo-elastic loading (Van Humbeek 1999).

As introduced above, the non-linear elastic behaviour that we call pseudoelasticity, is one part of the overall viscoelastic nature of this material. The presence of the loading and unloading plateaux connected to the evolution of stress-induced martensitic transformation is the main evidence of non-linearity in the stress-strain relationship; the area included between the loading and unloading branches is a measure of energy lost as an effect of internal friction and is itself largely dependent on the martensitic transformation. As will be described in this section, the relative dimension of the hysteresis area is a function of strain amplitude and strain rate. All of those observations lead to the definition of non-linear viscous-elasticity in NiTi.

Several models have been devised to describe this phenomenology (Malovrh et al. 2001; Soul et al. 2007; Yang et al. 2013; etc.), but they will not be introduced here for the sake of brevity.

Dependence on the composition and thermomechanical processing

The possibility to obtain pseudoelasticity at room temperature (say, T<20°) is linked to the Ni content in the quasi-equiatomic alloy. For an atomic content of at least 50.6% (Ni-rich) it is generally assumed that there is a basic chemical substrate for this to occur. However, the processing, in terms of cold working and thermal treatment (annealing, shape setting) is fundamental to fine-tune the value of the characteristic transformation temperatures, and hence the thermal and mechanical hysteresis. Furthermore, the precipitation of secondary phases, which is also dependent on the temperature and duration of the ageing, contribute to influence the mechanical characteristics, both in terms of stiffness, and plateau properties (height and length). For details on these general metallurgical aspects, the reader is referred to the relevant literature (Otsuka et al. 1999; Otsuka et al. 2005; Lagoudas 2008; etc.). Considering in particular the damping behaviour, it is evident that alloys with high $\sigma^{P \rightarrow M}$ and low $\sigma^{M \rightarrow P}$ values are the most interesting ones, because hysteresis is large (Van Humbeek 1999).

Dependence on the strain amplitude

For loading-unloading cycles occurring beyond the linear elastic domain, the strain amplitude not only affects the hysteresis area, but also influences the ratio between the hysteresis area and the input strain energy (i.e. the SDC or η). This is borne out by direct calculations of the loss coefficient from stress-strain graphs (Dolce et al. 2001), and by internal friction measurements (Piedboeuf et al. 1998). The equivalent damping increases almost linearly at low-medium strain amplitudes (1-5%), despite the increase of energy dissipation. This last effect has to be

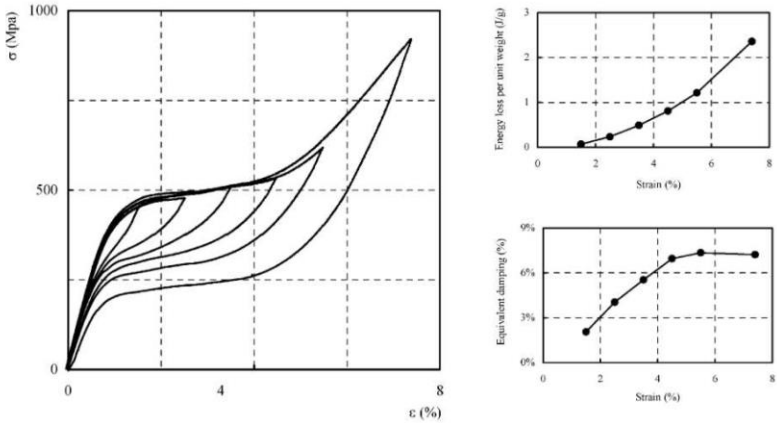

Figure 2.4 Cyclic loading-unloading tensile tests on austenite wire: influence of strain amplitude on the height of the plateaux and hysteretic area (*left*). On the *top right* is reported the energy loss per unit weight vs. strain and on the *bottom* graph the equivalent damping vs. strain amplitude. It is evident how the equivalent damping, after an initial linear increase, around 5% strain reaches almost a constant value because for further increment in strain a strong hardening that takes place in the pseudoelastic material (courtesy of Dolce et al. 2001).

ascribed to the strong hardening that takes place, during loading, as soon as the forward martensitic transformation ends (Fig. 2.4 and 2.5).

Dependence on the strain-rate

The dependence of the NiTi stress-strain relationship on strain rate is due to the competition between the time scale set by the loading and the time scale associated with the heat transfer between the specimen and the surrounding medium. This is demonstrated by measurements of the temperature change at the surface of the sample as a function of specimen deformation at different strain rates. These experiments show that at intermediate and large strain rates the superelastic cycle is no longer isothermal, and the temperature of the sample may change by

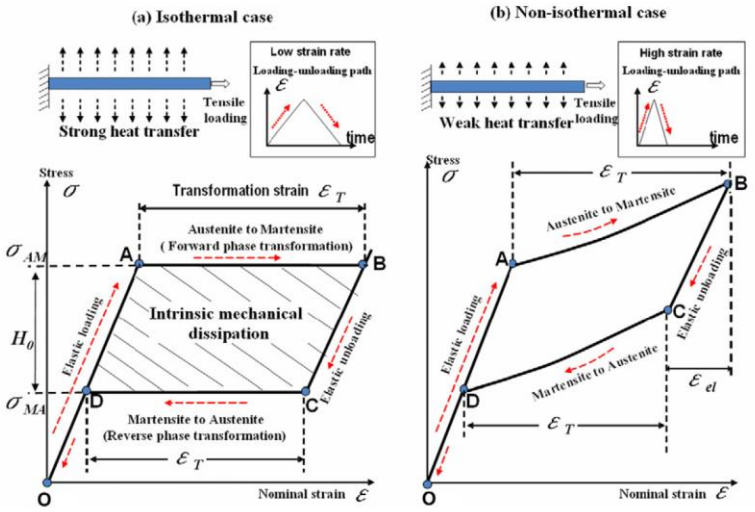

Figure 2.5 Sketch of the effects of strain-rate on the pseudoelastic NiTi alloy. Increasing the strain amplitude (from *left* to *right*) not only is the hysteresis affected, i.e. the reduction of the area, but also the (pseudoelastic) properties, i.e. the higher slope of the stress-strain curve (courtesy of He et al. 2010).

more than 1 K in the two directions of movement. The self-heating/cooling of the material by latent heat during the forward/reverse phase transition is mainly responsible for temperature oscillations in the specimen while the accumulated heat from the intrinsic mechanical dissipative work (internal friction) of the phase transition raises the specimen's mean temperature. After a number of loading cycles, stable cyclic thermal response of the material (a kind of 'steady state') can be reached. (He et al. 2010). These phenomena affect both the (pseudo)elastic and the damping behaviours (Figure 2.5).

(Pseudo)elasticity

The type of phenomenological elasticity (completely recoverable deformability) seen in shape memory alloys is truly a non-elastic

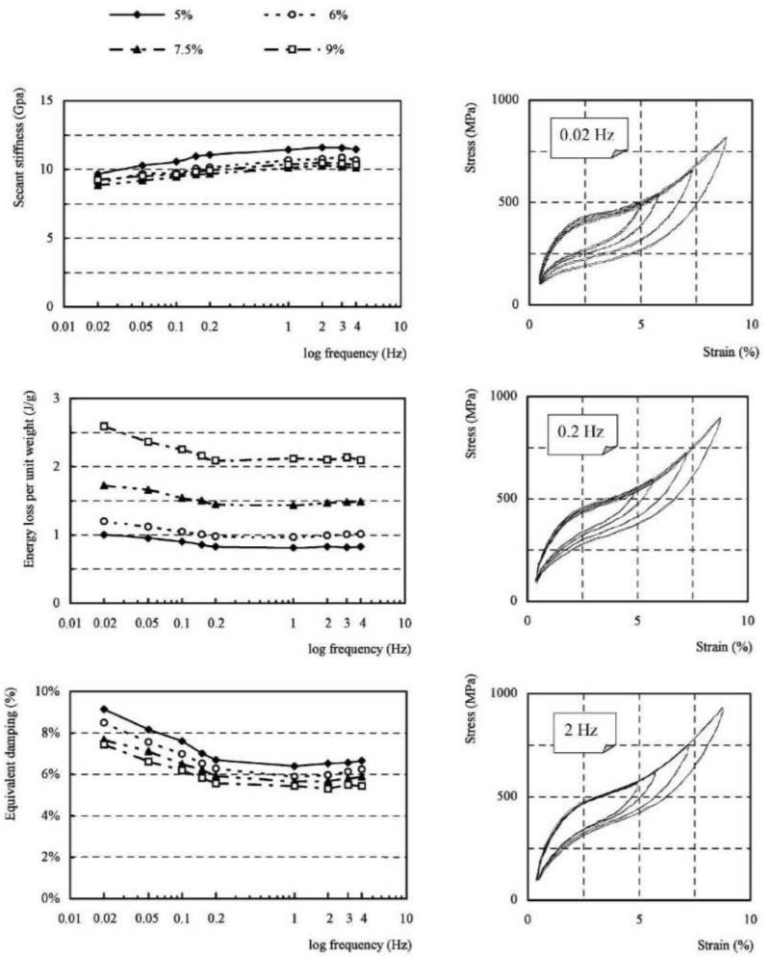

Figure 2.6 Cyclic tensile tests on pre-tensioned superelastic wires: mechanical behaviour as a function of strain amplitude frequency of loading (from *top right* to *bottom right*). On the left side is reported the trend of secant stiffness (*top*), the energy loss per unit weight (*middle*) and the equivalent damping (*bottom*) all of them vs the strain amplitude frequency of loading (courtesy of Dolce et al. 2001).

phenomenon, based on the existence of the thermoelastic martensitic transformation, so, it is coherently named 'pseudoelasticity' as mentioned above. Pseudoelasticity is characterised by a nonlinear stress-strain curve, so the stiffness can be defined in different ways, for instance, as the slope of the initial truly-elastic segment (Young's modulus), or as a suitable secant modulus, which is the slope of the line encompassing the stress and strain domains spanned during the loading phase. It is noteworthy that the shape of the tensile stress-strain cycle changes with the strain rate (figure 2.5). In particular, the secant modulus tends to increase for increasing loading speeds (Dolce et al. 2001), under the effect of self-heating and cooling of the alloy (via internal friction and the law of Clausius-Clapeyron) (figure 2.6 *top left*). What is also relevant for the application of this thesis is that the slope of the unloading branch increases with the strain rate (figure 2.6 *right*), because the stress values and the steepness of the unloading plateau determine the material spring-back force. Looking at the experimental results by different authors (Piedboeuf et al. 1998; Dolce et al. 2001; Soul et al. 2007; He et al. 2011; etc.) an estimate of those values at relevant strain rates is: unloading plateau stress: 200-450 MPa; unloading plateau slope (working spring-back modulus): 4-6 GPa.

Viscous damping

Considering the damping capacity, the experiments demonstrate that it has a non-linear relationship with the strain amplitude (Dolce et al. 2001) and even non-monotonic (Piedboeuf et al. 1998; He et al. 2010; Wolons et al. 1998) with the strain rate. In particular, the hysteresis area increases for intermediate strain amplitudes in tensile there is a strain rate for which the energy absorption is maximised and the absolute value of that maximum is found in correspondence of a critical transformation time equalling the time of heat transfer between the specimen and the environment (figure 2.7 and 2.8) (He et al. 2011). Hence, the damping is truly a function of the loading time (strain rate),

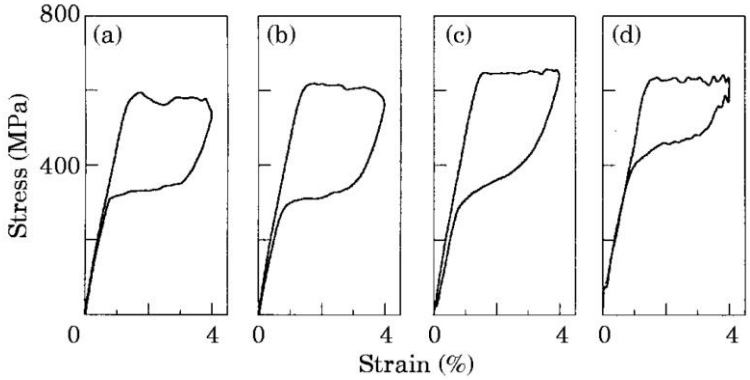

Figure 2.7 Stress-strain curves at 25°C and 4% of amplitude for four different frequencies: (a) 0.01 Hz; (b) 0.1 Hz; (c) 1 Hz; (d) 10 Hz. It is worth to notice that, after an initial increase of the hysteresis, the area starts do diminish, reducing the damping capacity (courtesy of Dolce et al. 2001).

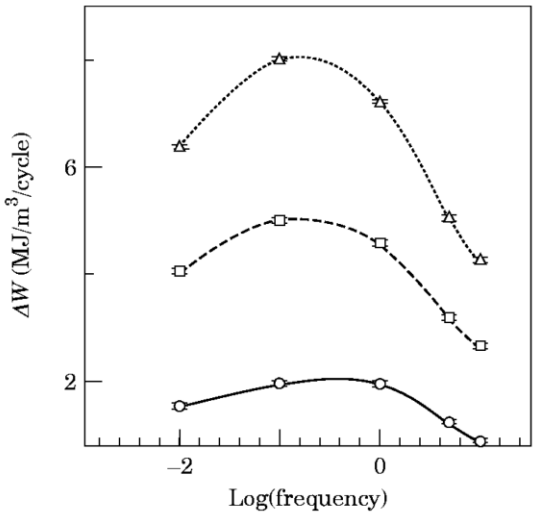

Figure 2.8 Variation of the average values of the dissipated energy with the cycling frequency at 2% (*top*), 3% (*middle*), 4% (*bottom*) of strain amplitude (courtesy of Dolce et al. 2001).

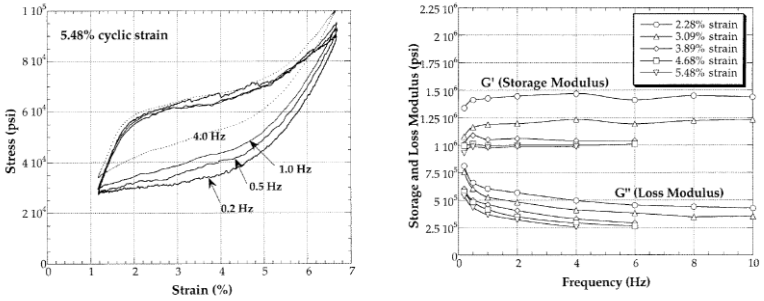

Figure 2.9 On the *left*, the stress-strain characteristic loading-unloading cycle shows the dependency of the SDC on the frequency: the higher the frequency the smaller is the area and thus the damping capacity. On the *right*, complex modulus variation with the frequency (the different curves are for different strain amplitudes) (courtesy of Piedboeuf et al. 1998).

ambient temperature, and sample geometry (heat transfer interfaces). For higher frequencies (e.g. 1-10 Hz), the loss modulus always decreases, while the storage modulus is approximately constant (Gandhi et al. 1999), so the damping capacity decreases (figure 2.9).

Referring to the cited works, the effective energy dissipation for slender elements at intermediate frequencies (0.01-2 Hz) and tensile strains (2-4.5%) are expected to be around 0.06-0.1 (equivalent damping η). This estimate is also consistent with the results for bending type loading (Ip 2000).

2.2.3 Comparison with other materials

In order to comprehend the relative advantages of using NiTi as a viscoelastic material for the production of our new orthoses, it is interesting to see them in comparison with other materials. That can be done by using material selection charts (Ashby et al. 2013). With the values extracted from the literature (cf. section 2.2.2), the position of NiTi (lower plateau) under working conditions is shown in the Specific

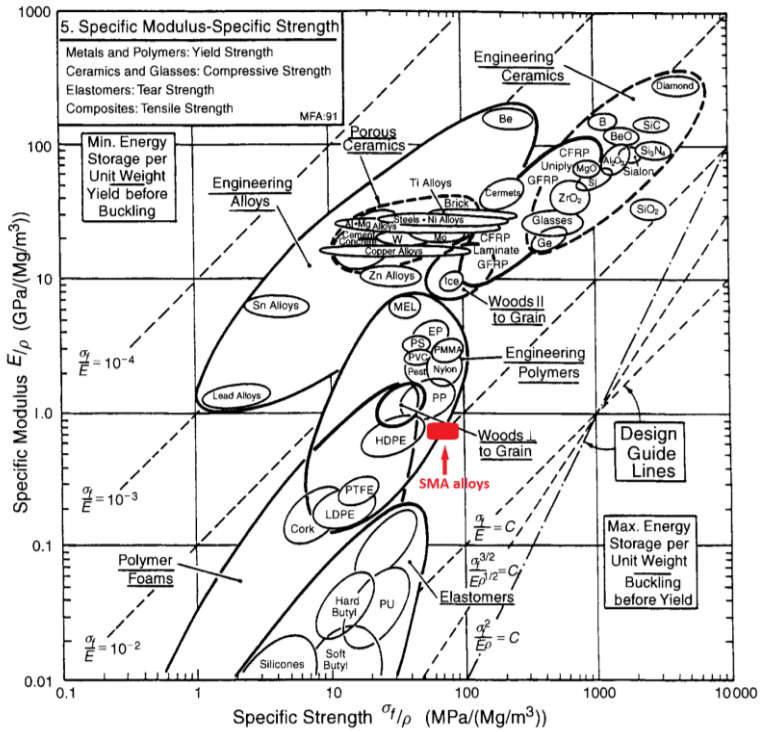

Figure 2.10 Ashby material selection chart. Comparison between Specific Modulus vs Specific Strength. The red rectangle identifies SMA alloys (modified from Ashby et al. 2013).

Modulus vs. Specific strength (Fig. 2.10) and Loss coefficient vs. Stiffness modulus (Fig.2.11).

It appears that, under dynamic conditions, NiTi behaves much like a polymeric material both in terms of rigidity, strength and damping capacity. On the other hand, given the lower density of polymers, should the functional element be made of plastic rather than NiTi, sections at

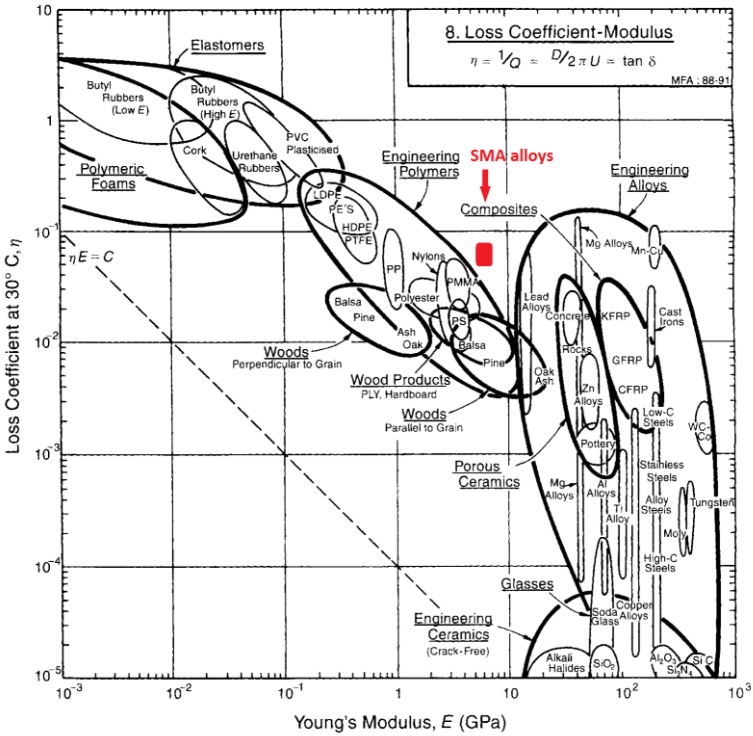

Figure 2.11 Ashby material selection chart. Comparison between Loss coefficient vs Young's Modulus. The red rectangle identifies SMA alloys (modified from Ashby et al. 2013).

least 6-8 times larger would be required to provide the needed mechanical behaviour. Furthermore, plastic materials of similar general characteristics (e.g. Polypropylene – PP) would tend to develop plastic deformations at the required cyclic working strain in our applications. This means that after a certain number of cycles the inability to recover completely will bring to a degradation of their functional performance.

2.2.4 Prior clinical experiences in the use of NiTi-based alloys for neuromuscular rehabilitation

There are several researchers who have exploited SMA characteristics for the design and use of devices for imparting forces on or producing movements of body segments, with the main purpose of assisting or replacing impaired functions. The most relevant experiences address biomedical problems such as the mobilisation of paralysed hands, fingers (e.g. Dittmer et al. 1993; Torri et al. 2006; Tang et al. 2013) and other segments (Pittaccio et al. 2009), the support of gait (e.g., Van Kuren et al. 2005; Pittaccio et al. 2010; Stirling et al. 2011; Deberg et al. 2014; Mataee et al. 2015) and limb repositioning (Viscuso et al. 2009). These literature items highlight the promising aspects of SMA technology in the rehabilitation field (Henderson et al. 2011) and also describe the limitations connected with its use.

Looking at the projects based on the shape memory effect, most studies mention the compactness and the possibility to develop flexible technologies as valuable aspects of SMA actuation, while the trade-off between torque or force output and actuation speed appears to be the main problem in rehabilitation applications. Another important issue to be taken into account is the actuator control; some researchers tried to manage it in different ways, depending on the target expected: the scientific papers on rehabilitation applications of SMA describe open-loop strategies focussed at simply triggering the start or pacing the repetition of actuation cycles (Pittaccio et al. 2009; Pittaccio et al. 2010); open-loop methods are also suggested to achieve particular movement trajectories (Torri et al. 2006; Tang et al. 2013); alternatively, more sophisticated closed-loop strategies are reported to achieve a more precise actuation control in terms of timing and output parameters (position, speed, force, …) (Zhang et al. 2013; Chen et al. 2014).

Figure 2.12 Two examples of active devices used for the neurorehabilitation designed by CNR-ICMATE. Both the mobiliser are activated exploiting shape-memory effect. It is worth to notice that *Toe-UP!* mobiliser (*left*) can be used by neurological patient in the early stages of their recovery process and it is provided with a NiTi-based linear actuator; on the *right*, the ankle mobiliser *Leia* is equipped with two patented rotary actuators including in NiTi wires, and its special design aimed at reducing electromagnetic emissions allows its use in very sensitive and strictly-ruled environments, such as MEG or MRI.

The use of pseudoelasticity is described in different studies mainly dealing with limb repositioning and gait rehabilitation (Viscuso et al. 2009; Deberg et al. 2014; Mataee et al. 2015). In those works, the deformability, adaptability and the nonlinear mechanical properties of SMA are considered as a means to design biomechanically compliant solutions to address the clinical necessities connected mainly with spasticity and paresis. The main aspects considered in the optimisation of those devices are the optimisation of alloy properties and the characterisation/modelling of their thermomechanical behaviour in order to deliver suitable static or dynamic corrective forces.

The experience of the CNR-ICMATE (formerly CNR-IENI) group, with whom the author has been working for the last six years, can be regarded as an interesting reference for the present research. Apart from the design of actuated systems exploiting shape-memory-effect devices (Fig.2.12) (Pittaccio et al. 2011; Pittaccio et al. 2013b; Pittaccio et al. 2013c), the group developed different wearable pseudoelastic orthoses for the treatment of spastic syndromes. The upper-motoneuron syndromes, whatever their aetiology (traumatic injuries, stroke, anoxia, etc.), are principally characterised by cortical lesions, from which a classic scheme of paresis, reflex-mediated hypertonic rigidity, muscular contracture, just to name the most prevalent motor symptoms. From the designer's point of view those applications are much more static, and the typical movement disorder traits, we are focussing on here, (dystonia, hyperkinesia) are most often absent. Nonetheless, some lessons can be learnt about the effects of pseudoelasticity on stretch-hypereflexia, the reduction in rigidity and the functional response to treatment.

The rationale in the use of devices with customisable pseudoelasticity in those cases included: (a) providing a corrective push that is correlated to the biomechanical, biometric, and clinical state of the patients, and to the likelihood that they will tolerate a given treatment intensity; (b) maximising acceptability and adherence to prescription times by making the corrective push mild enough and the orthosis sufficiently compliant to involuntary jerks that the pain induced by lengthening on spastic muscles is reduced; (c) avoiding limb fixity, thus improving joint mobility and the chances of a residual use of the limb; (d) avoiding the need to adjust spring preload as posture evolves, and the associated burden for caregivers; (e) self-regulating the strength of the orthotic action in relation to the direction of movement: thanks to SMA hysteresis, the stress during loading is higher than during unloading, so the perceived spring stiffness is higher for actions that are directed against the clinical goal (Pittaccio et al. 2015a; Pittaccio et al. 2015b).

Here we shall briefly describe the results obtained with this strategy in two studies that could be of help.

The first study (Pittaccio et al. 2013a) was conducted in collaboration with our clinical partners at Institute 'E. Medea' (Bosisio Parini, Italy). The pseudoelastic hinges were tested in cross-over trials against standard fixed-joint orthoses on 25 children (aged 7.75 ± 5.40 years) with mild to severe spastic tetraparesis as a consequence of central lesions (trauma, anoxia, encephalitis, etc…). The results suggest that pseudoelastic orthoses are much more tolerable for patients than traditional ones, and are as good in controlling posture. A great advantage of pseudoelastic devices over traditional ones is that, it was found, while traditional devices, due to the immobility and disuse they impose on the affected joint, tended to increase its viscoelastic stiffness (p=0.016) during a month's treatment, *pseudoelastic orthoses decreased viscoelastic stiffness* (p=0.026), over an equal period of time. In this application keeping the therapeutic force as slow as possible is recommended (Fig.2.13 *left*).

The second study (paper in preparation), is a recent one, done in collaboration with our partners at Ospedale Valduce (Clinica Villa Beretta, Costamasnaga, Italy). Six chronic hemiplegic (stroke) patients (age 56.16±7.22 years) were enrolled for the study and were prescribed to wear a custom-made orthosis for at least 6 hours a day for a month (Fig.2.13 *right*). Patients were evaluated before and after this period using several scales, including Fugl-Meyer (F-M), Modified Ashworth Score (MAS), and WOLF Motor Function Test (WMFT). Furthermore an accelerometer and an analogic potentiometer on-board the orthosis were used to evaluate quantitatively the performances of patients during the execution of motor tasks such as Reaching Foreward, Hand to Mouth and Timed Up-and-Go. The orthotic treatment produced mild improvements in several articular and functional parameters. For instance MAS (Elbow) decreased by 1±0.89 (p=0.02), F-M (items A-D)

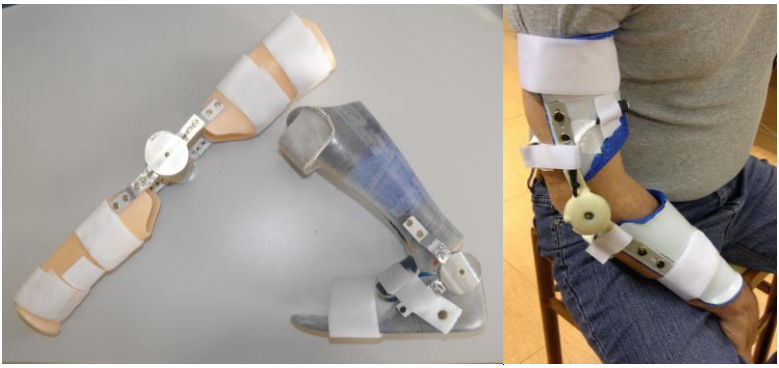

Figure 2.13 Two examples of passive orthotic devices used for the neurorehabilitation in spastic syndromes. On the *left*, pseudoelastic orthoses recommended for the repositioning and controlling posture of the elbow and ankle joints of paediatric patients with tetraparesis. On the *right*, a pseudoelastic personalised orthosis for the treatment of post-stroke upper-limb impairments in an adult patient.

improved by 1.66±1.13 (p=0.01) and WMFT increased by 4±4.35 (p=0.05). Improvement in movement speed in the hand-to-mouth task (from onboard sensor) seems to be greater for patients with high pre-treatment MAS (Pearson R^2=0.82). Reaching Forward times decreased by 19.1±20.5% (p=0.035). This pilot study showed that a *pseudoelastic orthotic treatment can promote moderate reacquisition of segmental mobility of the upper limb in chronic hemiplegic patients*.

2.3 Optimisation of the material characteristics in the design of the new orthoses for Childhood Dyskinesia

Considering the main objective of the present thesis, there is a need to optimise the properties of the NiTi functional elements) for the new orthosis. An interesting study has been conducted by the research group of CNR ICMATE about the development of a method for controlling shape memory alloy characteristics during shape-setting treatments in

the furnace (Pittaccio et al. 2014). The results of the study show how the selection of a defined thermomechanical treatment could influence the mechanical properties of the material and thus its behaviour and subsequent response in the specific application. Bearing in mind these considerations, in order to maximise the viscoelastic performance, we need to select a reference composition and an appropriate thermomechanical treatment able to endow the material with good pseudoelasticity (well-developed plateaux) and significant damping capacity (large hysteresis). The present section describes the optimisation of the selected alloy and its characterisation. It will also show the coherence between the obtained material properties and the mechanical characteristics required for the patients' needs.

2.3.1 Optimisation

In terms of composition, the necessity to have a material that displays pseudoelasticity leads to select amongst the Ni-rich alloys and in particular we selected a NiTi-based on Ni-rich side. Moreover, the specific field of application, i.e. the construction of a orthotic devices, imposes the choice of a materials that display their properties at room temperature (20°-30°C); in this respect, the composition considered is a "cold-alloy", i.e. a quasi-stoichiometric NiTi alloy with an A_f largely below the temperature range of use (A_f of the alloy, after solution treatment: -30°C). Finally, we choose a medical-grade alloy, which is characterised by smaller quantities of inclusion and impurities coming from the synthesis processes, that if present, by weakening the material, could shorten the life-span of the alloy and thus the orthosis.

Specimens of NiTi wires of the selected composition were cold drawn to a diameter of 2.0 mm with a final degree of cold working of 41% (cross-section reduction).

To optimise the properties of the alloy, we have tested different

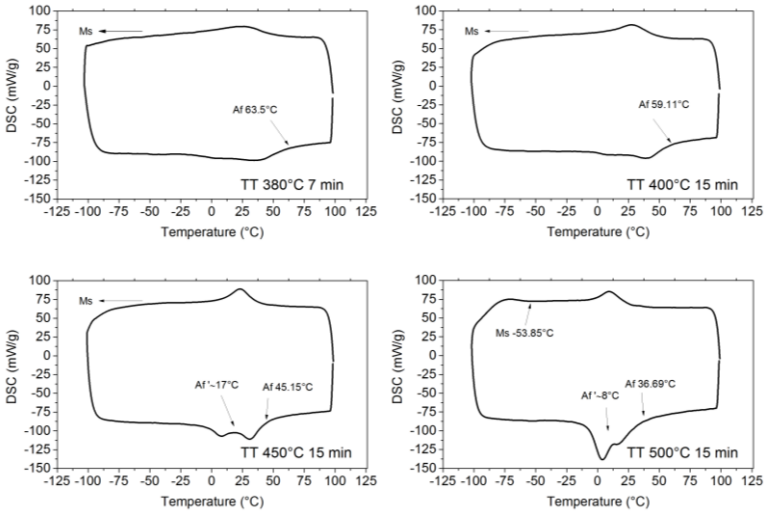

Figure 2.14 DSC curves for NiTi wire samples treated at different temperatures: 380°C for 7 min, 400°C for 15 min, 450°C for 15 min, 500°C for 15 min (from the *top left*). It can be noticed that there is a progressive increment of the thermal hysteresis and the transformation enthalpy with increasing temperature of the treatment.

thermomechanical treatments, at temperatures 380°C, 400°C, 450°C, 500°C (treatments carried out in the furnace in air environment, followed by water quenching). Samples of a few milligrams were used to carry out the calorimetric analysis with a differential scanning calorimeter (DSC Q100, TA Instruments, New Castle, DE, USA, heating-cooling ramp from -100°C to 100°C at 10°C/min). The characteristic transformation temperatures are reported in figures (Fig. 2.14).

It is evident from the DSC curves how the temperature influences the transition temperatures, the thermal hysteresis, and the transformation enthalpy (area under the peaks). With the present composition, all selected thermal treatments produce a two-step transformation with

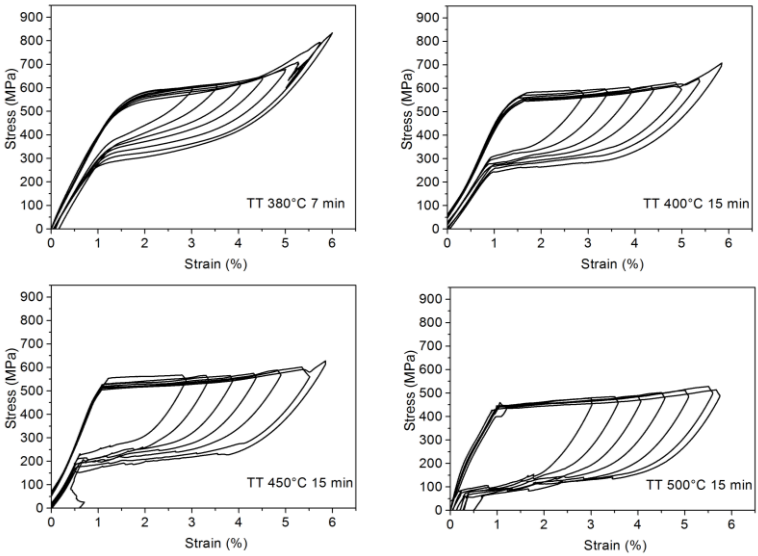

Figure 2.15 Tensile test curves for NiTi wire samples treated at different temperatures: 380°C for 7 min, 400°C for 15 min, 450°C for 15 min, 500°C for 15 min (from the *top left*). It can be noticed that, increasing the temperature of the treatment, there is a progressive increment of the mechanical hysteresis (damping capacity), as well as a reduction of the strength (height of the plateaux).

intermediate R-phase formation. This is due to the precipitation of a secondary Ni-rich phase (Ni_4Ti_3). Under these conditions, pseudoelastic behaviour is practically observed above the A_f' rather than the A_f temperature. The *Ms* temperature which is linked to the height of the unloading plateau becomes visible in the measurements range only for the highest treatment temperature (500°C).

Connected to this physical investigation, the analysis of the mechanical response to tensile loading-unloading has been carried out using the universal mechanical testing machine (2/M machine, MTS Systems, Eden

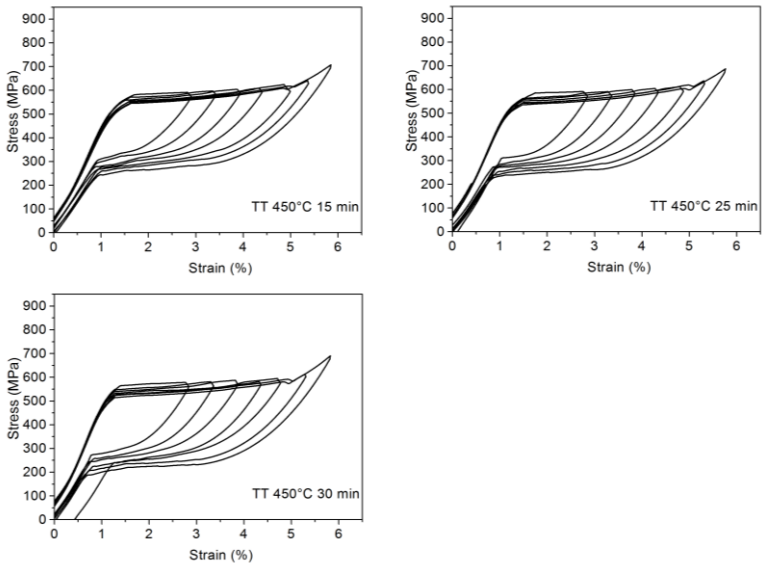

Figure 2.16 Tensile test curves for NiTi wire samples treated at the same temperature of 450°C for different time durations: 15 min, 25 min and 30 minutes (from the *top left*). It can be noticed that the effect of increasing the treatment time is to decrease the plateau stresses, especially the unloading one.

Prairie, MN, USA at a chamber temperature of 24°C, 1%/min, 0-6% strain control) (Fig. 2.15 and 2.16).

Coherently with the calorimetric observations, pseudoelastic behaviour is seen for all treatment conditions, but it is well developed only for temperatures of 400°C and above. The main effect of the temperature is that both the loading and unloading plateaux decrease in terms of stresses, but the unloading one decreases more, and thus the hysteretic area increases (Fig. 2.15). For the treatment at 500°C the unloading plateau looks excessively low, and the residual strain starts to accumulate. These observations suggest that a good balance for our application (good deformability, mild spring-back forces and good

damping capacity), can be obtained with a preferred treatment at 450°C. In order to fine-tune the treatment duration, additional tests were carried out at this temperature (Fig. 2.16). Increasing the treatment duration, it is possible to offset the balance toward a greater damping capacity and a lower strength.

Even if the specific application in rehabilitation, that we are considering, is dynamic, it is possible to conduct the optimisation of the viscoelastic response in quasi-static conditions, because the modulations of the material characteristics introduced by the dynamic variables (changing strain amplitude and strain rate), are expected to follow the well-known observed trends (cf. section 2.3.1). The fundamental assumption is of course that baseline pseudoelastic stability and damping capacity, once optimised in quasi-static condition will be carried over through the modulation by the dynamic variables.

In addition, it is worth noticing that the exact movement amplitudes or speeds, which will be employed by the patients in carrying out various real-life tasks, cannot be known *a priori*. Therefore, attempting an optimisation in specific dynamic condition, could be actually of little consequence.

2.3.2 Characterisation of bent NiTi elements and functional personalisation

In the previous section the optimisation of the stress-strain behaviour has been carried out using tensile tests, because they allow observing the pseudoelastic behaviour directly without interfering geometric parameters depending on the set-up. Now material response will be investigated in loading conditions more similar to the ones typical of the specific application, i.e. in the pseudoelastic orthosis for the upper limb. As will become more apparent in Chapter 3, the orthosis concept that we are developing will make use of NiTi bars loaded principally in

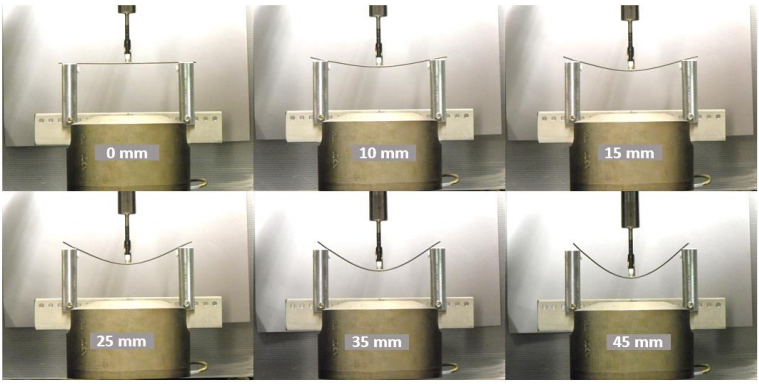

Figure 2.17 The picture shows the experimental set up to test NiTi wire samples, in three-point bending mode, during loading-unloading, at different crosshead displacement, from 0 mm to 45 mm of deflection as reported. These images are used to obtain the wire line-shape, using image analysis methods.

bending, with only secondary out of plane components. Hence, an *ad hoc* set-up has been constructed to test NiTi wires under cyclic loading-unloading in *three-point bending* mode (Figure 2.17) with the MTS machine. This has been done because the specific design and construction of the orthoses bring the material into a loading condition, which is comparable with due approximation: indeed, despite the fact that the extremities of the wires will be fixed on the orthoses, preventing any type of sliding and movement relative to each shell, they will still be able to rotate reciprocally around the articular joint centre, following the mutual rotation of the orthosis shells. For this reason the boundary conditions, in terms of deformations, are more similar to the three-point bending loading condition rather than, say, a dual-cantilever case, i.e. a much more severe constraint, by which the wire ends, being encastred, are not allowed to move relative to one another, and the stresses grow much larger than in the real application for similar midline bar curvatures. The main difference between the orthosis case and the three-point bending set-up is that, in the latter, the ends are drawn

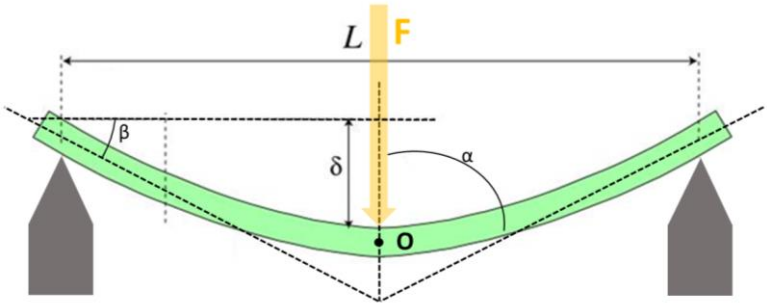

Figure 2.18 The scheme illustrates the geometrical parameters taken into account for the evaluation of the reaction forces and torques, during the experimental three-point bending test on the NiTi pseudoelastic wire. In particular, a deflection δ of the wire (crosshead displacement), corresponds to a load imparted by the moving punch (F); α is the angle of the bent sample ends to the vertical axis (2α has been considered to be a good model for the anatomical joint angle); β (90°- α) is the angle of the bent sample ends to the horizontal axis.

towards the midline while the punch lowers, so the length of wire tested between the supporting pins changes during the test.

For every displacement of the crosshead (δ), from 0 mm to 45 mm and thus a corresponding load imparted by the punch (F), there is an angle of elbow joint rotation, represented by twice the value of α in figure 2.18. During the test, pictures have been taken of the deformed wire. The corresponding curve, obtained from image segmentation and line fitting (5th degree polynomial) in MatLab, was analysed with an *ad hoc* subroutine to extract the line shape $l(s)$, its curvature and corresponding radius of curvature as reported in figure 2.19, besides the angle α.

All these parameters can be utilised to estimate the torque that the material is able to impart in the flexional loading condition, as a function of the joint angle. Using the measured values of force, the vertical

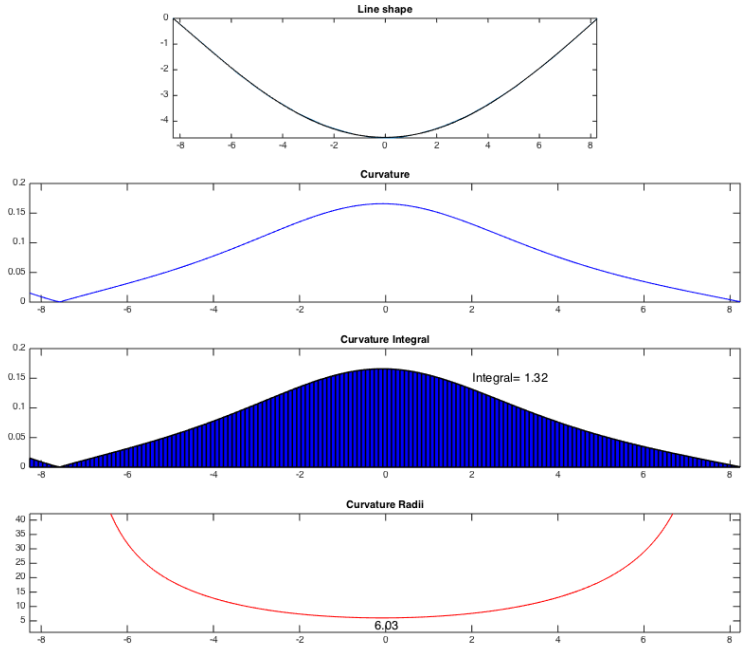

Figure 2.19 An example of the results of the MatLab analysis on the photo images to extract the line shape, the curvature, the area under the curvature and the radius (from *top* to *bottom*), for a defined deflection of the NiTi wire sample during three-point bending test.

reaction at the supporting pins is $F(\alpha)/2$, and the moment around the wire centre O (Figure 2.20) is $M(\alpha)= F(\alpha)\ L\ /4$.

However, this is an approximation, because, as mentioned previously, a difference with the real orthosis case is that in our present set-up the length of wire tested between the supporting pins changes during the test, while it does not change on the orthosis. In order to correct for this issue, we could try to estimate what force would be measured to obtain an equal curvature, should the wire length be conserved during the test.

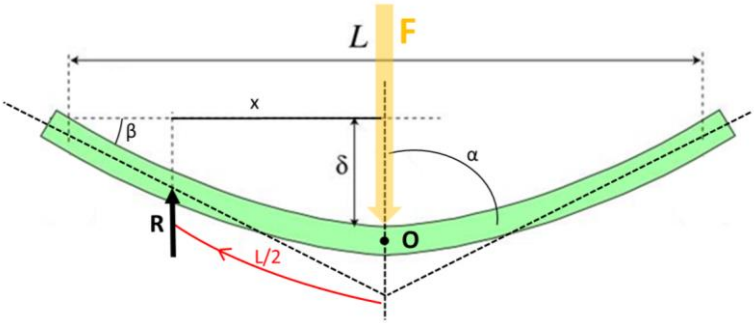

Figure 2.20 The scheme illustrates the geometrical parameters taken into account for the evaluation of the reaction forces and torques, during the experimental test of three-point bending on the NiTi pseudoelastic wire. In particular, R is the reaction force, applied in a point x, that is the horizontal distance from the crosshead action-line, where the line length of the wire sample is equal to $L/2$ (*red line*), due to the sliding occurring during flexion tests. Clearly the structure is symmetrical; therefore, in the scheme, for the sake of clarity, is reported only half side of the structure and the relative reaction force.

In order to do so, it must be recalled that (rigorously for small strains in elastic materials, e.g. <1-2%) the midline force F to obtain a given wire deflection δ is proportional to the inverse of cubed span length L:

$$F \sim \frac{1}{L^3} \qquad (2.6)$$

So, if we find the abscissa x such that, with the measured wire line-shape the wire length from the midline O to x is always $L/2$ (like at the start of the test, when the wire is suspended horizontal and undeformed), we can use equation (2.6) to obtain a better estimate of the moment (Figure 2.18). The required abscissa it calculated, for each α, by solving the following equation for the upper integration limit x:

$$\int_0^x \sqrt{1 + \left(\frac{dl(S|\alpha)}{ds}\right)^2}\, ds = \frac{L}{2} \qquad (2.7)$$

where $l(s|\alpha)$ is the shape of the line and is parameterised by the joint angle α, or equivalently the deflexion δ figure 2.20.

Now, the reaction force for a supporting pin located at x can be obtained by scaling the measured reaction force using equation (2.6):

$$R(\alpha) = \frac{F(\alpha)}{2} \cdot \frac{L^3}{x(\alpha)^3} \qquad (2.8)$$

Finally the new improved estimate of the moment originated by the bending of the bars (of fixed length) inflecting around O is given by:

$$M_x(\alpha) = R(\alpha) \cdot x(\alpha) \qquad (2.9)$$

for every specific deflection δ (corresponding to the measured α).

In this manner, if an orthosis mounts 2 NiTi wires working in parallel, it is predicted to impart a therapeutic moment $2M_x$. With the present tests we have calculated these values over a range of joint *flexion* angles between 0° and 90° (which correspond to joint α angles 180°-90° - for comparison the physiological range of motion of the elbow joint is 0°-130° of *flexion*), Figure 2.21.

It is also interesting to calculate the strains in the wires. Knowing the distance from the neutral axis y, together with the radius of curvature of the wire (r) the corresponding deformation $\varepsilon(y)$ in the wire sample, loaded during 3-point bending test is:

$$\varepsilon(y) = -y/r \qquad (2.10)$$

The average strain on the cross-section is obtained using y equal to half the wire diameter.

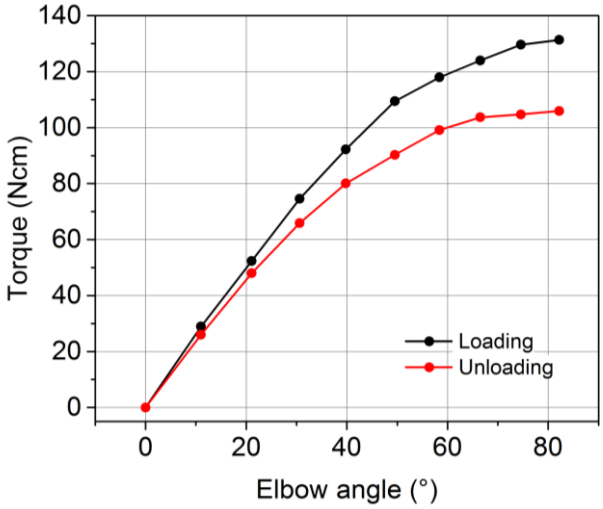

Figure 2.21 The graphs illustrates the torque ($2M_x$) that the two NiTi wires in the orthosis, treated at 450°C for 15 min, display during 3-point bending testing mode and thus the torque that the material could impart, if used a functional element in the construction of a dynamic orthosis.

With the methods described above, the samples tested provide the following reference values reported in Table 1. The characterisation has been carried out using a 2mm-diameter wires of NiTi, and a thermomechanical treatment at 450°C for 25 minutes, known to provide the NiTi sample with intermediate mechanical characteristics. It has already been discussed that, starting from this characteristic, a fine tuning of the material properties to obtain can be achieved modifying the temperature and duration of the treatment in the furnace, to change the balance between strength and damping capacity.. The length span L between the supporting pins was 165mm, generally compatible with the application.

The results of the *line analysis* on the images of the tested samples are reported in Table 1.

Table 1. *Line characteristics from image analysis. The strain (ε) is the mean value on the midline cross section calculated for a 2 mm-diameter NiTi wire (y=0.5 mm).*

δ (mm)	2α (°)	radius (mm)	ε (%)
5.0	169.0	485	0. 1
10.0	158.9	247	0.2
15.0	149.4	165	0.3
20.0	140.2	125	0. 4
25.0	130.5	101	0. 5
30.0	121.6	86	0.58
35.0	113.5	75	0. 66
40.0	105.4	67	0. 74
45.0	97.8	60	0. 83

All these considerations about the NiTi wires characterisation, offer the possibility to use a well customisable material, in terms of tuneability of the mechanical properties. In order to match the clinical requests and the patients' needs with the above mentioned properties, it is evident that the quantitative characteristics of the impaired limb play an important role. In doing this, in this study we tried to quantify the physiological torque to be controlled by the orthosis; the objective is to exploit the properties of the materials at their best to stabilise the joints without impairing the residual motor abilities of the patients (requisite of mild therapeutic forces).

To evaluate the forces necessary to control and support the movement of the upper limb, we calculated the biological forces, i.e. the torque necessary to keep the forearm horizontal with the elbow bent at 90° against gravity (M_{phys}), and the maximal voluntary isometric torques ($M_{isom\ max}$) that a patient is theoretically able to generate based on his/her anthropometric parameters. Notice that measuring these moments directly would be impossible, because the patients in general cannot be expected to maintain positions or perform maximal isometric contractions voluntarily).

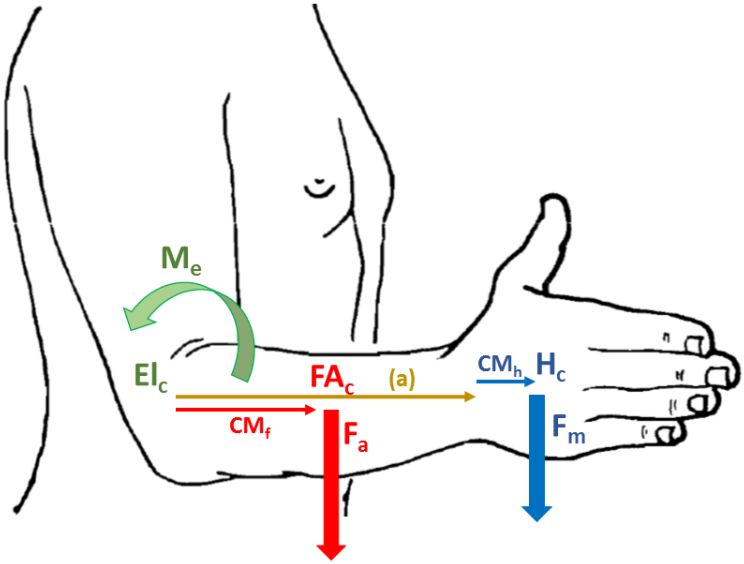

Figure 2.22 The figure shows the forces taken into account to calculate the equivalent torque at the elbow joint. In particulae, the torque at the elbow (M_e) is the sum of the torque generated by the weight force of the forearm (F_a) centred in FA_c and the weight force of the hand (F_m) centred in H_c. (a), CM_f, CM_h are the length of the forearm, the position of the centre of mass of the forearm and the position of the centre of mass of the hand, respectively.

Some parameters have been calculated directly as a combination of the others collected form the patient, in particular, the forearm mass (m_f) is:

$$m_f = d \times V \qquad (2.11)$$

Where d is the homogenised density of the forearm and V its volume.

The torques necessary to sustain the forearm when only the gravity force acts (M_{phys} centred in the elbow joint EL_c) is:

$$M_{phys} = m_f \times CM_f \times \frac{9.81}{1000} + m_h \times \left(CM_h + L_f\right) \times \frac{9.81}{1000} \qquad (2.12)$$

Where m_f is the forearm mass, CM_f is the centre mass of the forearm (centred in FA_c in figure 2.22), m_h is the hand mass, CM_h is the centre mass of the hand (centred in FA_c in figure 2.22) and L_f is the length of the forearm.

The evaluation of the maximal isometric torques (M_{isom}) have been done considering the constant values found in the literature (Falk et al. 2009):

$$M_{isom,50} = 0.78 \times CSA \times 100 \qquad (2.13)$$

$$M_{isom,87} = 0.98 \times CSA \times 100 \qquad (2.14)$$

for the 50th percentile and for the 87th, respectively, where CSA is the cross sectional area of the forearm evaluated from the reconstructed model in Rhinoceros (cf. Chapter 3).

Table 2 reports the anthropometric parameters of one of our patients, 8 years old, taken as an example, to calculate the torques necessary to sustain the forearm when only the gravity force acts (M_{phys}) (Figure 2.22) and the maximal voluntary isometric torques (M_{isom} max) used to estimate the possible limits of the therapeutic forces to impart with the orthosis.

Table 2. *Anthropometric parameters and calculated moments for an 8-year-old patient, taken as an example to show the procedure.*

ID	Patient 1
Age (y/o)	8.00
Body mass (kg)	20.00
Height (cm)	116.00
Mean arm density (g/cm^3)	1.40
Forearm volume (cm^3)	248.58
CSA (cm^2)	21.10
Forearm length (cm)	18.00
Forearm mass (g)	348.01
CM_f position (cm)	7.71
Hand length (cm)	14.50
Hand mass (g)	130.00
CM_h position (cm)	6.79
M_{phys} (Ncm)	57.90
$M_{isom,50}$ max (Ncm)	1645.80
$M_{isom,87}$ max (Ncm)	2067.80

In Table 2 in *blue* are reported biometric parameters, derived from a direct measurement on the subject; the *orange* parameters have been measured on the solid model of the arm and the forearm geometry, reconstructed in Rhinoceros, from the data collected with the stereophotogrammetric system on the patient (see further details in Chapter 3 of the present thesis). The *green* parameters come from the literature, because of the impossibility to calculate them with the data collected. The *black* parameters have been calculated directly as a combination of the others.

It can be noticed that the two NiTi wires, coupled to be employed in the orthotic device, can impart a maximum torque M_x, that is in the range between 105-130 Ncm, and, in the case of this patient, it is approximately twice the M_{phys} necessary to hold the forearm bent at 90° of flexion and it is between 9-10% and 4-5% of the maximum isometric torque at the elbow for the 50th and 87th percentile, respectively.

2.4 Discussion and conclusion

All the considerations and the analysis reported above show that the NiTi-based alloys are a promising class of materials to accomplish the requirements needed in the development of a wearable dynamic orthosis for the support of upper-limb rehabilitation in Childhood Dyskinesia. In particular, NiTi displays a good viscoelasticity, which is a fundamental characteristic in dynamic applications.

It was assumed that the alloy characteristics can be optimised looking at quasi-static measurements. The effects of strain rate are in fact known from the literature. It can be observed that patients with motor control problems, such as the ones affected by dystonia and hyperkinesia, often have difficulties in initiating the movements and in stabilising the positions. In this respect, from a theoretical point of view, the strain rate dependency of the NiTi, especially with higher damping capacity at low strain rate, could help in better controlling the initial phases of the motion; for higher movement velocities, and when then gesture is more developed, the higher speed brings the material in condition of lower viscosity and damping capacity; in this manner the second part of the movement may be less hindered by the orthosis itself, maintaining the control with mild forces.

The torque, which a couple of NiTi bars of 2mm in diameter can impart was demonstrated to be two times greater than the torque necessary to hold the hand and the forearm at 90° respect to the arm segment and in

the range of 10% respect the maximal voluntary isometric contraction force, for a patients of 8 years old. This means, on one side, that the force is sufficient to be well perceived by the subject wearing the device, but, on the other, it is far lower than the action the patient can express, an thus it cannot interfere too much with the possibility to move voluntary or stimulate a negative stretch-reflex response. The mild forces and consequently the mild torques imparted on the impaired limb, are in fact hoped to accomplish the important clinical requirement to reduce, or at least contain, symptoms such as the hypertone, the variability and the overflow, which are likely stretch-reflex dependant (van Doornick et al. 2009) or at least worsened by high force fields.

The possibility to fine-tune the mechanical properties of the material matches another of the patients' need, which is of paramount importance, i.e. the customisation. In this respect, the selection of the right thermomechanical treatment provides the material with the desired level of strength, deformability and the desired hysteresis; for subject's specific necessities of higher forces, a maximisation of the height of the plateaux will result in more elastic-like response with higher forces; on the contrary, if a higher damping is required, the choice of the thermomechanical treatment will be to maximise the mechanical hysteresis, and thus the SDC.

For these reasons, in order to achieve the final aim of the thesis we shall use NiTi wires with the diameter of 2mm, treated at different temperatures (range between 380°C and 500°C) for a time between 15 and 25 minutes, to design and develop the articulated part of the orthoses (see further detail in Chapter 3) for the upper-limb of patients affected by Childhood Dyskinesia. As a general rule, we will use the working assumption that corrective moments below 10% of the maximum isometric effort will not be a hindrance for the achievement of the voluntary motion. Furthermore, the same moments will have to be around twice or three times the torque necessary to support the

weight of the limb, in order to be clearly perceived. For patients with prevalent dystonic traits, it may be appropriate to keep this moment lower (a suitable value will be decided on a case-by-case basis), in order to avoid the stretch reflex response.

2.5 References

Ashby, M. F., & Johnson, K. (2013). Materials and design: the art and science of material selection in product design. Butterworth-Heinemann.

Chen, Z., Fan, S., & Zhang, D. (2014, December). An exoskeleton system for hand rehabilitation based on master-slave control. In *International Conference on Intelligent Robotics and Applications* (pp. 242-253). Springer International Publishing.

Deberg, L., Taheri Andani, M., Hosseinipour, M., & Elahinia, M. (2014). An SMA passive ankle foot orthosis: Design, modeling, and experimental evaluation. *Smart Materials Research*, *2014*.

Dittmer, D. K., Buchal, R. O., & MacArthur, D. E. (1993). The SMART Wrist-Hand Orthosis (WHO) for Quadriplegic Patients. *JPO: Journal of Prosthetics and Orthotics*, *5*(3), 73.

Dolce, M., & Cardone, D. (2001). Mechanical behaviour of shape memory alloys for seismic applications 2. Austenite NiTi wires subjected to tension. *International Journal of Mechanical Sciences*, *43*(11), 2657-2677.

Falk, B., Usselman, C., Dotan, R., Brunton, L., Klentrou, P., Shaw, J., & Gabriel, D. (2009). Child–adult differences in muscle strength and activation pattern during isometric elbow flexion and extension. *Applied Physiology, Nutrition, and Metabolism*, *34*(4), 609-615.

Gandhi, F., & Wolons, D. (1999). Characterization of the pseudoelastic damping behaviour of shape memory alloy wires using complex modulus. *Smart Materials and structures*, *8*(1), 49.

He, Y. J., & Sun, Q. P. (2010). Frequency-dependent temperature evolution in NiTi shape memory alloy under cyclic loading. *Smart Materials and Structures*, *19*(11), 115014.

He, Y. J., & Sun, Q. P. (2011). On non-monotonic rate dependence of stress hysteresis of superelastic shape memory alloy bars. *International Journal of Solids and Structures*, *48*(11), 1688-1695.

Henderson, E., & Buis, A. (2011). Nitinol for prosthetic and orthotic applications. *Journal of materials engineering and performance*, *20*(4-5), 663-665.

Ip, K. H. (2000). Energy dissipation in shape memory alloy wires under cyclic bending. *Smart Materials and Structures*, *9*(5), 653.

Yang, S., Dui, G., & Liu, B. (2013). Modeling of rate-dependent damping capacity of one-dimensional superelastic shape memory alloys. *Journal of Intelligent Material Systems and Structures*, *24*(4), 431-440.

Lagoudas, D. C. (2008). Shape memory alloys. *Science and Business Media, LLC*.

Lagoudas, D., Hartl, D., Chemisky, Y., Machado, L., & Popov, P. (2012). Constitutive model for the numerical analysis of phase transformation in polycrystalline shape memory alloys. *International Journal of Plasticity*, *32*, 155-183.

Liu, Y., & Van Humbeeck, J. (1997). On the damping behaviour of NiTi shape memory alloy. *Le Journal de Physique IV*, *7*(C5), C5-519.

Liu, Y., & Yang, H. (2007). Strain dependence of the Clausius–Clapeyron relation for thermoelastic martensitic transformations in NiTi. *Smart materials and structures*, *16*(1), S22.

Malovrh, B., & Gandhi, F. (2001). Mechanism-based phenomenological models for the pseudoelastic hysteresis behavior of shape memory alloys. *Journal of intelligent material systems and structures*, *12*(1), 21-30.

Mataee, M. G., Andani, M. T., & Elahinia, M. (2015). Adaptive ankle–foot orthoses based on superelasticity of shape memory alloys. *Journal of Intelligent Material Systems and Structures*, *26*(6), 639-651.

Melton, K.N., & Mercier, O. (1980) The mechanical properties of NiTi-based shape memory alloys. *Acta Metallurgica, 29*, 393-398.

Ortín, J., & Delaey, L. (2002). Hysteresis in shape-memory alloys. *International Journal of Non-Linear Mechanics*, *37*(8), 1275-1281.

Otsuka, K., & Wayman, C. M. (1998). Mechanism of shape memory effect and superelasticity. *Shape memory materials*, 27-48.

Otsuka, K., & Wayman, C. M. (1999). *Shape memory materials*. Cambridge university press.

Otsuka, K., & Ren, X. (2005). Physical metallurgy of Ti–Ni-based shape memory alloys. *Progress in materials science*, *50*(5), 511-678.

Piedboeuf, M. C., Gauvin, R., & Thomas, M. (1998). Damping behaviour of shape memory alloys: strain amplitude, frequency and temperature effects. *Journal of Sound and Vibration*, *214*(5), 885-901.

Pittaccio, S., Viscuso, S., Rossini, M., Magoni, L., Pirovano, S., Villa, E., ... & Molteni, F. (2009). SHADE: A shape-memory-activated device promoting ankle dorsiflexion. *Journal of materials engineering and performance*, *18*(5-6), 824-830.

Pittaccio, S., Viscuso, S., Beretta, E., Turconi, A. C., & Strazzer, S. (2010). Pilot studies suggesting new applications of NiTi in dynamic orthoses for the ankle joint. *Prosthetics and orthotics international*, *34*(3), 305-318.

Pittaccio, S., & Viscuso, S. (2011). An EMG-controlled SMA device for the rehabilitation of the ankle joint in post-acute stroke. *Journal of materials engineering and performance*, *20*(4-5), 666-670.

Pittaccio, S., Garavaglia, L., Viscuso, S., Beretta, E., & Strazzer, S. (2013a). Implementation, testing and pilot clinical evaluation of superelastic splints that decrease joint stiffness. *Annals of biomedical engineering*, *41*(9), 2003-2017.

Pittaccio, S., Garavaglia, L., Molteni, E., Guanziroli, E., Zappasodi, F., Beretta, E., ... & Passaretti, F. (2013b, July). Can passive mobilization provide clinically-relevant brain stimulation? A pilot EEG and NIRS study on healthy subjects. In *Engineering in Medicine and Biology Society (EMBC), 2013 35th Annual International Conference of the IEEE* (pp. 3547-3550). IEEE.

Pittaccio, S., Zappasodi, F., Tamburro, G., Viscuso, S., Marzetti, L., Garavaglia, L., ... & Pizzella, V. (2013c, July). Passive ankle dorsiflexion by an automated device and the reactivity of the motor cortical network. In *Engineering in Medicine and Biology Society (EMBC), 2013 35th Annual International Conference of the IEEE* (pp. 6353-6356). IEEE.

Pittaccio, S., & Garavaglia, L. (2014). Electric resistance monitoring as a method for controlling shape memory alloy characteristics during shape-setting treatments in the furnace. *Materials Science and Engineering: A*, *599*, 92-104.

Pittaccio, S., Garavaglia, L., Ceriotti, C., & Passaretti, F. (2015a). Applications of Shape Memory Alloys for Neurology and Neuromuscular Rehabilitation. *Journal of functional biomaterials*, *6*(2), 328-344.

Pittaccio, S., Garavaglia, L., Ceriotti, C., & Passaretti, F. (2015b). The Use of Dynamic Systems Based on Shape Memory Alloys for the Treatment of Neuromuscular Disorders. *IFAC-PapersOnLine*, *48*(20), 189-194.

Saadat, S., Salichs, J., Noori, M., Hou, Z., Davoodi, H., Bar-On, I., ... & Masuda, A. (2002). An overview of vibration and seismic applications of NiTi shape memory alloy. *Smart materials and structures*, *11*(2), 218.

Soul, H., Yawny, A., Lovey, F. C., & Torra, V. (2007). Thermal effects in a mechanical model for pseudoelastic behavior of NiTi wires. *Materials Research*, *10*(4), 387-394.

Stirling, L., Yu, C. H., Miller, J., Hawkes, E., Wood, R., Goldfield, E., & Nagpal, R. (2011). Applicability of shape memory alloy wire for an active, soft orthotic. *Journal of materials engineering and performance*, *20*(4-5), 658-662.

Tang, T., Zhang, D., Xie, T., & Zhu, X. (2013). An exoskeleton system for hand rehabilitation driven by shape memory alloy. In *Robotics and Biomimetics (ROBIO), 2013 IEEE International Conference on* (pp. 756-761). IEEE.

Torri, M., Viscuso, S., Pittaccio, S., Nespoli, A., & Besseghini, S. (2006). Biomechanical design of a shape memory alloy spring for the activation of a flaccid hand rehabilitation device. *Medical Device Materials III*, 237-242.

van Doornik, J., Kukke, S., & Sanger, T. D. (2009). Hypertonia in childhood secondary dystonia due to cerebral palsy is associated with reflex muscle activation. *Movement Disorders*, *24*(7), 965-971.

Van Humbeeck, J. (1996). Damping properties of shape memory alloys during phase transformation. *Le Journal de Physique IV*, *6*(C8), C8-371.

Van Humbeeck, J. (1999). Non-medical applications of shape memory alloys. *Materials Science and Engineering: A*, *273*, 134-148.

Van Humbeeck, J., & Kustov, S. (2005). Active and passive damping of noise and vibrations through shape memory alloys: applications and mechanisms. *Smart Materials and Structures*, *14*(5), S171.

Van Kuren, M. B., Gillette, S., Mejia, P., Stoever, T., & Walker, A. (2005). Design considerations for a wearable pediatric rehabilitative boot. In *Rehabilitation Robotics, 2005. ICORR 2005. 9th International Conference on* (pp. 400-403). IEEE.

Viscuso, S., Pittaccio, S., Caimmi, M., Gasperini, G., Pirovano, S., Villa, E., ... & Molteni, F. (2009). Pseudoelastic nitinol-based device for relaxation of spastic elbow in stroke patients. *Journal of materials engineering and performance*, *18*(5-6), 805-813.

Wolons, D., Gandhi, F., & Malovrh, B. (1998). Experimental investigation of the pseudoelastic hysteresis damping characteristics of shape memory alloy wires. *Journal of Intelligent Material Systems and Structures*, *9*(2), 116-126.

Xiao, T. (1993). Internal friction due to thermoelastic martensitic transformation. *Metallurgical Transactions A*, *24*(5), 1067-1071.

Zhang, J. J., Yin, Y. H., & Zhu, J. Y. (2013). Electrical resistivity-based study of self-sensing properties for shape memory alloy-actuated artificial muscle. *Sensors*, *13*(10), 12958-12974.

Chapter 3

Development and fabrication of new wearable smart-material-based orthoses for the control of Movement Disorders

The chapter presents an innovative method based on optoelectronic stereophotogrammetry for all-in-one-frame acquisition of upper-arm geometry and a process for the design and production of new customised dynamic wearable orthoses for the upper limb. It also describes the entire procedure to acquire data from the subject, virtually design the device, and physically construct and assemble it.

3.1 Introduction

This study shows a new method for the design and the construction of wearable orthoses to treat Movement Disorders in the young.

Several groups have now evidenced that orthotics can be valid alternatives to standard procedures in treating neurologic patients affected by Movement Disorders (Burtner 2008; Morris et al. 2011), and could bring a general improvement in the management of this kind of diseases also increasing the life-quality of the subjects affected; however, orthotics are not frequently prescribed by clinicians (Boyd et al. 2001; Autti-Rämö et al. 2006), as explained in more detail in Chapter 1 of this thesis.

Often, it seems, the efficacy of the splinting is hindered by the fact that the devices are standard, without a functional customisation. Problems are related to the fact that orthoses are bulky or uncomfortable, and patients, particularly the younger ones, encounter difficulties during the donning and doffing (Nicholson et al. 2001; Coghill et al. 2010; Morris et al. 2011). In the literature, some studies (e.g. Fish et al. 2001; Mavroidis et al. 2011; Pittaccio et al. 2012; Kumar et al. 2015) report how a good customisation is fundamental both to reach high levels of comfort (and consequently an increased daily application time) and to improve efficacy of the treatment. To obtain a good personalisation, the device should bring forth at the same time the best *anatomical adaptation* and the *functional customisation of the therapeutic action* imparted. While functional customisation is not usually taken into account in the design and construction of orthoses (see on the contrary Chapter 2), examples of anatomical design are obtained by means of different systems for body surface acquisition, like direct shaping of thermoplastics on the limb followed by casting in gypsum and manual refinement of the model, or more recently, point-cloud representation from a 3D scanner and CAD-assisted post-processing of the resulting mesh (Pizzi et al. 2005;

MacDonald et al. 2016). These methods are useful because they provide good results in terms of adherence to the real shapes of the limb under exam, but have some limitations. For instance, they require long time for the acquisition of the surfaces and during this time the subjects must remain steady or at least they should not move the affected limb. Considering the case of Movement Disorders, it is evident how these systems are inapplicable due to the sudden, non-repetitive and continuous movements that the patients involuntarily make.

The objective of the present study is to show a new method to build fully-customised orthoses and increase the personalisation also for dystonic and dyskinetic patients, with the purpose to improve comfort and the usability of the devices. A method to accomplish this aim is described, exploiting an optoelectronic stereophotogrammetric system, which provides the coordinates of reflective passive markers in space illuminated by infrared radiation during the acquisition time. By means of this well-known tool, already in use for motion analysis in many different fields (Medved et al. 2001; Capozzo et al. 2005; Jasper et al. 2011), we obtained point clouds of sufficient resolution to reconstruct the solid geometry of the specific part of the body under exam, during motion, without affecting the limb shape or posture, with accuracy and in a rapid way. The possibility to obtain also a measure of limb kinematics in standardised tasks served the purpose of functional personalisation because, when managing children with movement disorders, the first step is to identify movement patterns that are abnormal for the age of the child and classify their phenomenology (Koy et al. 2016). The following sections highlight the procedure to place the passive markers solving the problems connected with avoiding limb-model deformations and optimising placement and point-cloud structure, and to reconstruct data in order to obtain the final limb geometry. Furthermore, it shows the designing process of the valves and the fixtures to connect the functional metallic elements (designed and built as explained in Chapter

2) to the valves, and finally, the construction of all the parts and the assembling process to create fully customised wearable orthoses.

3.2 Materials & Methods

To design and construct a fully customised wearable device for the neurorehabilitation of dyskinetic and dystonic patients, using data acquired via the optoelectronic system, many different activities have been carried out: a first step of biomechanical design of the *concept orthosis*; a second step of marker disposition and methods to collect useful *point clouds*; a third step of *virtual design of parts*, including the CAD-aided image elaboration and the design of the valves and fixtures personalised on the individual subject; and a final step of *making and assembling* of all the parts to obtain the final device.

3.2.1 Biomechanical design

Biomechanical considerations are at the core of the development of the innovative wearable rehabilitation device presented in this study. Even though the main symptoms, that affect dystonic and dyskinetic patients, share many inter-individual similarities, the exact signs, that every subject displays, are different in terms of joint affected, residual range of motion (ROM), compensatory strategies and muscular synergies. For this reason, it is expected that the kind of motion to be corrected, the residual voluntary movements to be allowed, the level and direction of forces to be imparted, will be different, accordingly.

The plan is that the new dynamic orthoses should impart a dynamic constraint and a feedback force field in order to stabilise voluntary action and help movement control. To accomplish this objective, the device is required not only be comfortable light and wearable, but it should also provide forces applied along the right direction and of a prescribed

intensity related to each patient's characteristics and the clinical goal. Furthermore, the interfaces must be designed so that forces can be transferred to the patient's body effectively.

The design process includes two main steps: *conceptual design* and *personalisation*.

Conceptual design

The principal features of the new orthoses can be defined in general, and will remain valid across different patient-specific embodiments. They depend upon requirements such as the following, which must be met to make the devices readily adaptable to *personalisation*.

i. The orthoses will be able to act upon *one or several joints*. This implies that the concept will include multiple parts to adapt to different body districts, i.e. will set up supports available for the elbow, wrist and fingers, possibly connected together if requested.
ii. It is foreseen that *one or more degrees of freedom* (d.o.f) will have to be controlled. The orthosis will need to impart forces along different directions separately or in combination; the functional elements will have to produce an efficient overall effect, without impairing the residual voluntary movements and limiting cross-effects between different d.o.f.'s, which should be controllable independently. To do this, fixtures allow asymmetric placement of the pseudoelastic elements in order to produce a directional torque around the forearm, in addition to elbow flexion, or an in-plane bending to control radial-ulnar posture in addition to flexion of the wrist.
iii. In order to *avoid sliding or misalignment* of the shells, the pseudoelastic elements must be aligned with the joint centre of rotation and this alignment will have to be preserved as much as possible during motion, especially during the bending of the orthosis. Consequently, the fixtures have been designed to allow the shells to remain adherent to the limb as to transfer the action of the pseudoelastic elements, and to maintain the NiTi elements in the

correct alignment during motion, bearing in mind that their position might be asymmetric on the 2 limb sides, if a complex repositioning action is required.

We also designed the fixtures to be able to house more than one pseudoelastic wire per side in order to modify the force of the device, if needed. The shape of the fixtures has been designed once and their general concept can be readily modified to adapt to the specific requests of different subjects (cf. Personalisation, and the following sections).

iv. The *transfer of forces* towards the body will depend on the characteristics of the interfaces, in particular the valves have to be adherent to the limb following perfectly the anatomical features, considering that during motion soft tissues and muscles change their shape and position in some way; the shells are padded with different thicknesses also to absorb and to be compliant for these natural variations, and to increase comfort, especially around bony structures. The position on the limb has been chosen to maximise the force transmission and to minimise the contact where there is a large variation in the limb shape. We decided to place valves on the backside of the arm and forearm, hold the wrist on the volar side and the hand supporting the thumb, in order to balance the above-mentioned characteristics.

The concept therefore provides *in potentia* all the features useful to support the rehabilitation of many different upper-limb impairments of neurologic aetiology, and the general shapes and structures of the splint are already set up in a “primitive” form. By designing an orthosis with these characteristics, we are able to approach most clinical pictures, by personalising case-by-case only the features needed for the specific patient, without having to redo the design every time anew.

In support to a clever and satisfying virtual design, we had the opportunity to discuss and exchange views on some biomechanical criteria with a group of experts from Strathclyde University in Glasgow

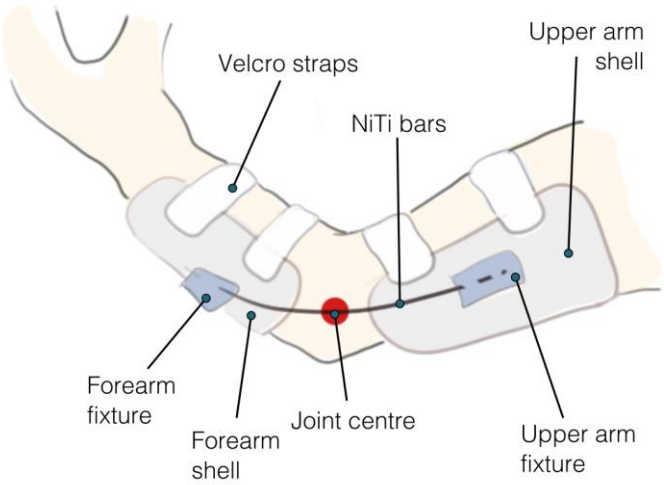

Figure 3.1 Concept of the new orthotic wearable dynamic device for rehabilitation support of the upper limb. The figure refers to the elbow joint, as an important example.

led by Professors Arjan Buis and Roy Bowers. Especially, we discussed the strategies to form the valves, to prevent movements between skin and shells, to keep the limb in the right position, reducing the quantity of material, increasing the comfort and the efficacy. Observing that the geometry of the arm and the forearm are not perfectly circular, but slightly oval, led us to decide that this anatomical feature can be exploited, from a biomechanical point of view, to impart a pinching action to constrain an exaggerated movement (especially prono-supination, which occurs around the forearm axis) even if the shapes remain unchanged and adherent to the limb. To achieve this effect, the chosen positioning of the valves on the ulnar side of the forearm is most suitable.

In the light of all the observations presented above, the overall design of the new orthosis is as depicted in Figure 3.1.

Personalisation

While the anatomical customisation will be dealt with in the following sections, the design methods for the functional personalisation are briefly described herein below.

In order to choose for each single patient the appropriate degrees of freedom, the intensity of the forces and their direction of action, a preliminary analysis of the specific mobility is conducted by means of the optoelectronic system. The analysis of kinematics provides the characteristics of the motor abilities of the subject (cf. paragraph of methods of this Chapter 4). In this manner, it is possible to understand if, during the execution of a standardised motor task, the subject has a specific impairment affecting one or more joints, which degrees of freedom are mostly compromised and in which way the subject tries to compensate for this impairment. Say that, during the pointing task, one would record no flexion or a hyperextension of the elbow, with a marked supination of the forearm; in that case, to complete the motor task, patients would likely compensate with a motion back and forth of the thorax, sometimes sideways. In such conditions, the degree of freedom to be favoured would be first and foremost the flexion of the elbow, also controlling the prono-supination. This is just an example, while it is observed that the picture can vary greatly, hence the need for scout acquisitions of the patient-specific kinematics. Information like this, coming from the preliminary kinematics evaluation, helped us in defining the specific neutral posture, position and the geometries of the valves and fixtures, starting from the virtual general concept, designed at the beginning.

In particular, the return (neutral) posture, towards which the pseudoelastic elements tend to bring the limb, is actually a fundamental aspect of personalisation, that has to do with both the pathologic habit of the limb, and conversely the optimisation/recovery of its functional

usability. As it is done for other details already mentioned, it is possible to decide upon this functional requirement during the virtual design phase in the construction of the personalised device (cf. section 3.2.3): the neutral angle of the device can be modified from the initial (measured) posture using the Rhinoceros software (Rhinoceros 3.0, Robert McNeel & Associates, Seattle WA, USA) as shown in Figure 3.2.

All these aspects, together with the biomechanically-informed choice about the forces to be imparted through the functional metallic elements in NiTi-based alloys (that are extensively discussed in Chapter 2), are the first step of the innovative method presented here, to construct a fully customised device to support the neurorehabilitation of patients affected by dystonia and dyskinesia.

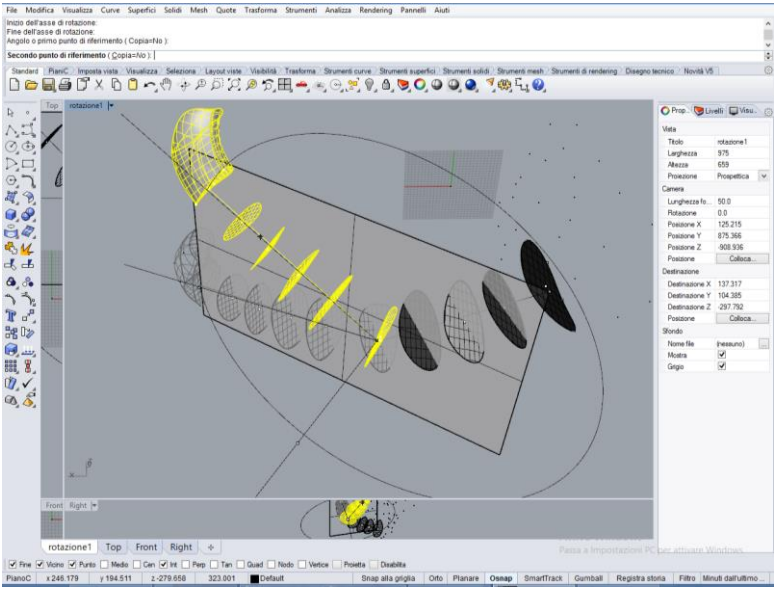

Figure 3.2 The screenshot depicts the CAD-aided realignment of the elbow model in order to select the desired neutral angle of flexion, before designing the personalised fixtures.

3.2.2 Marker set-up and image acquisition

Besides the concept and the functional personalisation, the design of the new devices includes the anatomical/geometrical customisation of the orthosis elements. The starting point is the acquisition of relevant body surfaces. The method is based on the following concept and considerations.

Point clouds used to describe surfaces are in general topologically unstructured (Remondino 2003), with points occurring at variable distances and mutual positions. Some *a-priori* knowledge of the acquisition system and the geometry to be described can help give a structure to the point data, thus optimising the number of samples and the well-posedness of the reconstruction problem with appropriate spatial resolution.

A BTS SMART-Elite System with 8 infrared cameras has been used to acquire the surface of the limb, coupled with passive reflective hemispheric markers of 6 mm in diameter. The optoelectronic system acquires marker positions in a desired and calibrated volume. A clever balance between the dimension of the field of view (FOV), related to the camera magnification, and the minimal spatial resolution of the system (10 mm), connected to the size and the number of the markers employed, must be established to maximise the accuracy of the acquisition avoiding confusion in the recognition of individual markers.

Another important key-point to be considered is the position of the markers. A generic surface can be divided into sections and then estimated from the section borders (Hohe et al. 2002; Colombo et al. 2006): this approach is also valid for human surface reconstruction (Colombo et al. 2013). Therefore, it is also possible to think of a limb as made of slices: the closer the slices, the better the surface description. In this respect, the method here presented tries to maximise the number

of “slices” that can describe the upper limb of the subject, and similarly the number of the markers should be sufficient to describe faithfully each “ring” (the border of the slice) itself, with a high number of them. Analysing the sizes and shapes of upper limb sections from children an youths, it appears that they have a more or less circular shape. If sections were perfectly planar and circular, their geometry could be reconstructed with only 3 points per slice. However, they are not circular and planar and so it is necessary to increment the number of markers, to describe in a more affordable manner the section borders.

Given those considerations, we set 12 rings to describe the upper limb (65 markers in total) plus 5 rows of 4 markers each, on the front and back side of the upper part of the chest wall to describe the shoulder and the upper thorax (adding 40 markers). More in details there are 5 equidistant rings on the forearm, starting from the wrist with 2 of them of 4 markers each and 3 of them of 6 markers each. One ring of 6 markers on the plane through the olecranon and centre of rotation of the elbow. Three planes on the arm, starting from the elbow, of 6 markers each and finally, to collect the surface of the shoulder, we placed 15 markers aligned on 3 convergent arches starting in correspondence of the axillary fold as depicted in (Figure 3.3).

The optoelectronic system allows acquiring the position of the markers placed on the limb surface (i.e. the positions of the centroids of the hemispheric markers, see Chapter 4 for further explanations). The subject is free to move in the calibrated FOV and in order to collect the entire surface it is sufficient that each marker is seen by at least 2 cameras in one and the same instant. No constraints for the limb and no deformation of the surface is provoked in this manner. Once the marker positioning is completed, normally the acquisition is rapid and takes no more than a few seconds. The acquisitions were carried out in the LARES laboratory (Laboratory of Respiration located in the Department of

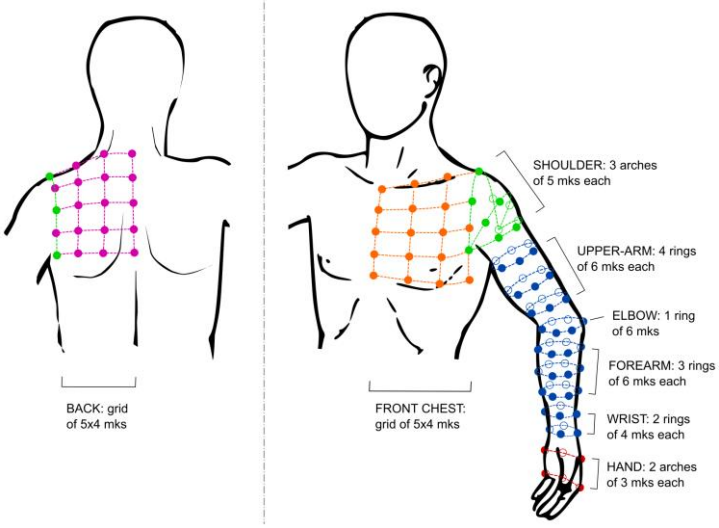

Figure 3.3 Sketch of marker placement on the upper limb and thorax. The position of each marker is adjusted in relation to precise anatomical fiduciary points, in order to be repeatable for every subject and allow obtaining a "quasi-structured" points cloud, useful to reconstruct a model of the surface of the limb in an easy manner.

Electronics, Information and Bioengineering of Politecnico di Milano, Milan – Italy) shown in Figure 3.4.

To validate the acquisition procedure, 2 healthy volunteers have been acquired; then, for one of them we validated the entire procedure, building from the reconstructed geometry an *ad hoc* set of shells that fit perfectly on the subject's limb (Figure 3.5). Based on this pre-assessment we decided to apply this method to construct fully customised dynamic wearable devices for the 5 paediatric patients (age range: 11.8 ± 5.1 years old) that took part in the clinical study (see Chapter 5).

Figure 3.4 Set-up for the limb surface acquisition. The optoelectronic system uses 8 infrared cameras. During the acquisition, the subject is free to move inside the FOV. By holding the subject's finger, the researcher gently controls any exceptional involuntary movements, favouring the optimal posture (close to a neutral arm habit), maximising marker visibility.

Figure 3.5 The figure *on the left* displays a personalised set of shells built for a healthy subject to validate the entire acquisition plus CAD-aided limb modelling procedure; the prototype fits perfectly on the subject's limb even without the necessity to add padding inside the valves, as shown *on the right*. The padding is employed to increase the comfort softening the interface between the soft skin and the rigid valve and to add secure pinching grip.

3.2.3 Surface reconstruction and virtual construction of the devices

The file collected through the BTS System is tracked using the SMART Tracker software (SMART Motion Capture System – BTS Bioengineering) to find the instant with the highest number of visible markers, corresponding to a close-to-the-desired posture (for further explanation about tracking procedure, see Chapter 4) and then processed with a *home-written* MatLab subroutine (MATLAB – MathWorks) to import the dataset into Rhinoceros (Rhinoceros – McNeel North America), where the model of the limb is built from the point cloud.

In particular, each ring is reconstructed by interpolating with a 3rd-order spline the points which belong to the same circle of markers. All the rings in the forearm and the arm become the basis for two corresponding lofted, third order NURBS surfaces, for the arm and the forearm, connected at the level of the elbow circle (Figure 3.6).

The virtual model of the arm is converted into stereolithographic *.stl* format that can be employed by a CNC machine (Computer Numeric Control machine) to create the positive model of the limb. The same

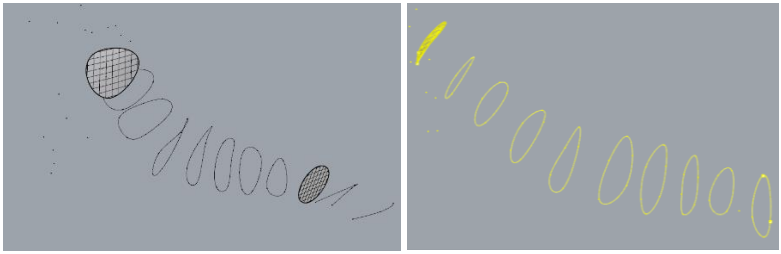

Figure 3.6 The figure shows the first step in the process to create the virtual arm model from the point cloud collected with the optoelectronic system. From the point cloud, each ring, that defines the contour of the limb, is reconstructed by interpolating with a 3rd-order spline the points that belong to the same circle of markers, or limb slice.

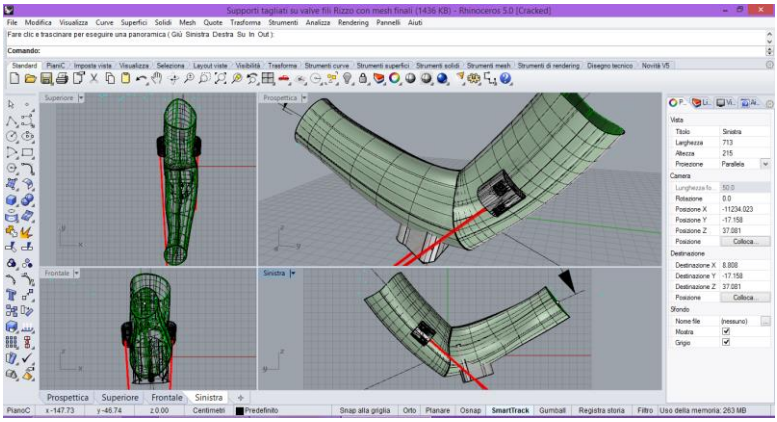

Figure 3.7 The screenshot shows how the virtual model of the limb, obtained from the point cloud, becomes the basis to design virtually the shells of the device (*light green*) and the fixtures (*grey*) which hold the functional metallic elements of the orthoses (*red*). The figure shows the alignment of the NiTi wires with the elbow centre of rotation: the personalisation of the fixtures requires that they have holes to hold the wires in this exact alignment, and thus the CAD drawing and the 3D printing will create them.

geometry is used to design virtually the valves of the device and the fixtures for the functional metallic elements of the orthoses (see Chapter 2). These fixtures are designed onto the surfaces of the valves and adapted to match perfectly the anatomical surface of each subject. They are cut and oriented on the valves to ensure a perfect alignment of the NiTi metallic wires with respect to the centre of rotation of the elbow joint (Figure 3.7).

3.2.4 Physical construction and assembling of the devices

The virtual model of the different parts, the valves, the fixtures and the NiTi wires were constructed by means of different technologies and tools. In particular, the fixtures were built in *ABS+* (i.e. poly(acrylonitrile-butadiene-styrene), proprietary formulation) with a 3D printer (3D Elite

Figure 3.8 The CNC machine in action: a 7-axis mill shapes the polyurethane foam block to obtain the positive limb model based on the virtual reconstruction from the point cloud converted into stereolithographic *.stl* format.

Dimension, Stratasys), which took as input the virtual model designed in Rhinoceros. The NiTi wires were shape set as explained in Chapter 2. Fixtures and functional elements were constructed in the laboratory of CNR-ICMATE (National Research Council of Italy, Institute of the Condensed Matter Chemistry and Technologies for the Energy, located in Lecco – Italy). Finally, the physical model of the arm was obtained with a 7-axis mill from a polyurethane (density 120 kg/m^3) foam block (Figure 3.8); this model is used as a positive mould to form under vacuum a sheet of polypropylene pre-heated at 180°C; the shells were refined and padded following the shapes defined for the specific subject requirement. This part of the construction, together with the entire assembling procedure was done in the factory of the orthopaedic centre COE (Centro Ortopedico Emiliano located in Reggio Emilia – Italy).

3.3 Results

The concept design of the new device was suitable to respond to all the varied personalisation requirements posed by different patients.

Optoelectronic kinematic analysis proved a valid tool to assess movement impairment and suggest a personalised approach to functional control of the upper limb.

The procedure to replicate formal anatomy into the orthosis shells required some trials, to understand the limits of the system in terms of discretisation and resolution; a final set-up was defined including 105 reflective markers as shown in Figure 3.9. For all the subjects of the study, we collected data coming from the optoelectronic system, like the ones in Figure 3.10; the point clouds in the FOV were imported into Rhinoceros through a *home-written* MatLab script for further processing. The points that belonged to the same "slice" of the limb were interpolated using a B-spline (Figure 3.11 *left*) and the surface of the arm was then reconstructed with a *loft* of the curves (Figure 3.11 *right*).

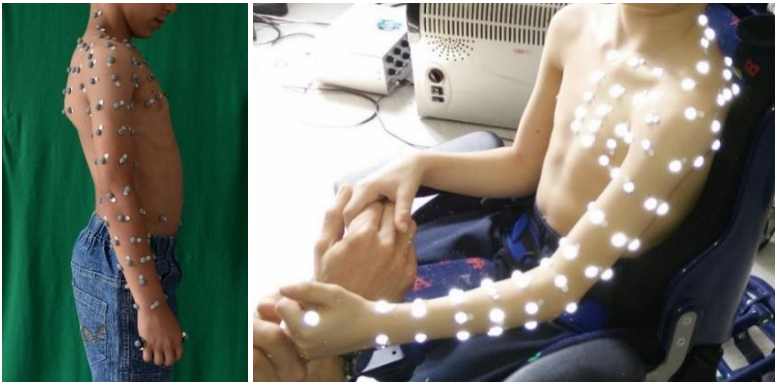

Figure 3.9 The figure shows markers positioned on the skin. The 105 reflective passive markers are positioned with a repeatable and defined scheme to obtain a structured points cloud, easier to replicate for every subject. *On the left* is depicted a healthy subject standing in the FOV; the acquisition of markers takes only a few seconds. *On the right* is shown the same marker placement for a dyskinetic subject. In this case, during the acquisition, even if the patient is left free to move in the FOV, the operator helps him stabilise posture to achieve the best arm positioning, by gently holding his fingers.

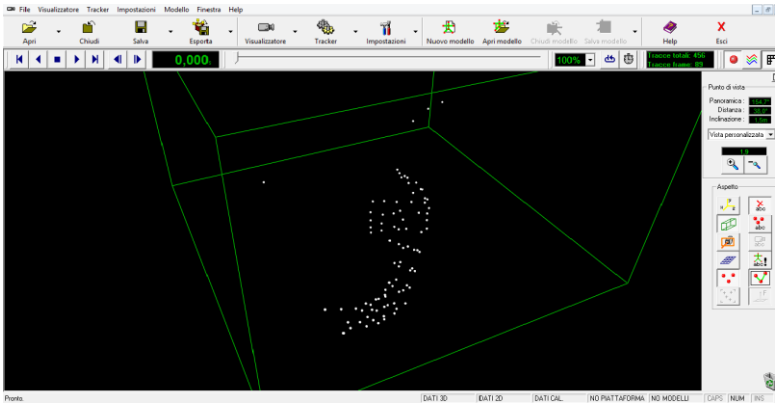

Figure 3.10 The figure shows how, using the software SMART Tracker, the reflective markers, placed on the limb surface and acquired by the optoelectronic system, can be visualised in the virtual FOV. The software allows scrolling through the few seconds' acquisition to select the frame with the best limb posture and maximum number of markers in view (collected).

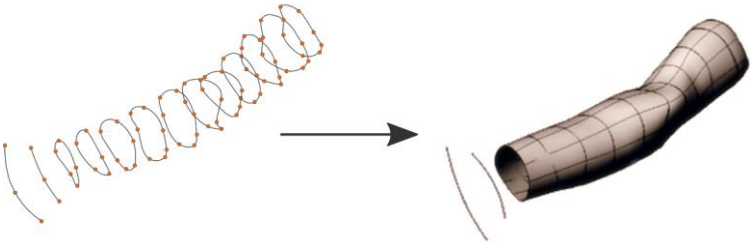

Figure 3.11 *On the left,* the figure depicts the "rings" that define the contour of the limb, reconstructed by interpolating with a 3rd order spline the points cloud acquired with optoelectronic system. *On the right*, all the rings in the forearm and the upper-arm become the basis for two lofted NURBS surfaces, to create the virtual model of the arm.

The virtual models of the upper limb (Figure 3.12) were the input files for the 7-axis mill that created corresponding polyurethane copies like the one shown in Figure 3.13 left. The shells were refined on each model

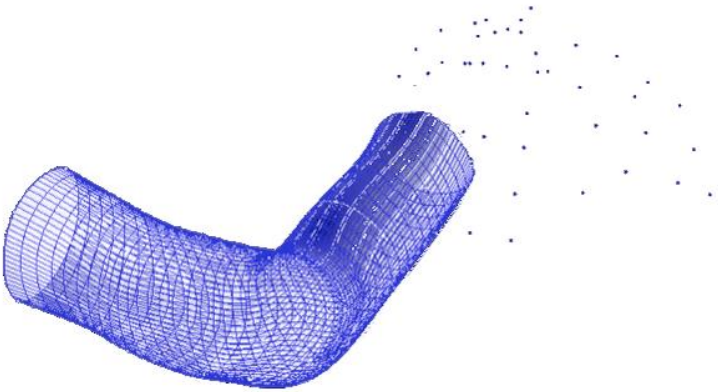

Figure 3.12 In the figure shows the virtual model of the arm, reconstructed from the point cloud and ready to be processed by the CNC machine. The two lofted surfaces of the arm and the forearm are merged in one and a mesh of the entire surface is created.

Figure 3.13 The figure displays, *on the left*, the physical model of the arm shaped by the CNC machine (7-axis mill) from a polyurethane foam. *On the right,* the polypropylene shells formed under vacuum using the model as a positive mould and cut following the biomechanical design.

in a customised way, depending on the specific individual requirements (Figure 3.13 right).

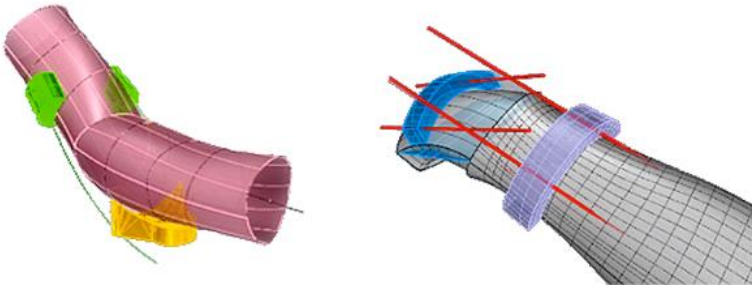

Figure 3.14 Images of the virtual design process of the fixtures. The shapes (of the valves and fixtures) and the alignments (of the wires and the fixtures) are modified in a patient-specific manner to finalise the device personalisation according to the surface of the virtual model of the arm and in order, to fulfil the biomechanical design prescriptions.

Some of the results of virtual design of the fixtures are reported in Figure 3.14. By means of 3D printing, the fixtures have been built in *ABS+* (Figure 3.15). They fitted perfectly to the surface of the valves and they could always be fixed easily in the position planned during the virtual design step, without the necessity of any further modification.

The NiTi wires have been shape-set as illustrated in Chapter 2. The entire assembling of the parts of the orthoses brought to the results illustrated in Figure 3.16 and Figure 3.17 that display some examples of the final devices personalised and worn by the patients who took part in the experimentation. Five dynamic orthoses, built following these criteria, have been prescribed to an equal number of paediatric patients affected by severe motor impairments due to Movement Disorders: in particular, 2 were mainly dystonic, 2 mainly dyskinetic and one with a more complicated clinical picture including dyskinesia, dystonia, spasticity and ballism. All of them were asked to use the device for at least 4 hours a day and none of them reported discomfort using the device up to 8 hours per day for the entire rehabilitation period (1 month or more: for further details about the experimental protocol, Chapter 5).

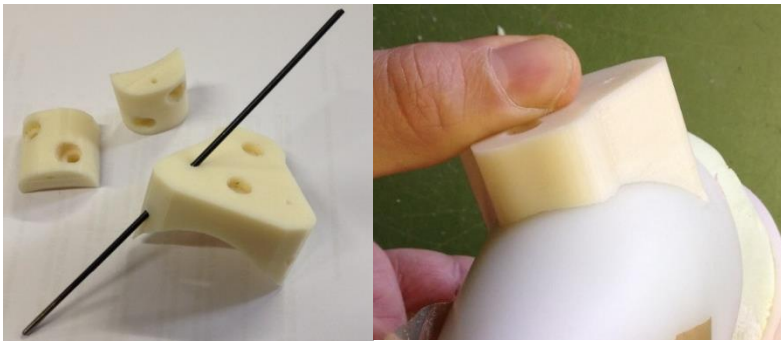

Figure 3.15 The fixtures printed in *ABS+* by means of a rapid prototyping 3D printer. *On the left* it can be observed how the fixtures are designed with all the personalised features required; consequently, once they are printed they are already provided with the shafts to hold the functional metallic wires and the holes for the fixing rivets, to connect firmly the fixtures to the shells. *On the right,* it is worth noting how the as-printed fixtures fit perfectly to the valve without the necessity for any further modification.

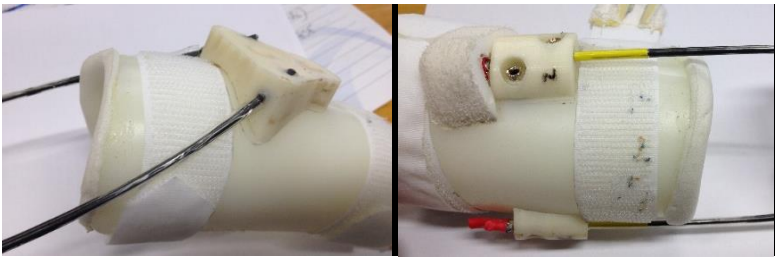

Figure 3.16 Figure shows the connection between the functional parts – NiTi wires, fixtures and valves. It is noteworthy how the fixtures fit perfectly to the shells and the NiTi wires run along them remaining adherent, without interference. The functional elements are locked in the fixtures; the proximal fixtures were sometimes padded, to prevent any possible discomfort, especially when the patients tended to maintain a very adducted habit of the shoulder.

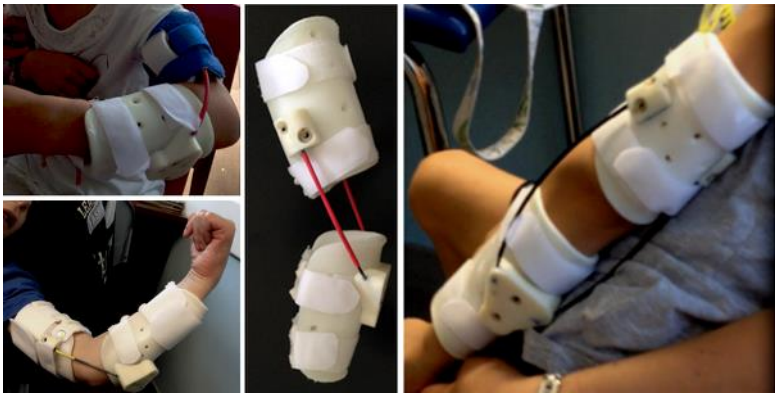

Figure 3.17 Some examples of the devices personalised, constructed and assembled *ad hoc* for 4 patients who took part in the study. It can be noticed how devices impart their corrective action, starting from different initial positions, related to the clinical characteristics and the specific needs of the subject; the orthoses are light and wearable even with clothes on, increasing the comfort perceived and, consequently, their usability.

3.4 Discussion

With the method presented in this study, it was possible to design and construct a type of dynamic wearable orthosis for the upper limb suitable for patients affected by dyskinesia and/or dystonia. The specific impairment of those patients requires that the valves and the fixtures should be designed, according to the functional criteria to obtain the placements of the wires along the desired direction to impart the corrective forces within the selected intensity range and along the chosen degrees-of-freedom. The alignment with the joint rotation centre is fundamental to avoid movement of the valves relative to the limb, which might generate friction and discomfort as well as a malfunctioning.

Precise planning supported every step of the building process that led to the manufacturing criteria for the development of a wearable, light, comfortable dynamic orthosis to support the rehabilitation of patients affected by dystonia and dyskinesia. The method *per se* is hard to validate in a quantitative manner, because a "real gold standard" does not exist. In fact, given a theoretically perfect reproduction of the limb, several other reconstructions a little different from that would be equally good, because during movements and changes of posture, muscles change size and position and therefore the size-constraints on the shells are relatively loose; furthermore the presence of variable padding, which is soft and compliant, can absorb some of the muscular size variations in the millimetres range. We have to interface a particular structure, the body, which is soft, compliant and changeable, with something more rigid, the valves; in this respect, it is not very useful to try and provide a strictly quantitative estimate of the residual size differences between the shells and the limb, because that will never be a constant in real life.

The procedure we adopted allows creating a fully customised device without forcing the subject into a fixed position for a long time; the process requires few seconds of acquisition after completing the positioning of markers on the surface of the limb in a completely harmless way. The acquisition technique does not imply any constriction of the patient in a prescribed position. The entire process of virtual design does not need the presence of the patient: the orthosis is designed, constructed and assembled without the necessity to have the patient available and this brings to a positive effect in the management of patients with these kinds of diseases. All of these patients experienced in the past orthotic treatments without improvements and often with discomfort and pain; the fact that they are young, set a constraint for the device, which should be really light and comfortable to allow residual voluntary motion and to preserve the interaction with their

environment, including playing, schooling and supporting activities of daily living. All of these features seem to be achieved by the devices constructed with the procedure presented here. In fact, the comments coming from the patients enrolled in the clinical trials (see Chapter 5) were positive and showed how the device supported their rehabilitation. All the patients have exceeded the minimal prescription of 4 hours per day, wearing the orthosis up to 8 hours per day; the parents and physiotherapists of four of them reported that they used the device also for some specific daily activities, such as playing games, feeding, writing, drawing and training sessions with the physiotherapists. None of the patients reported pain or specific discomfort, even though the rehabilitation period fell during the summer months; only two of them reported sweating problems after some hours of use in the heat of August. In addition, the donning and doffing practice has not been a problem, to either parents or physiotherapists or the patients themselves.

Some further technical improvements to the method could still be achieved; in fact, the employment of other kinds of materials such as different polymeric materials, could help towards a further integration between shells and fixtures, preventing fatigue failures at the interfaces and speeding up the assembling time. By exploiting the functionalities of advanced 3D printers, the whole valves could also be constructed by means of rapid prototyping (cf. Pittaccio et al. 2015), diminishing the construction and the assembling steps, and possibly decreasing overall costs. In order to achieve this, some manual procedures could be made partially automatic, e.g. using parameterisation of the CAD-aided steps.

3.5 Conclusions

The method presented in this section, shows how, by exploiting the functionalities of an optoelectronic system, generally used for motion

analysis and quite accessible to many clinical centres, it is possible to design and construct, even for patients affected by severe and complex neuromuscular problems including dyskinesia and dystonia, a dynamic wearable orthosis for the upper limb that is completely customised. The biomechanically and functionally inspired conceptual design allows for broad personalisation schemes. The precise limb surface reconstruction allows an accurate anatomical personalisation of the shells, increasing the comfort perceived by the patients and the usability, and the fine positioning of the fixtures as well as the functional NiTi elements, which are thus set in the best conditions to impart their corrective force. The procedure speeds up the entire process of device construction for the patient, because simplifying the operations of surface acquisition and virtual design, as well as the physical construction and assembling, greatly improved the management of the patients and their occupation in terms of fatigue, discomfort and use of their time. Future prospects could be aimed at the further automation of the entire production chain, also by combining the use of other biocompatible and functional materials such as different polymeric materials and composites.

3.6 References

Autti-Rämö, I., Suoranta, J., Anttila, H., Malmivaara, A., & Mäkelä, M. (2006). Effectiveness of upper and lower limb casting and orthoses in children with cerebral palsy: an overview of review articles. *American journal of physical medicine & rehabilitation*, *85*(1), 89-103.

Boyd, R. N., Morris, M. E., & Graham, H. K. (2001). Management of upper limb dysfunction in children with cerebral palsy: a systematic review. *European Journal of Neurology*, *8*(s5), 150-166.

Burtner, P. A., Poole, J. L., Torres, T., Medora, A. M., Abeyta, R., Keene, J., & Qualls, C. (2008). Effect of wrist hand splints on grip, pinch, manual dexterity,

and muscle activation in children with spastic hemiplegia: a preliminary study. *Journal of hand Therapy*, *21*(1), 36-43.

Cappozzo, A., Della Croce, U., Leardini, A., & Chiari, L. (2005). Human movement analysis using stereophotogrammetry: Part 1: theoretical background. *Gait & posture*, *21*(2), 186-196.

Coghill, J. E., & Simkiss, D. E. (2010). Do lycra garments improve function and movement in children with cerebral palsy?. *Archives of disease in childhood*, *95*(5), 393-395.

Colombo, G., Bertetti, M., Bonacini, D., & Magrassi, G. (2006, February). Reverse engineering and rapid prototyping techniques to innovate prosthesis socket design. In *Electronic Imaging 2006* (pp. 60560P-60560P). International Society for Optics and Photonics.

Colombo, G., Facoetti, G., Rizzi, C., Vitali, A., & Zanello, A. (2013, July). Automatic 3D reconstruction of transfemoral residual limb from MRI images. In *International Conference on Digital Human Modeling and Applications in Health, Safety, Ergonomics and Risk Management* (pp. 324-332). Springer Berlin Heidelberg.

Fish, D. J., Crussemeyer, J. A., & Kosta, C. S. (2001). Lower extremity orthoses and applications for rehabilitation populations. *Foot and ankle clinics*, *6*(2), 341-369.

Hohe, J., Ateshian, G., Reiser, M., Englmeier, K. H., & Eckstein, F. (2002). Surface size, curvature analysis, and assessment of knee joint incongruity with MRI in vivo. *Magnetic Resonance in Medicine*, *47*(3), 554-561.

MacDonald, K., Chinchalkar, S. J., & Pipicelli, J. (2016). Forearm Positioning and Its Functional Implications. *Journal of Hand Therapy*, *29*(3), 376.

Mavroidis, C., Ranky, R. G., Sivak, M. L., Patritti, B. L., DiPisa, J., Caddle, A., ... & Drillio, R. (2011). Patient specific ankle-foot orthoses using rapid prototyping. *Journal of neuroengineering and rehabilitation*, *8*(1), 1.Medved V. *Measurement of human locomotion.* Boca Raton: CRC Press; 2001.

Morris, C., Bowers, R., Ross, K., Stevens, P., & Phillips, D. (2011). Orthotic management of cerebral palsy: recommendations from a consensus conference. *NeuroRehabilitation*, *28*(1), 37-46.

Nicholson, J. H., Morton, R. E., Attfield, S., & Rennie, D. (2001). Assessment of upper-limb function and movement in children with cerebral palsy wearing lycra garments. *Developmental Medicine & Child Neurology*, *43*(6), 384-391.

Pittaccio, S., Garavaglia, L., Ceriotti, C., & Passaretti, F. (2015). Applications of Shape Memory Alloys for Neurology and Neuromuscular Rehabilitation. *Journal of functional biomaterials*, 6(2), 328-344.

Pittaccio, S., Garavaglia, L., Viscuso, S., Beretta, E., & Strazzer, S. (2013). Implementation, testing and pilot clinical evaluation of superelastic splints that decrease joint stiffness. *Annals of biomedical engineering*, *41*(9), 2003-2017.

Pizzi, A., Carlucci, G., Falsini, C., Verdesca, S., & Grippo, A. (2005). Application of a volar static splint in poststroke spasticity of the upper limb. *Archives of physical medicine and rehabilitation*, *86*(9), 1855-1859.

Fabio, R. (2003). From point cloud to surface: the modeling and visualization problem. *International Archives of Photogrammetry, Remote Sensing and Spatial Information Sciences*, *34*(5), W10.

Koy, A., Lin, J. P., Sanger, T. D., Marks, W. A., Mink, J. W., & Timmermann, L. (2016). Advances in management of movement disorders in children. *The Lancet Neurology*, *15*(7), 719-735.

Kumar, D. S., Gautham, G., Sadiq, M., Das, B. N., & Krishna, K. J. (2015). Characteristics of Foot Dimensions of Children with Cerebral Palsy and Standardizing Orthosis Size-Through an Anthropometric Pilot Study. *Anthropologist*, *20*(3), 727-734.

Jaspers, E., Desloovere, K., Bruyninckx, H., Klingels, K., Molenaers, G., Aertbeliën, E., ... & Feys, H. (2011). Three-dimensional upper limb movement characteristics in children with hemiplegic cerebral palsy and typically developing children. *Research in developmental disabilities*, *32*(6), 2283-2294.

Chapter 4

Acquisition and analysis of upper-limb kinematic data in paediatric dyskinesia

The chapter presents a specialised method to collect kinematic data from neurological patients affected by Childhood Dyskinesia. It describes the acquisition protocol, a home-written MatLab code to extract relevant kinematic parameters, and the process to evaluate patient's status or the results of a rehabilitation treatment.
Normality data from healthy young volunteers will be presented.

4.1 Introduction

4.1.1 General concepts

The study and the understanding of human motion have been the research focus of many scholars for centuries, who employed different approaches to describe and explain the fundamentals and the rules, by which human (and animal) "actions" are initiated and different movements are executed (Cheze 2014; Winter 2009). Kinematics, which is the quantitative description of movement, is that part of human motion understanding that does not look into the causes or controlling factors, but purely addresses the evolution of positions in space (Winter 2009). The first experiments of systematic human motion description, which were experimented as of 1885 (Marey 1885; Muybridge 1901), opened the path for a better quantitative understanding of movement. Since that time till present, many improvements have been done, leading to the current cutting-edge commercial digital technologies. The quantitative description of human movement, in general, requires a specific instrumentation, capable to acquire and measure the motion in an affordable and repeatable manner (Cheze 2014; Chiari et al. 2005; Della Croce et al. 2005; Leardini et al. 2005).

In the past few years, many new devices and tools have been developed and used to accomplish this target (Cheze 2014), so nowadays very high standards in terms of quality and quantity of signal are available. Amongst the best, in terms of balancing cost, efficacy, usability (readiness, easiness) there are the optoelectronic systems, especially the ones based on the stereophotogrammetric principles (Capozzo et al. 2005). The improvements in this technology have fostered the study of human movement in increasingly complex and accurate ways. In particular, the analysis of gestures in sports (Bartlett 2007), and new movements, whose description was precluded in the

past, have gained now a stronger interest, and especially the ones related to pathological conditions (e.g Perry 1992). Expanding the field of application to the clinics, new perspectives have become available in the study and comprehension of motor disorders, and consequently their evaluation and treatment. The first diseases, that took advantage of the modern motion analysis techniques, were the ones related to walking. Stereophotogrammetry applied to walking, i.e. the gait analysis, has been the first type of kinematic analysis to generate a measurable improvement in the management patients (Perry 1992, Whittle 2007; McGinley et al. 2009).

Less was done so far in the field of upper-limb motion (Freivalds 2011), where most results were obtained over the last two decades. Some authors, for instance, tried to study and understand rather specific motor tasks in sports actions (Payton et al. 2007; Bartlett 2007), and address some inherent problems such as the fact that upper-limb motion is non-cyclical, has a huge range of motion (ROM) and the protocols to evaluate motion are hard to standardise. All these aspects, in fact, stand as obstacles in computing kinematic parameters. The numerical evaluation of upper-limb motion in patients has not been a very popular subject of study, because, in addition to the above-mentioned problems, the unpredictable movements and the symptoms caused by neuromuscular pathologies clearly complicate the researchers' job. In particular, (i) the lack of a cyclical movement task akin to gait; (ii) the characterisation of the large range of motion at the shoulder ; (iii) the complexities of defining the shoulder joint centre using external markers; (iv) time normalisation and the subsequent ensemble averaging of non-cyclic data. Singularly and in combination these difficulties have hampered attempts to model, measure and interpret upper limb kinematics. (Reid 2010; Jasper 2009).

A reference paper for upper limb kinematics in developmental age has been provided by Petuskey et al. (Petuskey et al. 2007).

4.1.2 Movement analysis and Movement Disorders

The current treatments for neurologic disorders affecting movement (Movement Disorders in particular) are of different types (pharmacological, surgical, physical and orthotic), every one bringing along relative advantages and drawbacks (cf. Chapter 1 for an extensive discussion). The effects of those approaches are sometimes difficult to evaluate, due to the lack of quantitative measurements that can prove their efficacy. Their endorsement is left to personal observations (e.g. by clinicians and medical doctors), often with inter- and intra-operator variations. In the absence of a reliable quantitative description of movements through tracings and indices, severity and possible improvements in motor function can only be judged by means of clinical scales that, albeit validated, are often affected by subjective factors. Patient evaluation is also difficult because the overall improvements often arise as the sum of mild segment-specific variations, which the clinical scales are not always able to score (Butler 2010; Jasper 2009; Coluccini 2007; Mackey 2005). The assessment of changes in movement capability could take advantage of bioengineering methods that provide quantification of the effects. In this context, kinematic analysis could be of help in gaining more affordable information about, not only the treatments applied, but also the disease itself.

Especially, considering dyskinetic and dystonic patients, whose motor execution – even in standardised tasks – is extraordinarily changing, complex and unpredictable (cf. Chapter 1), it often occurs that their improvements stand out best in relation to informal activities in their daily environment, while evidence of changes at pre-defined time points and in clinical settings often turns out to be scant, when collected by clinical scales alone. For those cases in particular, the availability of additional quantitative measurements, provided by a suitable kinematic evaluation, could improve the possibilities to

highlight even moderate changes in their motor patterns and in particular disentangle the role of the single specific segments that produce the overall effect.

4.1.3 Movement analysis methods for Childhood Dyskinesia

Although normal child development is the basis on which the abnormal development is appreciated, it does not follow that assessment and treatment should rely upon a strict adherence to normal developmental schedules. Even 'normal' children show many variations from the 'normal' developmental sequences and patterns of development which have been derived from the average child. Cultural differences exist for normal motor development (Hopkins & Westra 1989). However, in any culture, the child with cerebral palsy will show additional variations due to neurological and mechanical difficulties. When managing children with movement disorders, the first step is to identify movement patterns that are abnormal for the age of the child—some movement disorders are benign or physiological during certain stages of development—and classify their phenomenology. (Koy et al. 2016). From a clinical perspective, combining spatiotemporal and kinematic parameters may facilitate the identification of the pathological movement patterns seen in children with Childhood Dyskinesia and thereby add to a well-targeted upper limb treatment planning (Jasper et al. 2011).

Such objective has been applied to the assessment of upper-limb movement patterns, compared to clinical evaluations, especially with the purpose to support the treatment planning for children with hemiplegic cerebral palsy (Butler et al. 2010, Jasper et al. 2011). Indeed, amongst the studies that used 3D kinematic analysis protocols for the upper limb in cerebral palsy, most address spasticity and hemiplegia (Butler et al. 2010 and references therein); only few (Butler

et al. 2010; Butler et al. 2012) dealt with hyperkinetic clinical pictures (which clearly are more complex, kinematically).

The clinical application of an upper-limb 3D measurements requires the establishment of a biomechanical model and a set of relevant tasks (Kontaxis et al. 2009). Although several biomechanical models have been proposed, they vastly vary in complexity, number of segments, joint degrees of freedom and marker configurations (Schmidt et al. 1999; Rab et al. 2002; Carpinella et al. 2006; Williams et al. 2006). While there are recommendations available, such as the International Society of Biomechanics (ISB) ones on the definition of joint coordinate systems and rotation sequences, to standardise the reports of upper-limb kinematics (Wu et al. 2005), most studies on upper-limb kinematics in developing children (Coluccini et al. 2007; Petuskey et al. 2007) and children with hemiplegic cerebral palsy (Jasper et al. 2009) have not yet incorporated these guidelines.

Very few studies have assessed the reliability of upper-limb kinematics in developing children (Butler et al. 2010; Reid et al. 2010). While both these cited studies reported a good within and between session reliability, only Butler et al. (Butler et al. 2010) provided an estimation of the measurement error in terms of angle deviation from the target (for healthy children): mean intra-session errors ranged from 0.6° to 3.4°, and mean inter-session errors ranged from 1.6° to 4.8°. In addition, Mackey et al. reported moderate levels of inter-sessional repeatability (mean CMCs shoulder 0.49 to 0.63; elbow 0.63 to 0.74 – CMC: coefficient of multiple correlation) for patients with hemiplegic cerebral palsy (Mackey et al. 2005).

There is no common consensus on which tasks should be assessed to collect the most informative data from the patients (Jasper et al. 2009). In discussing their protocol, Reid (Reid et al. 2010) noticed that good within-day and day-to-day repeatability of upper limb 3D kinematic

measurements is achievable on clinical population with suitable standardisation of the tasks and by choosing tasks such as front reach, side reach, pronation- supination and hand-to-mouth, that require sufficient range of motion. Also Butler reported good repeatability in Reach&Grasp Cycles (Butler et al. 2010). Due to the variety in upper-limb functions, it is crucial to design a comprehensive movement protocol containing a set of clinically relevant tasks.

For this thesis we devised a procedure including an *ad-hoc* biomechanical model largely based on ISB recommendations, specially conceived for the assessment of dystonic and dyskinetic children, i.e. utilising specific motor tasks, able to display their motor skills., We selected, in accordance with medical doctors, a number of simple motor tasks taken from the Melbourne Assessment Scale, which are in our opinion, varied enough to explore a good range of upper-limb motor capabilities.

The protocol and method described here can be used to assess changes in patients' status over a period of rehabilitation done with the support of a wearable dynamic device, as the one described in Chapter 3. The present Chapter first shows the characteristics of a specialised set-up to collect upper-limb kinematic data by means of an optoelectronic system in healthy subjects. It then introduces the modifications necessary to encompass the assessment of dystonia and dyskinesia, as well as the general features of the *home-written* MatLab code used to define the pool of Eulerian coordinate systems and degrees of freedom, by which kinematic data are extracted and consequently the results can be expressed and analysed.

4.1.4 The movement of children with dyskinesia: prior results

A number of interesting results have been very recently reviewed by Bertucco et al., whose paper (Bertucco et al. 2015) we quote as is

(references to be found in the original work, most interesting topics highlighted and most useful statements underlined):

***Kinematic (spatial-temporal) measures are used for upper extremities to quantify the features and severity of dystonia**. One study compared children with dyskinetic CP (all affected by dystonia) to children in a control group in terms of arm trajectory (hand path) during a finger-to-nose reaching task. Children with dystonia were found to have increased variability and lacked a straight-line trajectory (hand path) compared to children in the control group. In another study, children with dystonia demonstrated decreased speed and greater variability during an upper extremity reaching task. An examination of temporal-spatial parameters during a reach-and-grasp cycle in children with hemiplegic CP, compared to children in a control group, supported that children with dyskinetic CP have slower arm movements. Results from these studies are consistent with the hypotheses that children with dystonia have an inability to remove unwanted components of movement, resulting in reduced velocity to compensate greater spatial variability and muscle overflow. Another study demonstrated that **spasticity and dystonia in children with CP could be differentiated using kinematic measures**. Children with dystonia displayed lower velocities, curved hand paths during reaching, whereas children with spasticity tended to demonstrate higher peak velocities during reaches with less curved paths. Children with dystonia displayed greater overflow in the non-moving arm during active movement of the contralateral arm/hand. Measurements taken in this study were highly correlated with the clinical measures on the BAD and Modified Ashworth scale (a clinical scale to quantify the severity of spasticity). **Target size during reaching also influences the speed of movement for children with dystonia**. In studies of reach-to-targets of various sizes and distances, children with dystonia scaled movement speed with the target size, but moved slower than children in the control group for targets of identical size. These results support that children with*

dystonia require larger targets to achieve speed comparable to controls, suggesting that they compensate for the underlying motor variability by reducing speed. Functional implications of the speed-accuracy trade-off for human movements have been demonstrated to be particularly useful for the design of touch-screen communication devices used by children with CP. Moreover, the sensory-motor ability to trade-off between speed and accuracy in a pointing task using the upper extremities provides evidence for the usefulness and validity of speed-accuracy quantification as a diagnostic tool for dystonia in children.

Similar observations are also present in different experimental papers cited in this chapter (Gordon et al. 2006; Sanger 2006; Butler et al. 2010; Jasper et al. 2011).

4.2 Subjects & Methods

4.2.1 General approach and Methods overview

Although motion analysis and consequently all the topics related (from the marker placement to the reconstruction and analysis of data) are well known in general and many papers and books provide deep insights in the topic (Hall 2012; Capozzo et al. 2005), the specific study of the upper-limb motion, especially when Movement Disorders are concerned, is still worth a separate discussion. Our general approach to study upper-limb kinematics in Childhood Dyskinesia is reported in the flowchart of figure 4.1 and will be explained more in detail in the following sections.

In order to understand the upper limb motion in neuropathological patients, in particular during specific motion tasks and even wearing a dynamic device, it is of help first to study the motor abilities of healthy subjects, extract their kinematic parameters and derive a description of normal gestures during the tasks (*normality*). In this way, when dealing

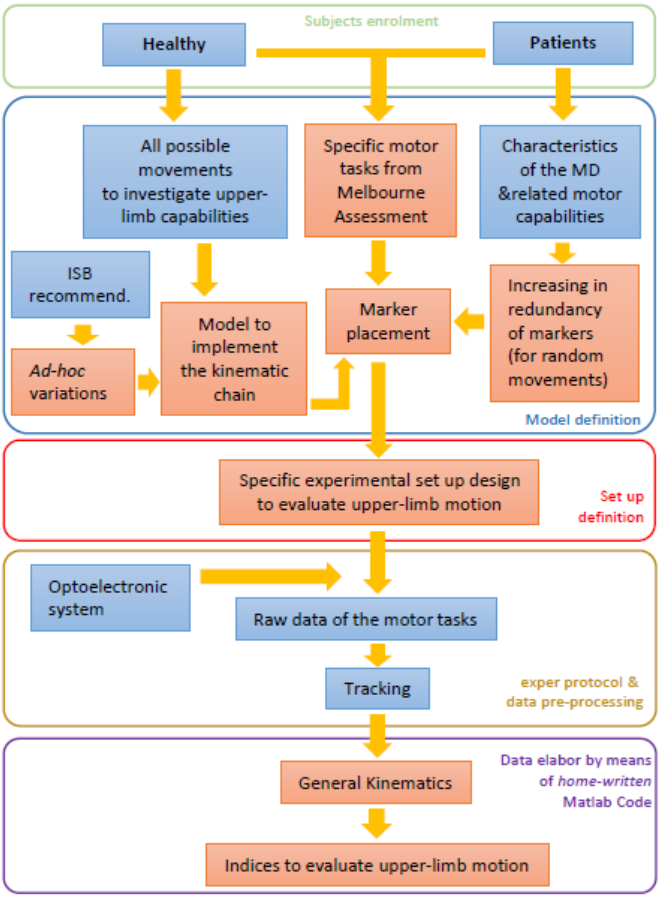

Figure 4.1 The flowchart shows the sequence of operations that we used to approach the kinematics evaluation of the upper limb. The methods employed in this study run from *top* to *bottom*; *in blue* are reported the operations in common use in movement analysis, *in red* are marked the steps, in which we mostly contributed with innovative methods.

with the neurological patients, we shall have a baseline available, against which pathological and presumably, distorted motion can be gauged (cf. sections 4.3.2, 4.3.3, 4.4.2, and 4.4.3).

In this study, we considered the human body and in particular, the upper limb as a kinematic chain composed by articulated rigid bodies. The mechanics of rigid bodies and its rules are a well-known topic, often also applied to human motion. We assumed that the thorax, arm, forearm and hand were rigid bodies articulated by the shoulder, elbow and wrist respectively, and we placed the markers on the skin in relation to precise reference points in the joints.

It is evident that a well-thought-out marker disposition is essential, not only to ensure marker visibility and for tracking reconstruction, but also to ease data analysis and the extraction of kinematics parameters and quantities. With the marker set-up, reported in section 4.2.4, it was possible for us to capture the motion of all the recruited subjects in a quite complete manner, collecting at the same time linear displacements and angular quantities.

Our kinematic analysis plans to solve the equations that link the degrees of freedom and rule the articulated system of rigid bodies (kinematics chain) by which we mimic the upper limb; the joints represent links between the limb segments, that block or restrict some of their degrees of freedom.

To write the equations for this problem, we associated an orthonormal coordinate system to each rigid body segment (Capozzo et al. 2005), mostly following International Society of Biomechanics (ISB) recommendations (Wu et al. 2005) as shown in section 4.2.3. The motion of each segment coordinate system was expressed relative to a reference coordinate system, considered to be fixed, which, in our case, corresponds to the table where the subject is seated. Section 4.2.3 will also describe how all the necessary coordinate systems for each segment were defined from the specific markers disposition presented in this chapter using *a home-written* MatLab script.

The subroutine also implements a method for data loss reduction (cf. section 4.2.6) exploiting the redundancy of the markers used on every segment. Another subroutine, described in section 4.2.5, computes a whole set of derived kinematic parameters able to describe the motion of the subjects enrolled in the study (cf. sections 4.2.7, 4.3, 4.4 and Chapter 5).

4.2.2 Subjects and experimental protocol

For the present study, we primarily enrolled 6 healthy boys (age 12.6 ± 4.9 years old). All subjects (or their parents) signed an informed consent after being informed on the aims and procedures of the experiments. Neurologic Institute "Carlo Besta" Ethics Committee (Milan, Italy) granted ethical approval for this research program. Participants underwent 3D upper limb kinematic analysis. During the optoelectronic stereophotogrammetry session, we asked the subjects to execute four standardised motor tasks:

i. pointing forward to a target;
ii. mimicking self-feeding;
iii. mimicking placing a pen into a box;
iv. mimicking placing a pen into a cup.

These exercises, taken together, were deemed appropriate to recruit different muscles that move the upper limb in a comprehensive and articulate enough manner to assess upper limb kinematics (and indirectly movement control). The exercises were also well suited to be performed by neuromuscular patients: in fact, they are part of the experimental set of motor tasks included in the Melbourne Assessment of Unilateral Upper Limb Function (*Melbourne Assessment* – see Chapter 5 for details). It was deliberately decided to exclude the grasping or releasing of objects, because those elements could be serious obstacles for the patients in initiating or terminating the limb motion tasks (Butler et al. 2010).

Figure 4.2 The photo shows the laboratory where the acquisitions were carried out. In particular, the BTS SMART-Elite System with 8 infrared cameras that has been used to acquire the motion of the upper limb, the table and the adjustable-in-height chair at the LARES laboratory (Laboratory of Analysis of the Breath located in the Department of Electronics, Information and Bioengineering of the Politecnico di Milano, Milan – Italy).

The experimental protocol included that the subjects repeat each exercise 5 times at a self-selected speed. The subjects were seated upright at a table in an adjustable-in-height chair (Figure 4.2).
The subjects were free to move in the calibrated FOV of the optoelectronic system and no constraints are set on the limb, so the subjects could execute freely the prescribed motor tasks. The acquisitions were carried out at the LARES laboratory (Laboratory of Respiration located in the Department of Electronics, Information and Bioengineering of the Politecnico di Milano, Milan – Italy) shown in Figure 4.5.

In addition to the healthy subjects, 5 patients of similar age range were recruited to test the protocol and refine the marker set-up (see sections 4.2.4, 4.2.6 and 4.3.1 for the methods, and Chapter 5 for the patients' characteristics).

Note: As the amount of data collected during these acquisitions was very large, for the present thesis it was only possible to analyse the part related to the pointing forward task.

4.2.3 Kinematic model

As already mentioned, we assumed that the thorax, arm, forearm and hand are rigid bodies articulated by the shoulder, elbow and wrist respectively (Kapandji 2011). To reconstruct the pool of coordinate systems representing the limb segments, we followed mostly the ISB recommendations, except for the shoulder coordinate system, where we considered a different order of axis multiplication to obtain the orientation we preferred, as shown in Figure 4.3. This was done, in order to express the results in accordance with straightforward clinical usage. In fact, the ISB prescriptions suggest to calculate for the shoulder joint the angles of (1) rotation of the plane of elevation, (2) axial rotation of the humerus (intra-extra rotation) and (3) elevation, because they suit best to a 3-D description of shoulder motion (multiplication order: Y-X-Y). On the other hand, we preferred to obtain the quantities, which are most commonly taken into account in medical language and most easily transferrable to clinical practice: i.e. shoulder flexion-extension, ab-adduction and intra-extra rotation. Since, using this terminology for rotations, flexion followed by abduction gives radically different results than abduction followed by flexion, we had to choose one of the two orders and chose the latter (multiplication order: X-Z-Y).

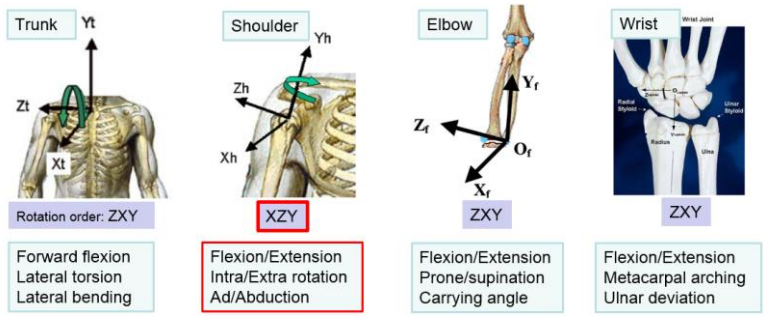

Figure 4.3 The figure illustrates the conventions used to define the coordinate systems of the body segments that permitted the study of the upper-limb kinematics. It also shows the angular quantities that the present approach allows calculating for each district (adapted from Wu et al. 2005).

4.2.4 Marker set-up

A BTS SMART-Elite System with 8 infrared cameras has been used to acquire the motion of the limb, coupled with passive reflective hemispheric markers of 6 mm in diameter. To our best knowledge, there is currently no ideal solution in the literature to position the markers to be sure to pick up their position, and consequently the movement of the limb segment, during every instant of acquisition during the execution of motor tasks. Placing at least 2 markers on a 1-D segment, it is possible to reconstruct its position in space and consequently trace its displacement during motion; however, it is not possible to collect the rotations of a specific 3-D body with only two markers: it is necessary to have at least three and that those are not aligned. In the study presented here, we used more markers on the same part of the limb (i.e. chest wall, spine, shoulder, elbow, wrist and finger), than the ones strictly needed for the reconstruction of the desired orientations of the upper limb and thorax segments. This was done, in order to improve the chances to collect the positions of at least the necessary markers (and consequently reconstruct the

movement of all districts), even if the subject should carry out unexpected movements, covering some of the markers from the view of the cameras. This is often the case when dealing with neurological patients affected by movement disorders.

The montage, constructed following those principles of redundancy and tested on the healthy volunteers, includes 25 reflective passive markers placed on the subject's body (as shown in Figure 4.4). The main anatomical landmarks used in this study to place the markers in a reliable and repeatable way are for the thorax: C7 – Processus Spinosus (spinous process) of the 7th cervical vertebra; T8 – Processus Spinosus (spinal process) of the 8th thoracic vertebra; IJ – Deepest point of Incisura Jugularis (suprasternal notch); PX – Processus Xiphoideus (xiphoid process), most caudal point on the sternum.

For the shoulder, we considered the acromium (A) and the volume of the acromial apophysis (ShF and ShB). For the elbow, we used as anatomical landmarks the olecranon and the opposite elbow fossa; for the wrist, the radial and ulnar styloids. All of those marks were employed to locate the joint centres of rotation. The anatomical landmarks for the hand were the bony prominences on the volar side of the hand on the knuckle of the second (MCP) and fifth metacarpus (MC5) and finally the interphalangeal knuckle of the index finger (PIP), plus the index finger-nail as reference for the markers on the finger (TIP). In addition, 4 markers identified the plane of the table; 1 marker was used to denote the starting and finishing point of the motor tasks on the table top. One marker, mounted on the target of the reach-forward task, was placed in front of the subject, shoulder-height, at a distance reachable with the extended arm, without moving the thorax, (see Figure 4.5).

Considering the patients, in addition to the 25 markers used on the body for the healthy subjects, we found it necessary to include a

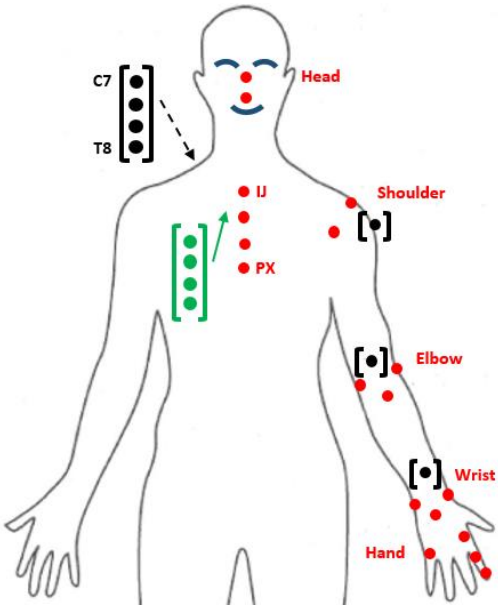

Figure 4.4 Layout of the reflective passive markers for the kinematics evaluation. The *red* markers are placed on the front side of the subjects. The *black ones* are on the back side, in correspondence of the top of wrist (volar side), the back of the elbow (olecranon), the back of the shoulder (aligned with the one on the front side), and on the back (along the spine, from C7 to the T8 vertebra). In case of peculiar movements by the subject, which caused the markers on the spine to be concealed from the cameras, a second row (*green*) fixed on the front side of the thorax, at the same height and laterally to the first sternal one provided an alternative for the definition of the central sagittal plane orientation. This set up was mainly employed for the patients (see Figure 4.5 and Chapter 5).

second line of 5 markers right of the sternum. The original 5 sternal markers (IJ to PX) were then shifted left by an amount, to be made symmetrical with the newly introduced ones. This device resulted in a more efficient system to track joint positions and orientations, especially in critical situations when vision of the limb or thorax by the

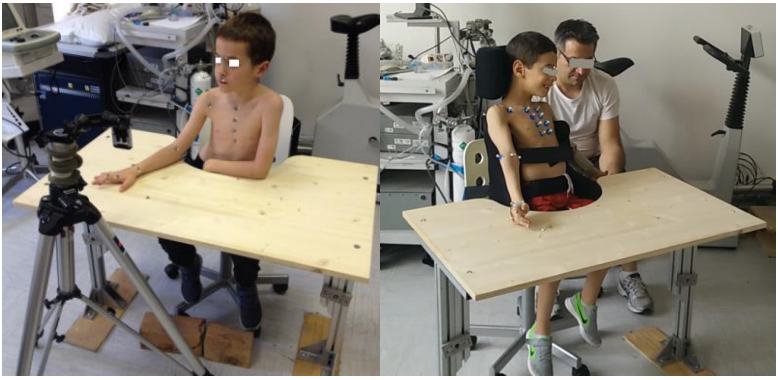

Figure 4.5 Set-up for the kinematic evaluation. The optoelectronic system uses 8 infrared cameras. During the acquisition, the subject is free to move inside the FOV. Healthy subject during a pointing task (*left*) and a patient during a hand-to-mouth exercise (*right*). It is worth to notice the different marker placement on the thorax used for the patients, i.e. with a double parallel row of reflective markers, to reconstruct the thorax coordinate system even when the patients push their backs against the containment chair.

cameras is severely blocked out by the moving patient's body. In fact, any set of three non-aligned markers out of the 10 para-sternal ones can be used to define a coronal plane, and the central sagittal one, orthogonal to that (see Figure 4.4 and 4.5). This different layout was employed for all the dyskinetic patients when their body motion did not allow collecting the marker positions by the cameras and when the markers placement on the spine felt uncomfortable due to the necessity for the patient to sit in a particular containment chair, for proper trunk support.

4.2.5 Reconstruction of marker paths and extraction of kinematic data

The data collected by the optoelectronic system are tracked with the SMART Tracker software (SMART Motion Capture System – BTS

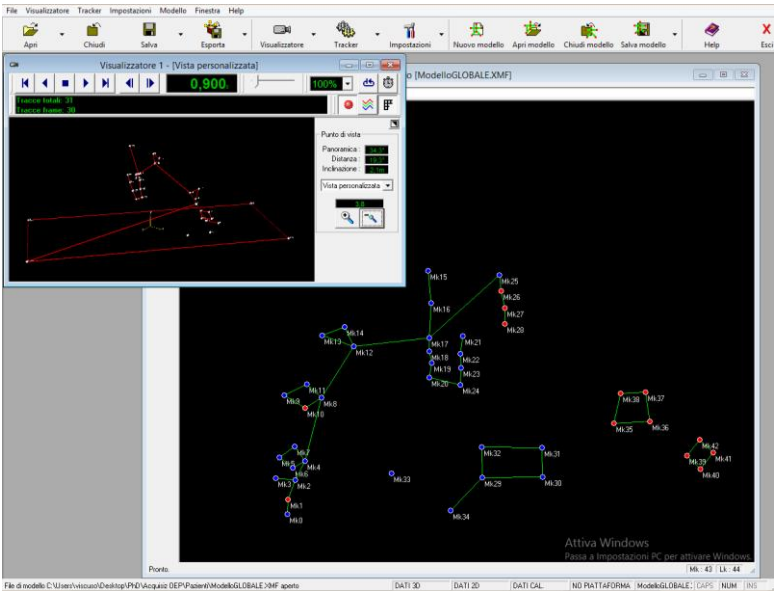

Figure 4.6 The screenshot shows the nodes-and-sticks model devised to assign (track) the raw data acquired by means of the optoelectronic system to the nodes of an appropriate kinematic chain. The SMART Tracker software allows labelling the markers across the execution of the motor tasks in order to generate nodal paths representing the motion of relevant points of the upper-limb kinematic chain in time.

Bioengineering), by which the markers are matched frame-by-frame to the nodes of an articulated model representing the kinematic chain (as explained in section 4.2.1 and shown in Figure 4.6). After this operation, the data are in the form of time-series expressing kinematic nodal positions in time. They are then processed using the main module of a *home-written* MatLab programme (MATLAB – MathWorks) to reconstruct from the nodes all the coordinate systems (orientations) that represent each limb segment, and the global space reference. Due to the established relationship between nodes (markers) and coordinate systems, it is possible to study, frame-by-

frame, the motion of the limb. The code, in particular, calculates the parameters of linear and angular kinematics for each segment and joint of the limb, and stores the numerical results.

4.2.6 Data loss reduction technique for lacunose datasets

As explained in the previous section, the *home-written* MatLab code takes as input the tracked data. It was already mentioned that patients' data are in general expected to be affected by severe lacunae, because of unpredictable gestures that repeatedly block out the lines-of-view of the cameras towards some markers during several timeframes.
In order to limit data loss, redundancy was introduced in marker placement, and consequently a method had to be devised to switch between different marker sets, encoding for the same segment-linked coordinate system, so that opportunities to reconstruct that coordinate system are maximised.
This was done by an *ad-hoc* algorithm that semi-automatically sets a pool of flow-controlling flags based on simultaneous marker occurrences (flowchart in Figure 4.7). The flags are a tool that we constructed to choose in a generalised or frame-by-frame (patching) manner among the different possible marker groups able to encode for a given segment position and orientation. In particular, they help decide whether to use:

i. double rows on the sternum or a single one plus the spine markers to define the thorax orientation;
ii. two markers at the sides of the shoulder or only the one on the acromion to identify the shoulder joint;
iii. which are the best couples of markers available (dorsal-volar, or medial-lateral) to calculate the centres of the elbow and wrist, depending on their relative occurrences in the dataset.

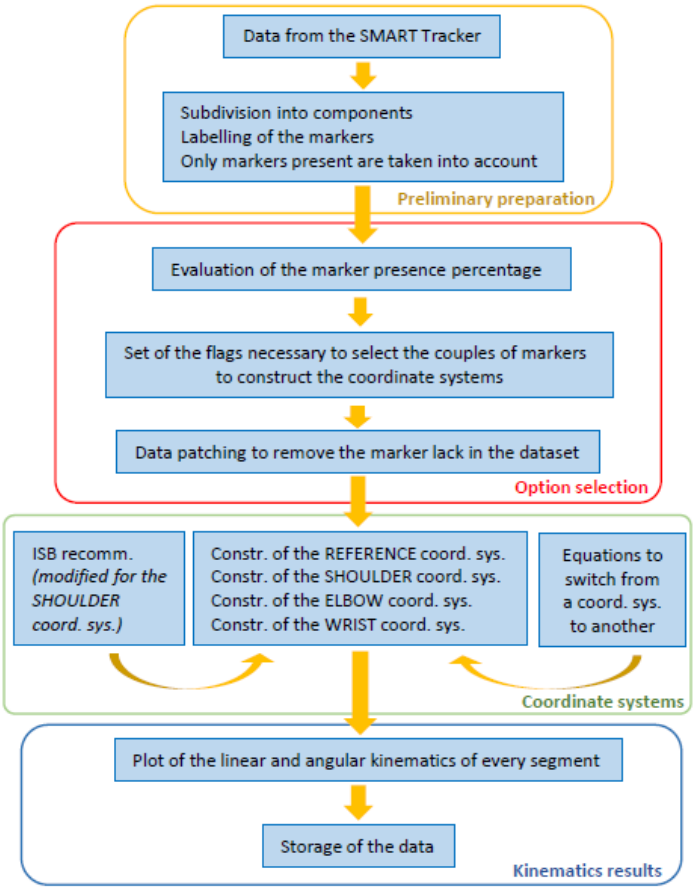

Figure 4.7 The flowchart shows the steps that the *home-written* MatLab code applies to process the tracked marker data and calculate the kinematic quantities characterising the upper limb during the execution of a defined motor task.

Figure 4.8 shows the first step of the algorithm to reduce the lacunae in the dataset. The percent presence of a couple of markers is plotted in comparison with that of the other couple available for that joint, i.e.

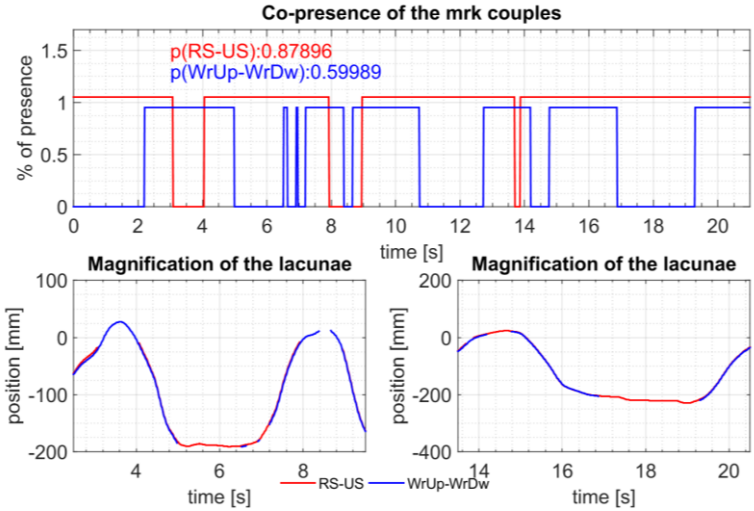

Figure 4.8 The figure shows the first step of the algorithm to reduce the lacunae in the dataset, in particular, the percent presence of the medial-lateral couple of wrist markers and the orthogonal one, for a typical healthy volunteer (*graph on top*). A magnification of the 3 lacunae present in the dataset, is shown in the *bottom* graph, where is plotted one of the 3 axial coordinates of the wrist centre, calculated with both of the couples of markers: medial-lateral (*red*) and volar-dorsal (*blue*). It can be noticed that, in this particular dataset, the loss of data only affects the volar-dorsal couple of markers.

medial-lateral or volar-dorsal for the wrist and medial-lateral or elbow fossa-olecranon for the elbow joint. From this percentage, we can evaluate the quantity of lacunae that we have in the dataset and thus the goodness of the acquisition, which will influence the subsequent possibility to calculate the coordinate system for that joint. The algorithm estimates the joint centre from the position of the markers in space, using both couples of markers (as shown for each coordinate in Figure 4.9 on the *left*). The final step consists in the reduction of the average difference between the two alternative centre estimates, evaluated with the couples available. We assumed that, for the elbow

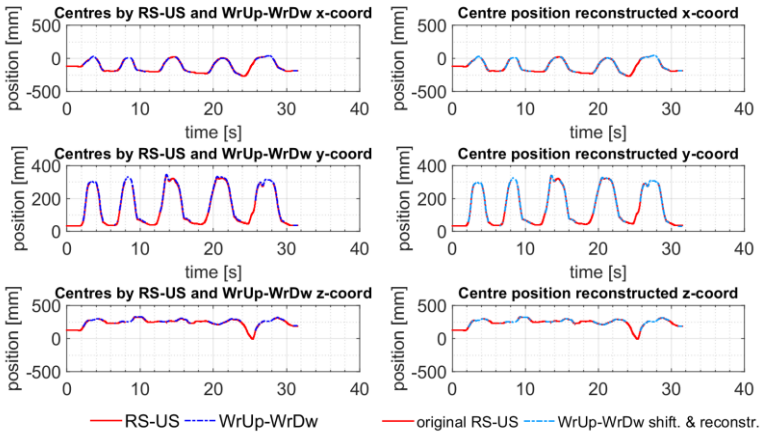

Figure 4.9 The figure shows the second step of the algorithm to reduce the loss of markers in the dataset. *On the left side* are reported the x- y- and z-coordinates of the wrist joint centres, calculated using the medial-lateral markers in *red* (anatomical landmarks on the apophysis of the radius and ulnae) and in *blue* the centre obtained with the markers placed on the volar-dorsal direction of the wrist. On the right are shown the x- y- and z- coordinates of the wrist joint centres, calculated using the medial-lateral markers in *red* and in *light blue* the ones of the centre obtained with the markers placed up-down, corrected using the coordinate-by-coordinate distance between the estimates.

and for the wrist joints, there is a preferable couple of markers, due to the fact that the anatomical landmarks are easier to find (for example the radial and ulnar styloide processes at the wrist); they are more symmetrically arranged relative to the joint centre, and furthermore the shape distortion during motion is less (e.g. at the elbow, along the medial-lateral direction rather than in the orthogonal one). Under this assumption, we always considered preferable the medial-lateral couple of markers, when present, and when they were not available, we used the other (orthogonal) couple corrected by subtracting the mean value

of the component-by-component distance between the centre estimates (Figure 4.9 *right)*.

The error committed in selecting one configuration with respect to the other in each case, has been evaluated over the cohort of six healthy subjects. We obtained an average mean error of 2.20 ± 1.25 mm considering the wrist joint, and 3.99 ± 2.27 mm for the elbow joint centre (Euclidean distances between the differently estimated centres).

4.2.7 Analysis of parameters and extraction of synthetic indices

In the assessment of motor performance, besides the analysis of the time courses of linear and angular parameters, some synthetic kinematics indices will be calculated to simplify the scoring. They could quantify not only the motion during a particular task, but also help explain the motor skills and the different compensatory strategies that a subject uses to try and reach the target. The evaluation of these synergies can be done if appropriate types and amounts of parameters are taken into account simultaneously.

The output of the calculations explained in sections 4.2.6 and 4.2.5 provides all the data that we used to extract the kinematic parameters and synthetic indices. In particular, the program stores for the thorax, the frontal and the lateral bending and the torsion; the flexion/extension (of shoulder, elbow and wrist), the ab/adduction, the intra/extra rotation for the shoulder, the prono/supination for the elbow and finally the ulnar deviation of the wrist; the linear displacement of the index fingernail.

We developed a separate MatLab subroutine (flowchart in Figure 4.10), that, by a segmentation process, subdivides the entire acquisition into periods of rest and motion, and works out, during the repetitions of the motor task, the following quantities:

Parameters related to the index fingernail movement

i. *D* - minimum distance from target;
ii. *N* - number of movement repetitions;
iii. *V* - mean speed to reach the target;
iv. *S* - stroke during the execution of the task (maximum distance covered by the index fingernail marker during movement);
v. *tT* - total duration of the motor task;
vi. *tN* – total duration of the repetitions;
vii. *tTm* - total time in motion (sum of the forward and backward motion time over the repetitions);
viii. *tTt* - total time around the target (sum of the time spent on the target over the repetitions) ;

Parameters related to distances covered by single segments

ix. *ShF*, *ShA*, *ShI* - maximum ROM of the 3 shoulder angles (flex/extension, ab/adduction, intra/extra rotation) utilised during the motor task;
x. *ElF*, *ElP* - maximum ROM of the 2 elbow angles (flex/extension, prono/supination) utilised during the motor task;
xi. *WrF*, *WrU* - maximum ROM of the 2 wrist angles (flex/extension, ulnar inclination) utilised during the motor task;
xii. *ThX*, *ThY*, *ThZ* - maximum linear displacement of the thorax along the three coordinate axes;
xiii. *ThFF*, *ThLF*, *ThT* - maximum angular movements of the thorax around the three Euler axes (forward flexion, lateral flexion, torsion).

Indices related to movement flow and smoothness

xiv. *Ic* – Index of curvature calculated on the spatial coordinates *d(t)* of the MCP marker (second metacarpus) during the motor task;
xv. *NMU* – Number of movement units, calculated based on the norm of the MCP velocity vector *v(t)* during the motor task;
xvi. J^2 – Squared jerk, mean norm of the first derivative of the acceleration vector *a(t)*, squared

A brief explanation is required for points xiv., xv. and xvi.

In order to obtain the *d(t), v(t), a(t) and J^2(t)* parameters, a pre-filtering step was applied to the raw MCP coordinates tracings. The chosen smoothing filter is the GVC, developed and validated by the International Society of Biomechanics (ISB) and implemented by a MatLab subroutine (C-implementation for MATLAB of Woltrings General Cross Validation Spline smoother, from ISB software).

The kinematic parameters (*Ic, NMU, J^2*), we found in the literature to be *common indices* used to assess kinematic performance at a glance. They are defined as follows: *Ic* is the *index of curvature*, calculated as the ratio between the curved path followed by the marker on the MCP joint and the straight distance between the starting point on the table and its final position close to the target (which is ideally the shortest possible track). The closer *Ic* is to 1 the straighter and more direct is the movement towards the target, without detours. The second index calculated is *NMU*, which is the *number of movement units*, calculated as the number of velocity changes that a subject's limb displays during the execution of each repetition of a motor task. This corresponds to the number of peaks in the velocity tracing with a height greater than 10% of the maximum value for each repetition. For each repetition, the NMU is ideally equal to 1, i.e. a subject shall not vary more than one time his speed profile during the execution of the forward movement. Larger values mean that in one or more repetitions the movement was executed less fluidly and with some hesitations. The third index calculated, *J* is the *jerk,* i.e. the third derivative of the spatial coordinates (first derivative of the acceleration) of MCP during the motor task, and thus J^2 is the square value. The lower the *jerk* the smoother the movement. In evaluating *Ic*, *NMU* and J^2, the marker selected was the MCP (metacarpal phalangeal prominence of the second finger).

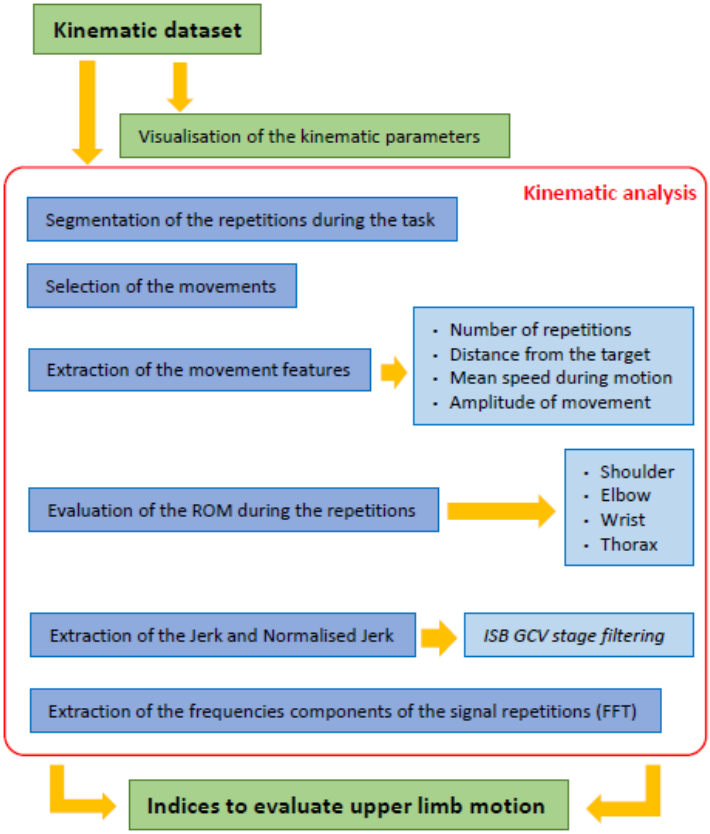

Figure 4.10 The flowchart shows the steps that the *home-written* MatLab code applies to extract the kinematic parameters from the data collected by means of the optoelectronic system for a subject during the execution of a standardised movement.

In this manner we took into account the posture and the motion of the wrist, but we did not consider the variations introduced by the motion of the fingers during the execution of the motor task: that could be a strong quasi-random effect in the patients' evaluation while on the

contrary, it tends to be a steady value for the healthy subjects, close to the length of the finger.

The interpretation of all these direct and derived parameters is expected to complement the scoring of the motor tasks execution in a quantitative way and help evaluate the motion of the subjects more in general, understanding if there are some recurrent synergies that are exploited during the execution of movements.

To this end, reference values of the parameters (mean and standard deviation) are calculated for the healthy group. Furthermore, an analysis of cross-correlation is provided.

4.3 Results

4.3.1 Data loss minimisation

With the tools described in section 4.2.6, we analysed systematically all the data collected from the healthy subjects, finding the already-mentioned mean errors. Furthermore, the method was applied to the patients' data (that are more lacunose). The *home-written* code, devised for the analysis, allowed us to extract more information from lacunose datasets, especially the ones collected from the patients. Figure 4.11 shows how the algorithm for patching the missing values is efficient in retrieving the information available, even when the initial dataset is quite corrupted i.e. with many lacunae.

The patching step, together with the selection of the flags for each dataset, improve consistently the possibility to define all the coordinate systems, specific for the body parts of interest: trunk, shoulder, elbow, and wrist. With these coordinate systems, together with the matrix of transformation between one coordinate system to another one, we evaluated the linear and angular kinematics of all the body segments.

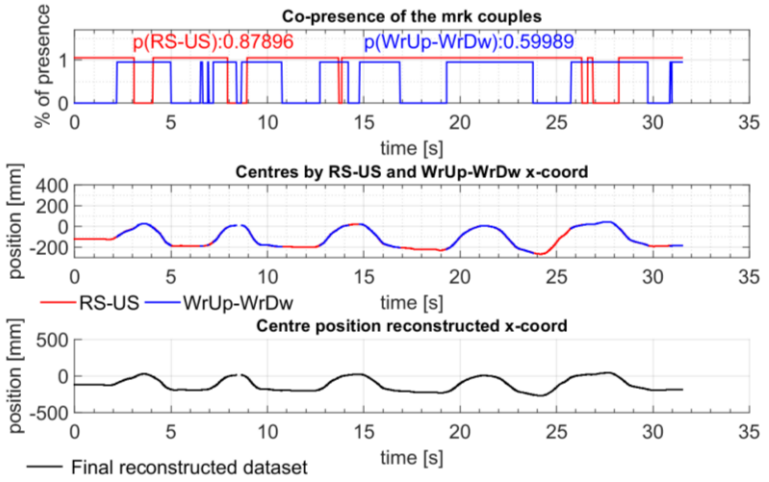

Figure 4.11 The figure shows the results of the algorithm to reduce the loss of markers in the dataset of one patient. The *top* graph shows the percentage of presence of the two couples of markers on the wrist during the pointing motor task in the original dataset: when the value is 1 the marker is present and so allows calculating the joint centre, *vice versa* the marker is not present when the value is 0. The graph in the *middle* reports the two centre coordinates X calculated on the original data, without patching. It is worth to notice the lack of data in correspondence of the missing markers, displayed in the top graph. The graph at the *bottom* shows the results of the patching algorithm and the data actually used to calculate the wrist joint centre.

The results of these steps are shown in Figure 4.12 for a successful case and in Figure 4.13, for a limit case in which neither the marker redundancy, or the patching algorithm are sufficient to prevent the data loss. This situation corresponds to a severe patient with generalised hyperkinesia affecting both arms and the trunk: the uncontrolled movements of the body often cover the sight to all the markers representing a certain reference point, despite the redundancy. Furthermore, the loss of markers for many contiguous timeframes does not allow to recover continuity by interpolation.

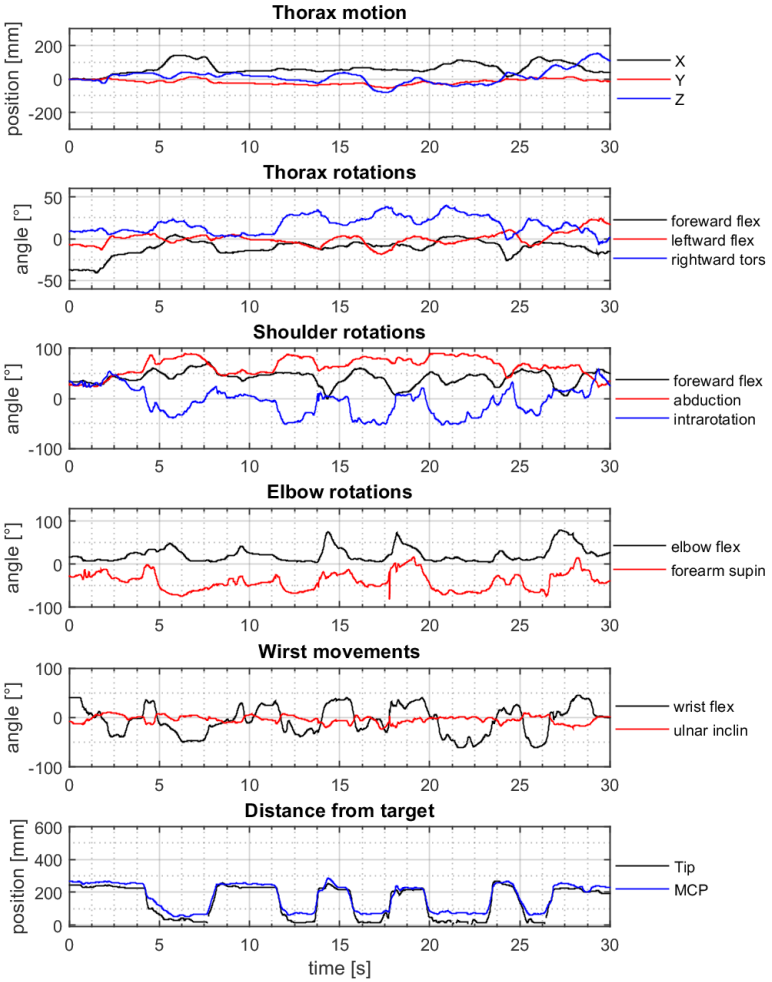

Figure 4.12 The figure reports the results of the kinematic analysis on a dystonic patient using all the available data recovered using the data-loss-minimisation algorithm. In this case it is possible to understand the general coherence and correspondence between the movements of the different districts, the initial position of the joints used during the specific motor task, the fluctuations around the target and the distance from it.

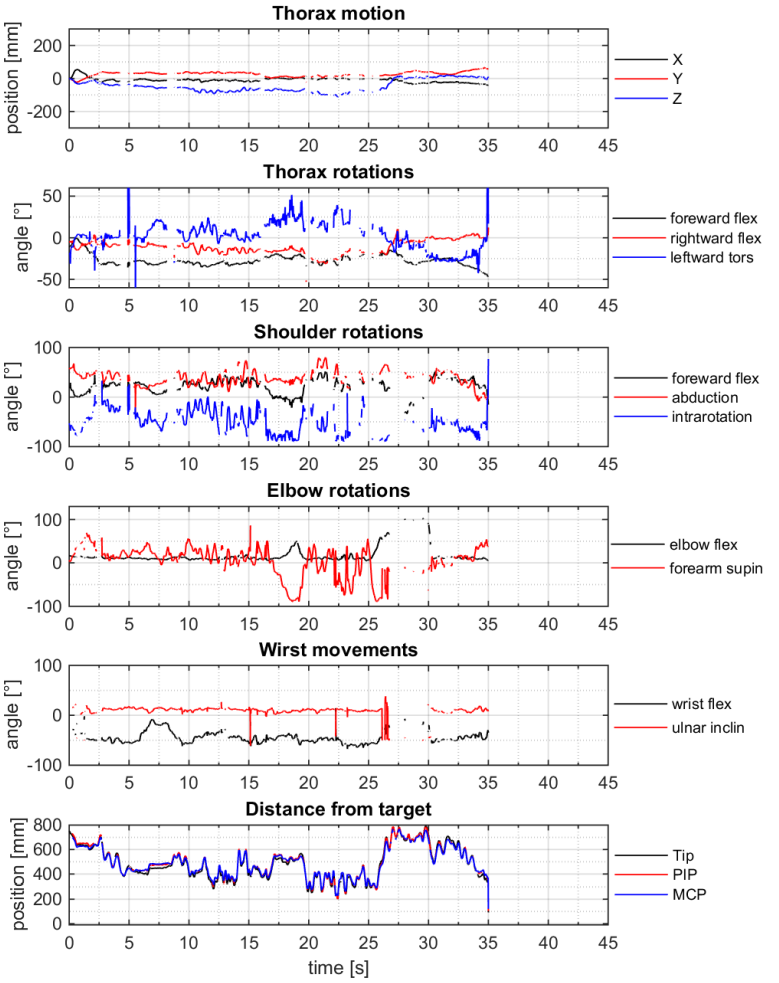

Figure 4.13 The figure reports the results of the kinematic analysis on a severely hyperkinetic patient using all the available data recovered using the data-loss-minimisation algorithm. In this case, it is not possible to reconstruct the continuous tracings because the generalised movements of the trunk and limbs, cause the loss of all the markers identifying a certain body point, despite the redundancy.

The entire process, which leads from the acquisition of data to the application of the algorithm through home-written MatLab codes, brings as result the kinematics of the upper-limb, as reported in the Figures 4.12, 4.13. From the graphs, it is possible to extract preliminary considerations about the general execution of the specific motor task (here the pointing forward), such as the number of repetitions, the total time necessary to execute the task, the general trends of angular kinematics of shoulder, elbow and wrist joint, the linear displacements and the angular movements of the trunk. More in detail, the direct correlation in the time course, of the data, gives the possibility to show the phase relationship between the parameters within the same joint and between the joints, in order to evaluate the execution of the movement of a patient with respect to the same execution carried out by the healthy population (cf. next section). In addition looking at the displacement of the fingernail during the pointing forward task as movement outcome, we also calculated the velocity, the acceleration and the jerk squared in order to give, besides the distances from the target, also an impression of the fluidity of the motor action and the capability to repeat the exercise in a relatively similar manner.

4.3.2 Healthy reference data: tracings

From the tracings obtained for the healthy subjects, (Figures 4.14, 4.15) it is possible to get a global impression of the execution of the motor task; in particular, taking as an example the kinematic report, resulting from the pointing-forward task of a healthy subject, the angular kinematics of the shoulder and the trunk define clearly the pacing of the task repetition; in addition the phase between elbow flexion-extension movements, angular parameters of the shoulder, together with the linear and angular kinematics of the trunk, identify the relationship between the body segments during the execution of the motor task. Furthermore the other kinematic quantities, which do not vary in time, such as the wrist flexion-extension or forearm supination,

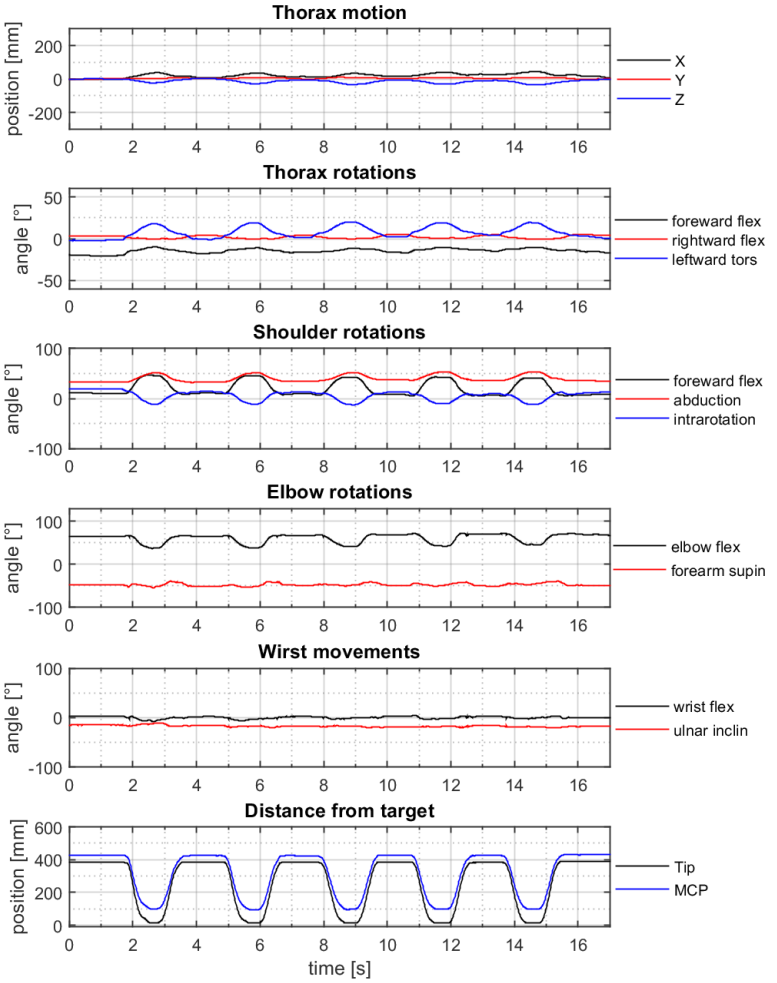

Figure 4.14 The figure reports the results of the kinematic analysis for one healthy subject. From the graphs, it is possible to understand rapidly the dataset quality, the general coherence and correspondence between the movements of the different districts, the speed of movement, the fluctuation in the distance from the target and the repeatability in the execution of the motor task in a qualitative or semi-quantitative way.

add information about which districts are or are not involved in the motor task execution and which are the synergies recruited to carry out the movement in the most efficient manner. The fluidity of motion and the constant pacing can be observed more in detail, looking at the parameters of displacement, velocity and acceleration in time Figure 4.15.

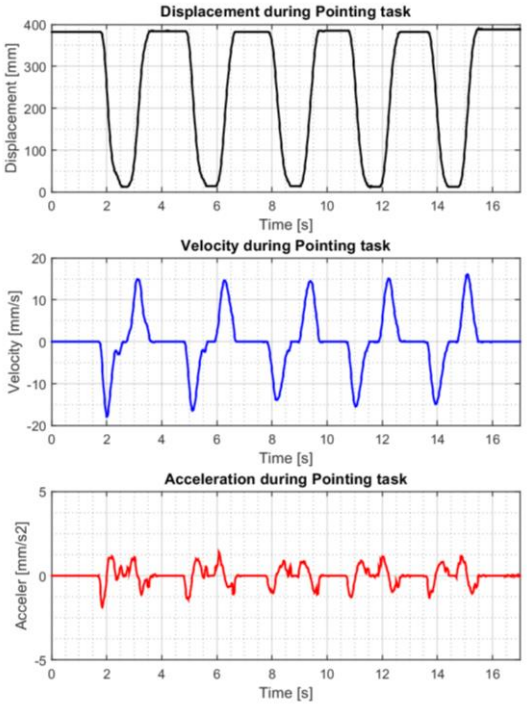

Figure 4.15 The graphs show the displacement of the fingertip during the pointing forward task (*top* graph), the velocity and the acceleration (*second* and *third*, respectively). This comparison give, at a first glance, an estimation of the fluidity of the movement, provide the distances from the target and shows the capability to repeat the motor task. They collectively represent a basic visualisation of the movement outcome, as the performance of the end-effector.

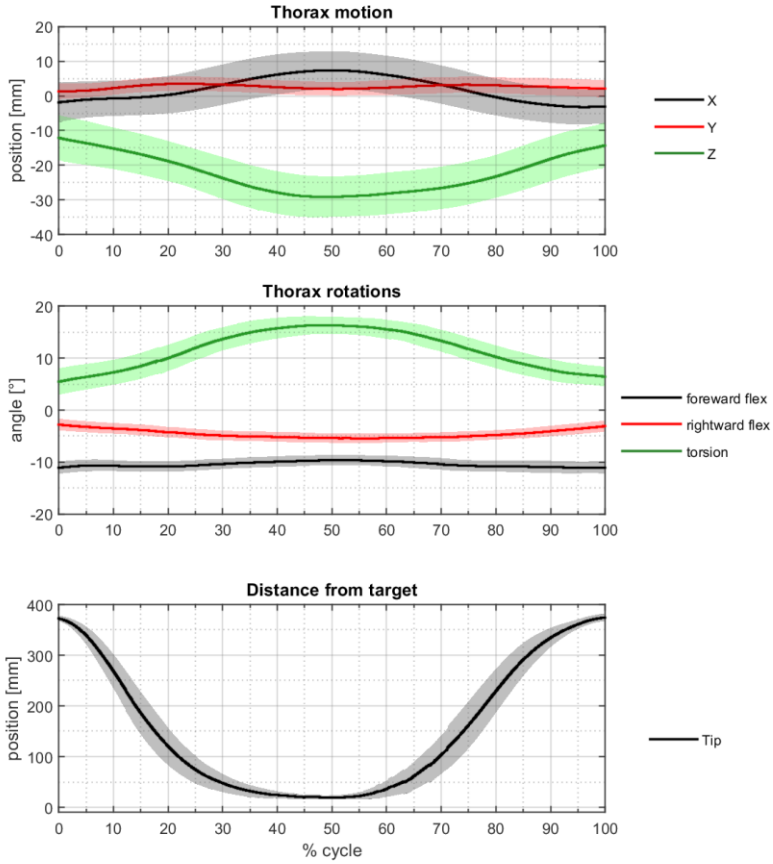

Figure 4.16 Mean (line) and st. dev. (shade) of normalised results of the kinematics for all the healthy subjects enrolled in the study. In particular, at the *top* are depicted the linear movements of the thorax, the corresponding angular kinematics *in the middle*, phase-referenced to the displacement fingernail tip (at the *bottom*) during the execution of the pointing forward motor task. The values are obtained from the mean of all the repetitions of the motor task for every subject (normalised in time to obtain the percentage of the cycle), then averaged over all the subjects who took part in the study.

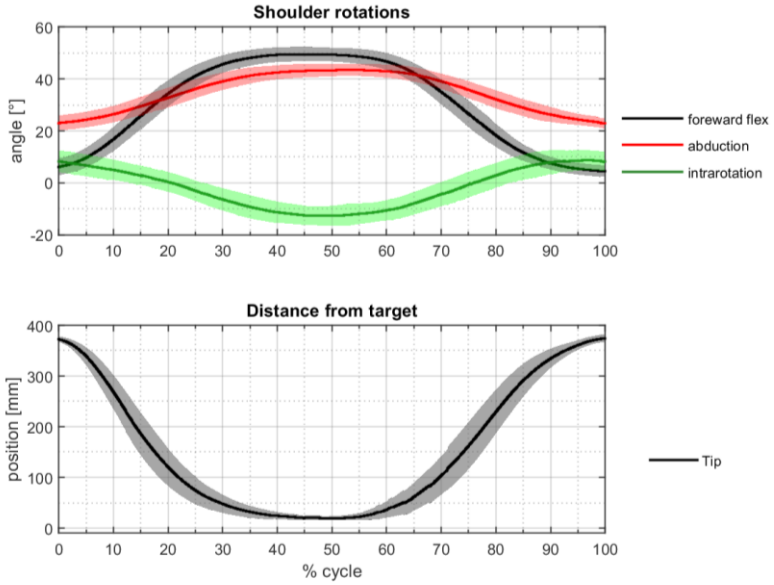

Figure 4.17 Mean (line) and st. dev. (shade) of normalised results of the kinematics for all the healthy subjects enrolled in the study. In particular, at the *top* are depicted the angular kinematics of the shoulder joint, phase-referenced to the displacement fingernail tip (at the *bottom*) during the execution of the pointing forward motor task. The values are obtained from the mean of all the repetitions of the motor task for every subject (normalised in time to obtain the percentage of the cycle) then averaged over all the subjects who took part in the study.

The information presented so far comes from the kinematic results of a single subject; by looking at the whole cohort of healthy control, volunteers, whose tracings can be averaged, we can obtain a more general description of task execution. Thanks to the normalised kinematic trends, obtained from the healthy population and depicted in Figures 4.16, 4.17 and 4.18, it is possible to visualise a reference tracing for each kinematic parameter devoid of the specificity of an individual

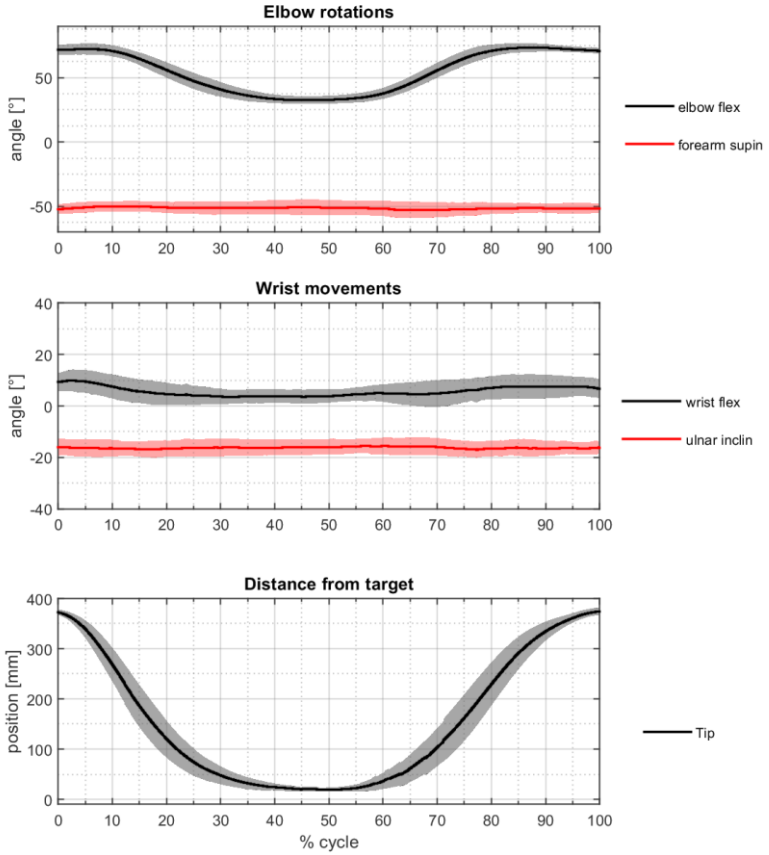

Figure 4.18 Mean (line) and st. dev. (shade) of normalised results of the kinematics for all the healthy subjects enrolled in the study. In particular, at the *top* are depicted the angular kinematic of the elbow joint, the wrist angular kinematics *in the middle*, phase-referenced to the displacement fingernail tip (at the *bottom*) during the execution of the pointing forward motor task. The values are obtained from the mean of all the repetitions of the motor task for every subject (normalised in time to obtain the percentage of the cycle) then averaged over all the subjects who took part in the study.

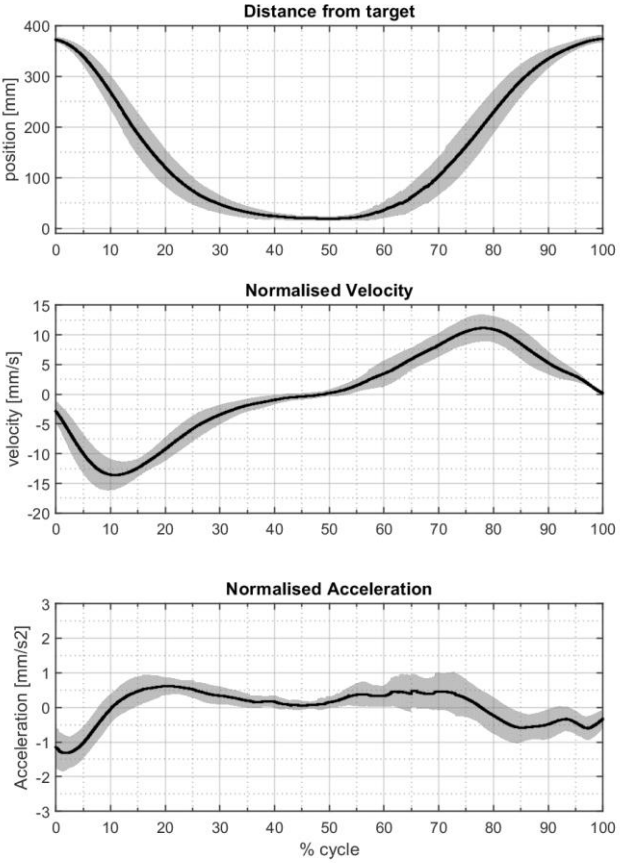

Figure 4.19 The graphs show the normalised displacement of the fingertip during the pointing forward task (*top* graph), the normalised velocity and the normalised acceleration (*second* and *third*, respectively). First, we obtained the mean value of all the repetitions for one subject (normalised in time to obtain a standard cycle equal for all the subjects) and then the values displayed are the average over the entire healthy population enrolled in the study (*lines*: mean value; *shades*: st. dev.).

subject, such as the execution time, the amplitudes, the speed etc. We calculated the normalised kinematic results for every subject, as the mean of all the time-normalised repetitions and then averaged between all the healthy control subjects. In the same manner, the parameters of displacement, velocity and acceleration during the motor task execution, have been calculated as shown in Figure 4.18.

4.3.3 Healthy reference data: synthetic parameters

Table 4.1 reports all the synthetic kinematic parameters calculated for the 6 healthy subjects enrolled in the study. For healthy volunteers, the dominant-side and contralateral movements were assumed to be equivalent. Hence, the corresponding values of the same parameter, obtained for each subject carrying out the task with the right and left hand, were averaged; the descriptive inter-subject statistics was calculated using those averaged values including only the forward part of the movement (to the target).

Pearson product-moment correlation has been estimated between all pairs of segment-related parameters collected from the healthy group. The results are reported in Table 4.2 and 4.3.

Table 4.1 *Values of all the synthetic parameters, evaluated over the entire healthy population enrolled in the study, for the forward reaching movement.*

Variable	Max	Min	Mean	St.Dev.
tT [s]			12.41	
tN [s]	1.09	0.76	0.91	0.14
tTt [s]	0.40	0.15	0.26	0.10
tTm [s]	2.01	1.60	1.78	0.16
D [mm]	22.43	14.81	17.97	3.01
S [mm]	364.83	349.21	357.12	6.57
V [mm/s]	485.00	338.68	409.56	59.25
ShF [°]	49.69	40.47	45.09	3.87
ShA [°]	25.90	18.16	21.87	3.26
ShI [°]	29.76	18.93	23.08	4.45
ElF [°]	45.26	37.41	41.64	3.26
ElP [°]	17.11	8.67	12.31	3.43
WrF [°]	17.39	7.28	12.06	4.27
WrU [°]	12.55	3.80	7.14	3.52
ThX [mm]	23.59	9.76	16.19	5.57
ThY [mm]	7.76	3.78	5.74	1.61
ThZ [mm]	24.84	12.58	17.83	4.91
ThLF [°]	4.59	1.95	3.23	1.07
ThT [°]	4.35	2.01	3.02	0.96
ThFF [°]	15.48	9.03	11.57	2.57
J^2 [mm/s^3]	1.15	0.00	0.05	0.04
Ic [-]	1.12	1.03	1.06	0.05
NMU [-]	1.07	1.00	1.01	0.05

Table 4.2 *The table reports the Pearson product-moment correlation coefficients (R-values) between the parameters expressing the segment specific maximum ROMs, evaluated for the entire healthy population enrolled in the study. In the matrix are highlighted the higher values showing statistic significance (see table 4.3)*

R_h.	ShF	ShA	ShI	ElF	ElP	WrF	WrU	ThX	ThY	ThZ	ThLF	ThT	ThFF
ShF	1												
ShA	-0,27	1											
ShI	0,28	0,36	1										
ElF	0,92	-0,03	0,59	1									
ElP	0,50	0,49	0,80	0,74	1								
WrF	-0,43	0,97	0,44	-0,08	0,58	1							
WrU	-0,06	0,90	0,66	0,30	0,82	0,92	1						
ThX	0,40	-0,41	0,62	0,49	0,29	-0,21	-0,04	1					
ThY	0,68	-0,33	0,52	0,64	0,34	-0,34	-0,12	0,64	1				
ThZ	0,84	-0,45	0,44	0,71	0,44	-0,31	-0,08	0,81	0,82	1			
ThLF	0,41	-0,33	0,61	0,42	0,28	-0,20	-0,07	0,96	0,78	0,84	1		
ThT	0,26	0,28	0,35	0,18	0,51	0,29	0,27	-0,08	0,64	0,26	0,19	1	
ThFF	0,35	-0,06	0,91	0,52	0,67	0,27	0,40	0,83	0,51	0,76	0,82	0,06	1

Table 4.3 *The table reports the p-values corresponding to the Pearson product-moment correlation coefficients of Table 4.2. In the matrix are highlighted the values indicating statistical significance (p<0.05).*

P_h.	ShF	ShA	ShI	ElF	ElP	WrF	WrU	ThX	ThY	ThZ	ThLF	ThT	ThFF
ShF	1												
ShA	0,61	1											
ShI	0,65	0,55	1										
ElF	0,02	0,96	0,30	1									
ElP	0,39	0,40	0,11	0,09	1								
WrF	0,57	0,03	0,56	0,89	0,31	1							
WrU	0,94	0,10	0,34	0,63	0,09	0,03	1						
ThX	0,44	0,41	0,26	0,33	0,58	0,73	0,95	1					
ThY	0,14	0,53	0,37	0,17	0,51	0,58	0,85	0,12	1				
ThZ	0,04	0,37	0,46	0,11	0,39	0,61	0,89	0,03	0,025	1			
ThLF	0,43	0,53	0,27	0,40	0,59	0,75	0,92	0,00	0,04	0,02	1		
ThT	0,62	0,59	0,56	0,74	0,30	0,63	0,66	0,87	0,12	0,57	0,68	1	
ThFF	0,50	0,92	0,03	0,29	0,15	0,66	0,51	0,02	0,25	0,05	0,02	0,89	1

Amongst all the possible correlations between parameters, we firstly considered the ones that from a statistical point of view correlated

more strongly and were statistically significant (p<0.05). The analysis of correlation showed that many strong interactions between the parameters exist (high values of Pearson's R), but not all of them have a high significance (low associated p-values). Amongst the most interesting effects, we found the following:

i. Shoulder flexion ROM and elbow flexion ROM (ShF vs. ElF) *positive correlation*;
ii. Medial-lateral displacement of the thorax and shoulder flexion ROM (ThZ vs. ShF), *positive correlation*;
iii. Shoulder abduction ROM and wrist flexion ROM (ShA vs. WrF) *positive correlation*;
iv. Shoulder intrarotation ROM and thorax forward flexion ROM (ShI vs. ThFF) *positive correlation*;
v. Wrist flexion ROM and wrist ulnar inclination ROM (WrF vs. WrU) *positive correlation*;
vi. Linear displacements of the thorax (along different directions X, Y, Z) *positive correlations*;
vii. Lateral bending of the thorax and thorax forward flexion ROMs (ThLF vs. ThFF) *positive correlation*.

4.4 Discussion

The results presented above show how the methods devised in this study are able to provide an efficient tool to analyse the movement of a subject during the execution of a specific motor task, extracting many kinematic parameters, useful to describe the upper-limb motion in a quantitative way.

4.4.1 Data loss minimisation

The minimisation of data loss regarding the elbow and/or wrist joint centres was found to be a fundamental step in the retrieval of

information, especially about joint orientations and angular degrees of freedom. The method that was presented has several advantages, and works for the more static dystonic cases. With the severely hyperkinetic pictures it does not seem to be completely effective, but it is likely that most methods would fail because it seems actually impossible to avoid that the bending trunk or twisting limbs of the patients moving in uncontrolled ways sometimes cover an essential subset of the markers needed to reconstruct body point positions, and that would be true even changing the position or number of the cameras or markers. To substantially decrease the data loss, it would be probably necessary to look at different technologies, such as inertial or other, although the signal in those cases may be somehow more difficult to post-process, interpret and use in clinical settings.

4.4.2 Role of normality

The results obtained from the evaluation of 6 healthy subjects helped define the standard motor-patterns of execution of the specific exercises, which involve several districts of the upper body. In this respect, the normality dataset could be used *to identify the ranges of values* which characterise the movement of a specific body segment; more in detail, to allow *the interpretation of the relations between different districts*, e.g. whether they are in phase with each other or not; *to highlight the possible synergies*, which drive to the global execution of the movement in exam. Finally, the normality tracings provide *information about the general execution of the movement* also in terms of fluidity and achievement of the target requested.
Those findings are also useful to understand better, by comparison, the motor skills of the patients. This analysis shall be carried out wisely in order to extract all the possible quantitative information from the patients' dataset, without missing the objective of such comparison: interpret "different" types of subjective performance understanding all the facets, which characterise patients' capability to execute a

proposed motor task. Under these preliminary considerations, the normality dataset can be used to control the *general capability of a patient*, to accomplish the movement proposed. More in detail, it is possible to observe if *a specific body district* moves differently from what the healthy cohort does. In this case, the presence of such differences in the body segments motion afflicts more than a district or just few, the finding might be ascribed to the establishment of a "new", even if pathological, synergy of motion. This "distorted" and some way "awkward" mode of task management by the patient should not necessarily be considered automatically a complete failure in motor control. Rather, taking into account that the patient is striving in the direction of *target accomplishment* (as opposed to perfect segmental execution), it should be evaluated whether the new scheme is functionally effective, or in what manner it is not. In this respect, it can be expected that if one or more districts do not behave in a foreseen, normal manner, the motor control system would *try* to reprogram all the other segment linked in the kinematic chain to compensate for the impaired one and reach the target anyway. These compensatory strategies even if they cannot be reckoned *per se* as optimised or at least physiological, when compared with normality values, may unveil some underlining attempt by the patient to overcome the unavoidable impairments.

This approach to the use of the normality information is not the only possible one. For instance, some other authors make direct quantitative comparisons degree-of-freedom by degree-of-freedom. A good example is the formulation of condensed indices such as PULMI (Butler et al. 2012), proposed to score in a quantitative way the execution of a defined motor task. The normality is used as a baseline to calculate numerical deviations in every degree of freedom taken independently. Every difference from the normality sums up to form a negative score, and thus it is completely disregarded that a difference in one degree of freedom could be caused (due to compensatory

strategies) by a difference in another degree of freedom: i.e. that *the degrees of freedom are not independent*!
In our opinion similar approaches, albeit simple, straightforward, and aimed at condensing information in few numerical scores, are too mechanistic and may ultimately fail to render the complexity of the problem.

4.4.3 Discussion on some correlations between kinematic parameters, and on the values of the smoothness indices

The statistical analysis of the synthetic parameters provides insight into the numerical relationships linking the parameters that describe the limb motion. More in detail, the analysis of correlation suggests interesting synergies in the healthy subject during the execution of some task (e.g. the pointing forward exercise), which could be considered as a clue to the motor pattern that subjects tend to apply in a repeatable manner. The following comments try to find an explanation to these behaviours and highlight the coordinated contributions of the segmental components of movement to reach the motor objective, in particular:

i. The ROMs of flexion of the shoulder and elbow used are linked together by a direct proportionality because, in order to carry out the motor task, covering of the stroke is shared and split especially between those joints, and degrees-of-freedom.
ii. More peculiar is the correlation between the medial-lateral displacements of the thorax with the shoulder flexion ROM. An explanation of this direct proportionality is that, while the elevation of the arm, during the pointing forward task, mainly implies a flexion of the shoulder (and some abduction), the lateral inclination of the thorax is used to hone the medio-lateral positioning of the body in front of the target.

iii. The *direct proportionality* between the ROMs of shoulder abduction and wrist flexion can be explained considering the fact that during motion the abduction complements the lifting of the shoulder and defines the direction (angle) of approach to the target: which is also achieved in a combined way by controlling the wrist flexion.

iv. The *direct proportionality* between the forward flexion of the thorax and shoulder intrarotation ROM can be explained considering the execution of the motor-task. In fact during a pointing action, the closer a subject goes to the target, with his thorax, the larger becomes the angle between the shoulder-to-target direction and the sagittal midline, so it will be necessary to compensate with an intrarotation of the shoulder, to reach the target.

v. The flexion of the wrist and the ulnar inclination are linked together by a *direct proportionality* because of anatomical reasons: the hand is not attached to the wrist in a straight manner and so a change in the flexion of the wrist brings along a change in ulnar deviation.

vi. The ROMs of lateral bending and forward flexion of the thorax are linked together by a *direct proportionality* because, in order to fulfil the motor task for a fixed target, a change in sagittal proximity requires an adjustment in medio-lateral alignment.

The low value of J^2, during the reaching phase, (reported in Table 4.1) is related to the fact the healthy population completed the motor task in a fluid (mean value across the repetitions) and repeatable (std value) way. Similarly, values of J^2 have been calculated for the patients (cf. Chapter 5 for specific results and details); if they are found to be higher than normal, it could be an indication of a less fluid conduction of movement, especially with abrupt accelerations or decelerations.

Connected to this findings, the result obtained calculating the *NMU*, look at movement smoothness in terms of velocity (rather than acceleration). In fact, the normal mean value of 1 with a std of 0, for the healthy group (Table 4.1), shows how healthy subjects execute the motor task in one stroke, without vacillations or changes in the speed or direction of motion; it is expected, on the contrary, that dyskinetic patients might generally display larger *NMU* with a greater variability.
Looking at the *Ic* reported, it is worth to notice how this index can give an idea of the goodness execution of the movement in terms of adherence to an optimal path. In fact, while the mean value for the healthy subjects is quite similar to 1 (basically they move the hand along a straight line between the starting point and the target, during reaching task) and the standard deviation quite small (high repeatability), the value obtained for the dyskinetic patients is expected to be higher, both mean and std (cf. Chapter 5 for specific results and details).
Looking at the kinematic parameters of velocity and acceleration it is possible to observe that in particular the acceleration (mean value in Fig. 4.19) shows a noisier trend, derived from a less fluid movement, during the return towards the initial position, while completing the pointing forward task. Also, the movement is slower in this phase. It can be argued that this happens, probably due to the fact that subjects mainly focus on reaching the target, moving their arm in the most efficient (and also fluid way), but, once the target is reached, they do not care anymore about the next part of the motion, not having a return target to reach, until the next pointing action.

4.5 Conclusions

By exploiting the functionalities of an optoelectronic system, used for motion analysis and quite accessible to many clinical centres, it is possible to analyse the subject's motion extracting kinematics

parameters that allow to describe in a qualitative and quantitative way the motor abilities of a subject during a particular motor task. The aim of this chapter was to provide an effective method based on that technology to study the complex motion of the upper limb in patients affected by Movement Disorders (and in particular Childhood Dyskinesia). This aim was practically achieved by designing *ad hoc* tools, such as, for example a redundancy scheme in the marker set-up, and an algorithm for the reduction in movement-dependent data loss.

The general method also makes available some normality values, in order to set a comparison baseline to understand better the patients' outputs.

Apart from its usefulness in characterising the state and severity of patients' conditions, the tool that was devised, makes also possible to evaluate in a qualitative and quantitative manner, the changes produced by a specific treatment, such as the use of the new dynamic wearable orthosis which is the subject of this thesis (cf. Chapter 3: *device* and Chapter 5: *clinical trials*).

4.6 References

Bartlett, R. (2007). *Introduction to sports biomechanics: Analysing human movement patterns*. Routledge.

Bertucco, M., & Sanger, T. D. (2015). Current and emerging strategies for treatment of childhood dystonia. *Journal of Hand Therapy*, *28*(2), 185-194.

Butler, E. E., Ladd, A. L., Louie, S. A., LaMont, L. E., Wong, W., & Rose, J. (2010). Three-dimensional kinematics of the upper limb during a Reach and Grasp Cycle for children. *Gait & posture*, *32*(1), 72-77.

Butler, E. E., & Rose, J. (2012). The Pediatric Upper Limb Motion Index and a temporal–spatial logistic regression: Quantitative analysis of upper limb movement disorders during the Reach & Grasp Cycle. *Journal of biomechanics*, *45*(6), 945-951.

Chèze, L. (2014). *Other Titles from ISTE in Bioengineering and Health Science*. John Wiley & Sons, Inc..

Cappozzo, A., Della Croce, U., Leardini, A., & Chiari, L. (2005). Human movement analysis using stereophotogrammetry: Part 1: theoretical background. *Gait & posture*, *21*(2), 186-196..

Carpinella, I., Mazzoleni, P., Rabuffetti, M., Throsen, R., Ferrarin, M. (2006). Experimental protocol for the kinematic analysis of the hand: definition and repeatability. *Gait & Posture*, *23*, 44-54.

Chiari, L., Della Croce, U., Leardini, A., & Cappozzo, A. (2005). Human movement analysis using stereophotogrammetry: Part 2: Instrumental errors. *Gait & posture, 21(2)*, 197-211.

Coluccini, M., Maini, E. S., Martelloni, C., Sgandurra, G., & Cioni, G. (2007). Kinematic characterization of functional reach to grasp in normal and in motor disabled children. *Gait & posture, 25(4)*, 493-501.

Della Croce, U., Leardini, A., Chiari, L., & Cappozzo, A. (2005). Human movement analysis using stereophotogrammetry: Part 4: assessment of anatomical landmark misplacement and its effects on joint kinematics. *Gait & posture, 21(2)*, 226-237.

Eberly D. (2014). *Euler Angle Formulas.* Geometric Tools, LLC. http://www.geometrictools.com/

Freivalds, A. (2011). *Biomechanics of the upper limbs: mechanics, modeling and musculoskeletal injuries*. CRC press.

Gordon, L. M., Keller, J. L., Stashinko, E. E., Hoon, A. H., & Bastian, A. J. (2006). Can spasticity and dystonia be independently measured in cerebral palsy?. *Pediatric neurology*, *35*(6), 375-381.

Hall, S. J. (2012). *Basic Biomechanics* (6th Ed.). New York: McGraw-Hill, Inc..

Hopkins, B., & Westra, T. (1989). Maternal expectations of their infants 'development: some cultural differences. *Developmental Medicine & Child Neurology*, *31*(3), 384-390.

Jaspers, E., Desloovere, K., Bruyninckx, H., Molenaers, G., Klingels, K., & Feys, H. (2009). Review of quantitative measurements of upper limb movements in hemiplegic cerebral palsy. *Gait & posture, 30(4)*, 395-404.

Jaspers, E., Feys, H., Bruyninckx, H., Harlaar, J., Molenaers, G., & Desloovere, K. (2011). Upper limb kinematics: development and reliability of a clinical protocol for children. *Gait & posture, 33(2)*, 279-285.

Jaspers, E., Desloovere, K., Bruyninckx, H., Klingels, K., Molenaers, G., Aertbeliën, E., ... & Feys, H. (2011). Three-dimensional upper limb movement characteristics in children with hemiplegic cerebral palsy and typically developing children. *Research in developmental disabilities*, *32*(6), 2283-2294.

Kontaxis, A., Cutti, A. G., Johnson, G. R., Veeger, H. E. (2009). A framework for the definition of standardized protocols for measuring upper-extremity kinematics. *Clin. Biomech. 24(3)*, 246-53.

Leardini, A., Chiari, L., Della Croce, U., & Cappozzo, A. (2005). Human movement analysis using stereophotogrammetry: Part 3. Soft tissue artifact assessment and compensation. *Gait & posture, 21(2)*, 212-225.

Kapandji, A.I. (2011). *Anatomia Funzionale, Volume I.* (6th Ed.). Monduzzi Editoriale.

Koy, A., Lin, J. P., Sanger, T. D., Marks, W. A., Mink, J. W., & Timmermann, L. (2016). Advances in management of movement disorders in children. *The Lancet Neurology*, *15*(7), 719-735.

Marey, E. J. (1885). *La Méthode Graphyque dans le Sciences Experimentales*. G. Masson. Paris.

Mackey, A. H., Walt, S. E., Lobb, G. A., & Stott, N. S. (2005). Reliability of upper and lower limb three-dimensional kinematics in children with hemiplegia. *Gait & posture*, *22*(1), 1-9.

McGinley, J. L., Baker, R., Wolfe, R., & Morris, M. E. (2009). The reliability of three-dimensional kinematic gait measurements: a systematic review. *Gait & posture*, *29*(3), 360-369.

Muybridge, E. (1901). *The Human Figure in Motion.* Chapman & Hall, London.

Payton, C., & Bartlett, R. (Eds.). (2007). *Biomechanical evaluation of movement in sport and exercise: the British Association of Sport and Exercise Sciences guide*. Routledge.

Perry, J., & Davids, J. R. (1992). Gait analysis: normal and pathological function. *Journal of Pediatric Orthopaedics*, *12*(6), 815.

Petuskey, K., Bagley, A., Abdala, E., James, M. A., Rab, G. (2007). Upper extremity kinematics during functional activities: three-dimensional studies in a normal paediatric population. *Gait & Posture, 25*, 573-9.

Rab, G., Petuskey, K., Bagley, A. (2002). A method for determination of upper extremity kinematics. *Gait & Posture, 15*, 113-9.

Reid, S., Elliott, C., Alderson, J., Lloyd, D., & Elliott, B. (2010). Repeatability of upper limb kinematics for children with and without cerebral palsy. *Gait & posture*, *32*(1), 10-17.

Sanger, T. D. (2006). Arm trajectories in dyskinetic cerebral palsy have increased random variability. *Journal of Child Neurology*, *21*(7), 551-557.

Schmidt, R., Disselhorst-Klug, C., Silny, J., Rau, G. (1999). A marker-based measurement procedure for unconstrained wrist and elbow motions. *J. Biomech. 32*, 615-21.

Teulings, H. L., Contreras-Vidal, J. L., Stelmach, G. E., Adler C. H. (1997). Parkinsonism reduces coordination of fingers, wrist, and arm in fine motor control. *Exp Neurol., 146(1),* 159-70.

Williams, S., Schmidt, R., Disselhorst-Klug, C., Rau, G. (2006). An upper body model for the kinematical analysis of the joint chain of the human arm. *J. Biomech. 39*, 2419-29.

Winter, D. A. (2009). *Biomechanics and motor control of human movement*. John Wiley & Sons..

Whittle, M. W. (2014). *Gait analysis: an introduction*. Butterworth-Heinemann.

Wu, G., Van der Helm, F. C., Veeger, H. D., Makhsous, M., Van Roy, P., Anglin, C., ... & Werner, F. W. (2005). ISB recommendation on definitions of joint coordinate systems of various joints for the reporting of human joint motion—Part II: shoulder, elbow, wrist and hand. *Journal of biomechanics*, *38*(5), 981-992.

GVC Software: https://isbweb.org/software/

Chapter 5

A pilot series of five single-case clinical trials

The chapter presents the results of five single-case trials on patients affected by Childhood Dyskinesia, namely upper-limb dystonia and hyperkinesia. The clinical trials are aimed at assessing the effect of the pseudoelastic orthoses, developed in Chapter 3, on posture and movement control, and include the evaluation of the patients in 2 different conditions (with and without orthosis) at 2 milestones: before and after a one-month's rehabilitation treatment. The methods comprise clinical scales, videos, interviews, and the ad-hoc quantitative kinematic analysis presented in Chapter 4.

5.1 Introduction

The present study is aimed at evaluating some patients affected by Movement Disorders, in particular Childhood Dyskinesia, during a month's treatment with the new wearable passive orthosis developed for the support of the voluntary actions of the upper-limb. The particular disease that affects these children impairs severely their daily activities, reducing life-quality itself. Sudden, unpredictable, non-repeatable and hard-to-be-controlled movements sometimes prevent even the simplest motor tasks from being completed, although these subjects can understand them perfectly. Standard treatments, nowadays in use, are often unable to bring a real advantage and are not rarely inefficient, sometimes even harmful, and include pharmacological treatments, surgical interventions, standard orthoses and manual therapies, as explained in greater detail in Chapter 1 of the present work. An alternative could come from the use of in non-invasive therapies, e.g. in the form of an orthotic device that supports the residual voluntary motion of the patient and stabilises posture dynamically, i.e. without being a fixed constraint. This hypothesis however must be tested before any such device can be safely adopted.

We designed and constructed innovative devices of that kind, as reported in the Chapter 3 of this thesis. The objective of the present Chapter is to describe the procedure, by which they have been tested on 5 patients affected by Childhood Dystonia of different type and severity, and the results obtained.

All the subjects have been evaluated with a multiparametric experimental protocol, including, but not limited to, the methods devised and explained in Chapter 4, and the results coming from the kinematic analysis are the main endpoint of the present chapter. Due to the strong differences existing between the subjects enrolled, and their limited number, the present work does not aim to draw statistically compelling conclusions, but the results will rather be discussed

separately, on a single-patient basis, in order to highlight various positive aspects that could be of help in designing future investigations based on this pilot study, with a larger cohort of patients and a refined clinical indication.

5.2 Subjects & Methods

5.2.1 General approach and Methods overview

Five children affected by Movement Disorders and in particular, secondary dyskinetic and dystonic problems, were investigated during the execution of a set of motor tasks involving the upper limb. This was done through clinical scales, videos, interviews and by kinematic motion analysis: an optoelectronic system and reflective passive markers were used to assess the detailed execution of the motor tasks. Data collected with this technique were processed as described in detail in Chapter 4.

The resulting tracings and indices are compared across the conditions (*with* and *without* orthosis) to provide an impression of the instantaneous effect of the device, and across the milestones, to allow a comparison of the rehabilitation treatment, i.e. *pre-* and *post- a treatment duration of 1 month*. The kinematic parameters, extracted by the analysis of the data, provide results that are used to describe the outcomes of a month's orthotic treatment as an adjunct to the daily rehabilitation treatments of those patients. Statistical analysis was not attempted, due to the limited number of experimental subjects, but some general qualitative trends will be described. Normality, as obtained in Chapter 4, was used for baseline qualitative (but not quantitative) comparison, for the reasons explained in section 4.4.2.

Cross-comparisons with other treatments or a control group was not included, coherently with the pilot nature of the study, the complexity of enrolling patients with matching presentations, and the reduced time

for the study (which prevented a cross-over scheme, for instance). Nevertheless, the clinical history of the patients is known, and they were all enrolled after a long series of different treatments, mostly of limited effect.

5.2.2 Patients' population

We enrolled 5 patients (age 12.2 ± 5.6 years old), affected by Movement Disorders, in particular: 2 patients were mainly dystonic/hemiplegic, 2 patients had a clinical picture of spastic-dyskinetic tetraplegia with hyperkinetic components, and one patient was mainly dyskinetic with behavioural complications; all of them were evaluated in relation to the affected upper limb. Among the inclusion criteria, the subjects were required to possess the capability to remain seated at least in their customised seat, collaborate and be able to understand and follow instructions. Exclusion criteria were fixed upper-limb articular limitations, upper-limb pain, pharmacological treatment variations during the previous 6 months and during the trial, skin allergies and cutaneous problems that might preclude the use of orthoses.

They were proposed the experimental treatment electively, as an adjunct to their current pharmacological and physiotherapeutic regimes.

The parents of all the subjects signed an informed consent after having been made aware about the aims and procedures of the experiments. The Ethics Committee of Neurologic Institute "Carlo Besta" (Milan, Italy) granted ethical approval for this research programme.

Patient #1

Young boy of 17 years old with right-sided hemiplegia and mainly dystonic picture, as a result of an ischemic vascular lesion in the left lenticular capsule, with a major impairment to the upper-limb. Normal cognitive level (IQ > 70). He was not on physical therapy.

As regards the postural-kinetic aspects and the walking skills, he showed mild functional impairment to the lower limbs: in fact, he reached Level I in the Gross Motor Function Classification System (GMCFS), compatible with walk without restrictions both in and outside the home environment. Looking at the upper limb skills, he ranked at Level III of the severity classification in the Manual Ability Classification System (MACs functional Scale), with difficulties in manipulating objects and in need to be helped in organising and/or modifying activities. The execution is slow and is carried out in a not-satisfactory manner as regards both quality and quantity. The activities are performed independently if they have been previously prepared or adapted. The results of the Communicative Function Classification System (CFCS) have shown good skills both on the receptive and productive domains (Level I) (Hidecker et al. 2011).

In addition, on the MD-CRS (Movement Disorders – Childhood Rating Scale), the patient has reached the Level II (mild severity) with regard to the Functional Score, while he obtained Level I (normal level) in the Severity Score, thus achieving in Motor Global Score of mild severity (Level III).

Patient #2

Young boy of 17 years old, with a clinical picture of acquired hemiparesis, due to a possible encephalitis 6-months after birth; co-presence of spasticity and dystonia, impairment mainly to the upper-limb. Mild cognitive impairment and difficulties in learning, sometimes connected to the social environment (IQ > 70).

Physical therapy since childhood, suspended at 10 years old. Treatments with upper-limb botulinum toxin injection at the age of 10 and 11 years old, with poor exits. The boy walks autonomously (GMFCS level 1) with impairment in exploiting bimanual skills and handling. Slow and

inefficient execution of movements and fulfilling of tasks, even the ones previously adapted.

The results of functional communicative classification (CFCS) reports quite good capabilities in comprehension even if he is affected by dysarthria. He reached Level III (hard severity) in the MD-CRS for both Functional Score and Severity Score, therefore the Motor Global Score impairment is mild (Level III).

Patient #3

Young boy of 8 years old, affected by infantile cerebral palsy, of the spastic-dyskinetic type. Tetraparesis associated with hearing loss, outcome of kernicterus. He underwent cochlear implantation at the age of 16 months. Cognitive development clinically good and appropriate behavioural aspects (IQ > 70).

As regards the postural-kinetic aspects and the walking skills, he showed very severe functional impairment to the lower limb: in fact, he has been classified at Level V in the GMCFS classification.

Looking at the upper limb skills, he ranked at Level III of the severity classification in the functional MACs Scale, with difficulties in manipulating objects and the need to be helped in organising and / or modifying activities. The execution is slow and is carried out in an unsatisfactory manner as regards both quality and quantity.

In the classification of communicative function (CFCS), he obtained Level II: the child's communication is effective, but is slower in rhythmicity between speaker and/or listener, both with known and unknown partners. The child independently alternates the role of speaker and listener with most people and in most contexts, but the frequency of conversational switch is slow and can make the conversational interactions more difficult.

In addition, on the MD-CRS the patient has reached Level III (high severity) with regard to Functional Score, while he obtained Level IV (hard severe motor disorder) in the Severity Score, thus achieving in Motor Global Score high severity (Level IV).

Patient #4

Male child of 8 year old followed for non-developmental encephalopathy, spastic dyskinetic quadriplegia, outcome of perinatal suffering in child born on time. The neuroradiological picture was normal also after repeated checks: for this reason, a diagnostic study in metabolic genetics has been made, which showed non-pathological features, leading to the conclusion of a PCI picture. Normal cognitive level (IQ > 70).

From a clinical point of view, the child shows a tetraparesis with a component of quadriplegia mainly hypotonic and non-postural: the head control is not stable yet; in addition, there is an important hyperkinetic component affecting all 4 limbs that impairs every voluntary action. He continues the physical therapy with a frequency of 4 times/week. As regards the postural-kinetic aspects and the walking skills, he showed very severe functional impairments to the lower limbs: in fact, he reached Level V in the GMCFS classification: severe impairments even with the support of devices. He is not able to maintain the sitting position, neither to control stably the head without an aid. He has to be transported and assisted in all postures.

With respect to the functional use of the upper limbs, according to the MACs classification, he reached Level IV, characterised by possibilities of manipulation, in adapted situations, of a limited number of objects, easier to manage. He completes the activities with high effort and limited success. He requires continuous support and assistance and / or an adapted situation, even to carry out only a part of the activity.

In the functional communicative classification (CFCS), he achieved Level III: able to communicate quite effectively with known partners, while communication is not effective with the majority of the unknown partners.

In addition, on the MD-CRS the patient has reached Level III (high severity) with regard to the Functional Score, while he obtained Level IV (hard severe motor disorder) in the Severity Score, thus achieving in Motor Global Score high severity (Level IV).

Patient #5

Young girl of 6 years old, with a clinical picture of encephalopathy of unknown origin, diagnosed at the age of 17 months with microcephaly and psychomotor retardation (IQ < 70). All genetic investigations carried out so far were negative. The MRI showed normal findings apart from a slight thickening of the cortex left para-hippocampal gyrus and a slight expansion of the cortical gyri.

From a clinical point of view, the child is affected by dystonic quadriplegia with greater impairment in the upper extremities, more to the right side. She sees a physiotherapist twice a week for physical therapy and once a week hydrokinesitherapy.

Considering the postural-kinetic aspects, the patient has been assigned to a II level GMFCS: she is able to walk indoor and outdoor without manual devices, but sometimes with manual assistance over longer distances. As for the manipulative-praxic aspects, according to the MACS classification she is classified at level V: unable to handle objects bimanually and severely limited skills in executing even simple actions.

Coming to the communicative aspects, the language is absent but the understanding is good. The patient uses methods of Augmentative Communication. She reaches level IV of the CFCS classification, failing to

communicate on a regular basis with known partners, either as a speaker or listener.

5.2.3 Experimental protocol

The experimental protocol (Figure 5.1) included 2 milestones (*cond. T1 and T2*) separated by a treatment period of one-month; during this period the patients were asked to wear the dynamic upper-limb orthosis

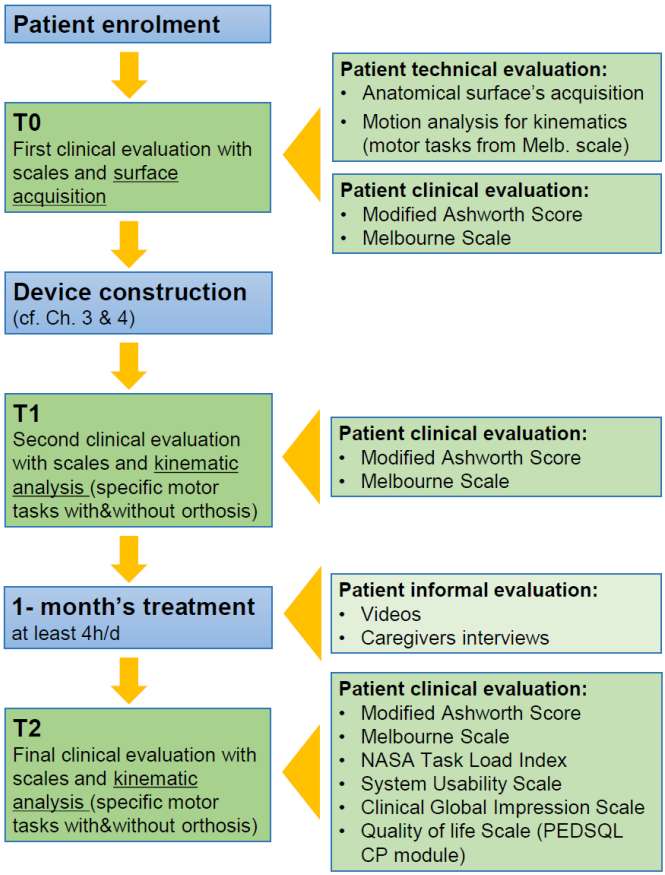

Figure 5.1 Experimental protocol devised to evaluate the patients.

for at least 4 hours a day, during the execution of their daily-life activities. The same trained clinician and physiotherapist evaluated all the patients with different Clinical Scales; in particular, at T1 they used the Modified Ashworth Score (MAS) and the Melbourne Assessment of Unilateral Upper Limb Function Scale (MULA), while at T2 they employed also the Quality of Life Scale (PEDSQL CP module) in addition to the scales executed at T1.

Participants also underwent 3D upper limb kinematic analysis at both milestones following the newly developed approach described in Chapter 4 of the present thesis. During the 3D optoelectronic evaluation, we asked the subjects to carry out 4 different selected movements, which were a subset of tasks adapted from the MULA consisting in:

i. Reaching forward to a target at the height of the shoulder;
ii. Carrying out a hand-to-mouth task that involved mimicking lifting a biscuit, from a standardised starting position on the table, to their mouth;
iii. Place a pen in a box, mimicking lifting a pen or a pencil, from a standardised starting position on the table, to the box on the table;
iv. Place a pen in a cup, mimicking lifting a pen or a pencil, from a standardised starting position on the table, to the cup or a glass on the table.

As described in the Melbourne Assessment Manual, the endpoint of the reaching task was the point where the participant made contact with the target. The endpoint of the pen-in-a-box or pen-in-a-cup task was the placement of the object in the box/cup. The endpoint of the hand-to-mouth task was the point when the biscuit contacted the mouth.

The experimental protocol included that the subjects repeated each exercise 5 times at a self-selected speed. During the assessments, the subjects were seated upright at a table in their own adjustable-in-height

chair, allowing their elbows to rest in 90° flexion on the tabletop (Fig. 5.2). The acquisitions were quite rapid and did not bother the children, generally they took no more than 30 minutes for both condition (the 4 motor tasks, *with* and *without* the device). The acquisitions were carried out at the LARES laboratory (Laboratory of Breathing Pattern Analysis located in the Department of Electronics, Information and Bioengineering of the Politecnico di Milano, Milan – Italy) shown in Figure 5.2. The methodology used for the kinematic analysis of the patients is described in detail in Chapter 4.

Besides the quantitative and qualitative measurements and evaluations carried out by clinicians and researchers, interesting and valuable results

Figure 5.2 The photo shows the laboratory where the acquisitions were carried out. In particular, the BTS SMART-Elite System with 8 infrared cameras that has been used to acquire the motion of the upper limb, the table and an adjustable-in-height chair (not a personalised one, as patients generally employed) at the LARES laboratory (Laboratory of Breathing Pattern Analysis located in the Department of Electronics, Information and Bioengineering of the Politecnico di Milano, Milan – Italy).

came from the comments of the families especially parents, but also physiotherapists and medical doctors who saw the patients before, during and after the clinical experimentations. Videos (Koy et al. 2016) taken by caregivers during the physiotherapy sessions or at home during daily activities, such as eating, playing, studying, drawing ect. helped us and the medical doctors understand better some hidden aspects or sometimes unclear trends in their quantitative results, i.e. the clinical scale scores and kinematic results.

5.3 Results and discussion for each single-case trial

5.3.1 Foreword

In general it was observed that our patients displayed many of the features already described in the literature, such as slow and variable movements with increased curvature and accompanied by exaggerated axial motion (cf. section 4.1.4). The detailed results obtained from the analysis of the patients who took part to the experimentation, will be presented separately for each patient, as independent single-case clinical trials, due to the strong specificity of the subjects. Only 4 out of the 5 enrolled patients have been evaluated with the optoelectronic system or clinical scales: this was in fact impossible for Patient #5, due to serious behavioural issues. Furthermore, only the data acquired for the pointing-forward task could be analysed within the timeframe of this thesis. The data for the remaining tasks will be the subject of future publications.

5.3.2 Patient #1

Patient #1: Personalisation of the orthosis

The orthosis for this patient was constructed aiming to control primarily the right wrist and hand postures, which were initially held in a very tight flexion scheme (Fig. 5.3 *left*). The pseudoelastic elements were used to

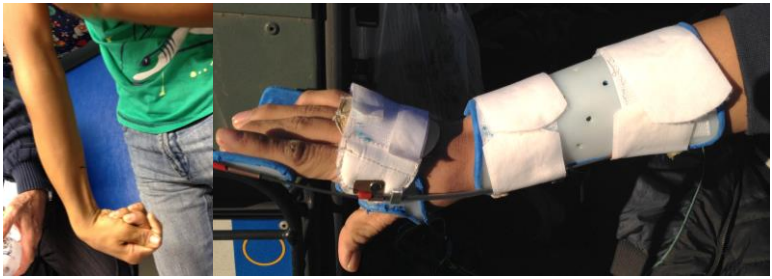

Figure 5.3 Pathological posture of the wrist in Patient #1 (*left*). Personalised orthosis designed and constructed for the same patient (*right*). It is worth to notice how the device promotes a repositioning towards a more physiological neutral wrist flexion and a relaxation of the thumb muscles, which stops pressing tightly against the index as shown on the left photograph.

generate an extension torque that was driving the wrist and fingers towards a reference angle of around 0° of flexion while also correcting the ulnar deviation, without fixing joint positions. An extended support for the fingers was used to release their hyperflexion, also decreasing the painful posture, reducing contraction, and allowing a more functional use of the fingers. The patient wore the orthosis for a month, 8/9 hours a day, with good acceptance.

Patient #1: Results

The clinical scales reported a little variation in MAS (pre: 5; post: 6, overall values for the upper limb) and a decrease in MULA (pre: 64.7%; post: 53.0%). The results coming from the kinematic analysis are reported in Figures 5.4, 5.5, 5.6. Considering the thorax motions, the mean Thorax lateral flexion decreases towards normality and the oscillations are task-related; the Thorax torsion reduces excessive movement amplitude and becomes more similar to the normal case (especially without the orthosis). The Thorax forward flexion on the other hand, becomes normal at T2, with the orthosis, while without the device the posture is a little too much backwards (Fig. 5.4). Looking at

the shoulder motions, the improvements are connected to all the degrees of freedom, with effective ranges of motion becoming globally closer to normal by T2 (Fig. 5.5). Wearing the orthosis has a very evident effect on the elbow joint flexion that improves in both average value and effective range after the treatment (T2). The best achievement is with the orthosis (Fig. 5.6). The wrist joint posture improves after the treatment: the orthosis can maintain the flexion angle around the neutral position; without orthosis the wrist collaborates to carry out the motor task with task-related movement.

Table 5.1 *Mean values of the temporal (tT, tN, tTt, tTm) and spatial parameters (D, S, V) for Patient #1. The kinematic parameters shown are the mean values across the 5 repetitions of the reaching target task: pre- and post- one-month's treatment, and with and without the orthosis. In the bottom row, the corresponding values for the healthy population enrolled in the study of Chapter 4. The definitions of these parameters are found in Chapter 4.*

ID	cond.	tT	tN	tTt	tTm	D	S	V
#1	T1	25,65	3,73	3,29	21,80	18,65	465,79	157,41
	T1ort	17,39	1,67	0,57	13,97	15,44	280,14	170,55
	T2	23,11	1,71	5,70	14,75	52,90	338,77	225,68
	T2ort	27,42	2,01	1,02	18,87	46,37	367,74	189,63

ID	tT	tN	tTt	tTm	D	S	V
Healthy	12,41	0,91	0,26	10,47	17,97	357,12	409,56

Table 5.2 *ROMs of the angular and linear parameters resulting from the kinematic analysis for the patient #1. The kinematic parameters shown are the mean values across the 5 repetitions of the reaching target task: pre- and post-one-month treatment, and with and without the orthosis. In the bottom row, the corresponding values for the healthy population enrolled in the study of Chapter 4. The definitions of these parameters are found in Chapter 4.*

ID	cond.	ShF	ShA	ShI	ElF	ElP	WrF	WrU	ThX	ThY	ThZ	ThLF	ThT	ThFF
#1	T1	32,50	43,44	74,72	16,79	43,28	22,41	8,41	26,93	15,87	62,15	4,00	12,30	10,85
	T1ort	20,55	18,95	25,94	6,71	7,18	1,90	1,00	8,81	4,66	25,60	2,13	5,08	4,29
	T2	29,03	19,04	37,64	27,04	38,37	41,72	12,75	24,76	8,10	26,37	5,10	4,03	7,97
	T2ort	22,78	39,54	43,73	29,33	20,00	5,64	12,98	25,94	10,36	66,85	5,11	8,47	12,07

ID	ShF	ShA	ShI	ElF	ElP	WrF	WrU	ThX	ThY	ThZ	ThLF	ThT	ThFF
Healthy	45,09	21,87	23,08	41,64	12,31	12,06	7,14	16,19	5,74	17,83	3,23	3,02	11,57

Table 5.3 *Indices Ic (index of curvature) and NMU (number of movement units) for Patient #1. The kinematic parameters shown are the mean values across the 5 repetitions of the reaching target task: pre- and post- one-month treatment, and with and without the orthosis and (last row) the mean value of the healthy population enrolled in the study of Chapter 4. The definitions of these parameters are found in Chapter 4.*

ID	cond.	Index	Max	Min	Mean	StDev	Index	Max	Min	Mean	StDev	Nrep
#1	T1	Ic	3,90	1,24	1,92	1,32	NMU	4,00	1,00	2,00	1,41	4,00
	T1ort	Ic	1,20	1,07	1,13	0,06	NMU	1,00	1,00	1,00	0,00	5,00
	T2	Ic	1,28	1,02	1,17	0,11	NMU	2,00	1,00	1,60	0,55	5,00
	T2ort	Ic	1,33	1,04	1,19	0,11	NMU	3,00	1,00	1,60	0,89	5,00
Healthy		Ic	1,12	1,03	1,06	0,05	NMU	1,07	1,00	1,01	0,05	5,00

The ulnar deviation improves especially without the orthosis on (Fig. 5.6). The kinematic analysis yielded interesting results (cf. Table 5.1, 5.2, 5.3); in particular, the parameters *Ic* and *NMU* varied between T1 and T2 in both condition, with and without the orthosis. Alongside the standardised measures, additional information became available through informal reports by the patient about his daily activities. In particular, the patient noticed a decrease in pain to the wrist, a decreased need to stretch the hand and fingers manually (which was usually a continual necessity), an improved ease in conducting bimanual tasks during study and play time.

Patient #1: Discussion

Patient #1, affected by dystonic rigidity, after the rehabilitation period shows a modification in the thorax angular kinematics, which tends to become more similar to normality; in addition, there is an increment in the ranges of motion of the shoulder and the elbow joints, even if the initial functional limitations were more concentrated about the wrist joint – which determined the decision to make a hand-wrist orthosis in the first place, excluding the more proximal upper-limb districts. The overall effect was to decrease the excessive stereotyped tendency to

stiffen the limb posture, as if in search a biomechanically stable point. In this case, breaking the scheme at a distal level opened the way to a multi-joint approach to the task, which started to look more physiological. On the other hand, the results of the clinical scales did not suggest any global functional improvement. It was noticed that part of the reason for the poor performance at T2 depended on the patient's being quite apprehensive that day, which resulted, especially, in worsening of the

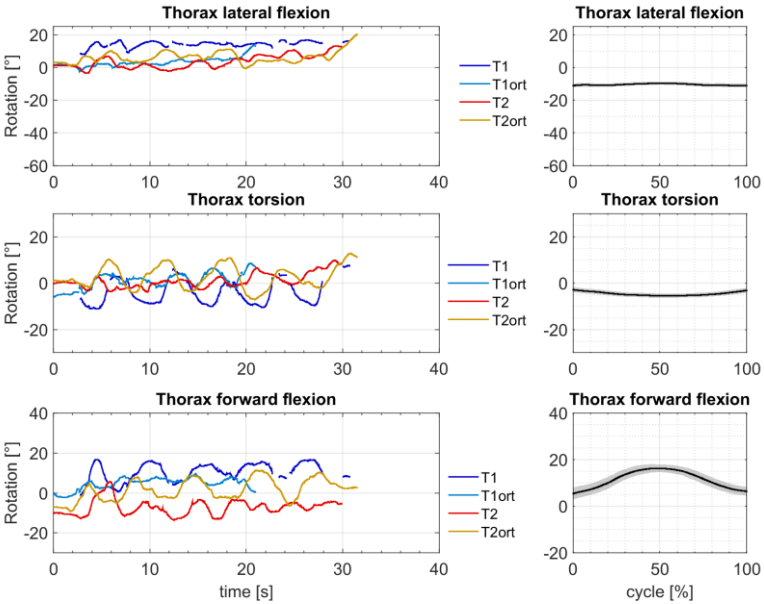

Figure 5.4 The graphs report, for Patient #1, the tracings of the angular kinematics of the *Thorax* during the pointing-forward task. The timecourses for the different degrees of freedom (*left side*) are compared with normal trends of the same parameters (*on the right* – average ± st. dev. over the subjects, against normalised repetition time, i.e. % of the cycle). The Thorax lateral flexion (*top*) is the oscillation left (negative) and right (positive) of the upper body; the Thorax torsion (*middle*) is the motion around the vertical axis of the body (positive leftwards) and the Thorax forward flexion (*bottom*) is the back (negative) and forth (positive) motion of the upper body.

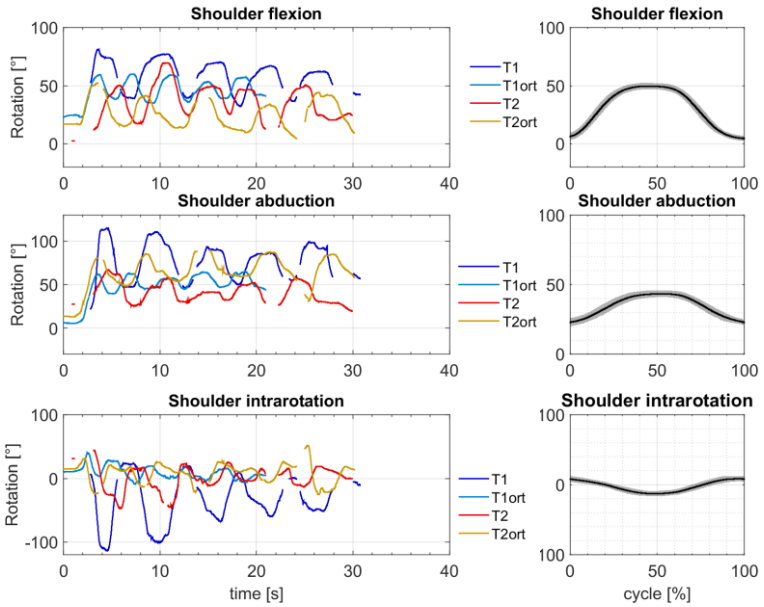

Figure 5.5 The graphs report, for Patient #1, the tracings of the angular kinematics of the *Shoulder* during the pointing-forward task. The timecourses for the different degrees of freedom (*left side*) are compared with normal trends of the same parameters (*on the right* – average ± st. dev. over the subjects, against normalised repetition time, i.e. % of the cycle). The Shoulder flexion (*top*) is the back (negative) and forth (positive) flexion of the shoulder joint; the Shoulder abduction (*middle*) is the motion that brings the arm from closer (negative) to the body to far (positive) from it laterally; and the Shoulder intrarotation (*bottom*) is the motion of the arm around its longitudinal axis (positive towards the body midline).

grasping actions (Butler et al. 2010), which are the precondition for many of the MULA items (but not the kinematic analysis tasks). The observed variations in the kinematic parameters *Ic* and *NMU* suggest that wearing the orthosis had an instantaneous effect at T1 more than at T2: it could be argued that the patient got used to the device action

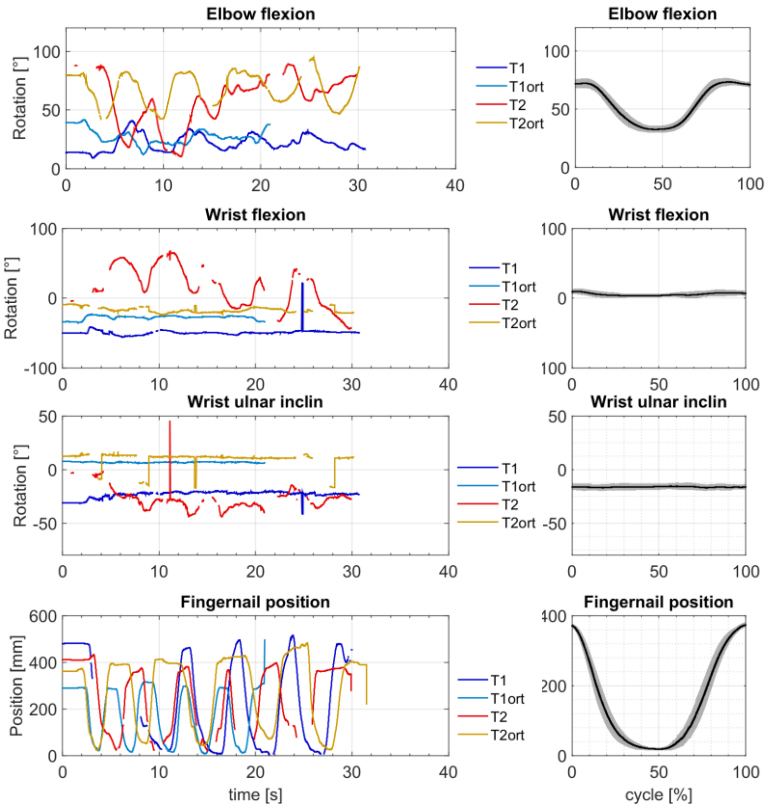

Figure 5.6 The graphs report, for Patient #1, the tracings of the angular kinematics of the *Elbow* and *Wrist*, and the *Distance of the Fingernail from the target* during the pointing-forward task. The timecourses for the different degrees of freedom (*left side*) are compared with normal trends of the same parameters (*on the right* – average ± st. dev. over the subjects, against normalised repetition time, i.e. % of the cycle). The Elbow flexion (*top*) is the rotating motion (flexion positive) around the joint centre of rotation in the plane of the humerus and forearm; the Wrist flexion (*second from the top*) is the rotating motion (volar positive) around the axis linking the radial and ulnar styloids; the Wrist ulnar inclin (*third*) is the medial/lateral deviation of the wrist joint (positive towards the ulnar side). The Fingernail distance from target (*bottom*) is always positive and decreases getting close to the target.

after one month of treatment. Furthermore the reduction of both parameters at T2, especially without the orthosis, suggests a positive effect and a stabilisation of the therapeutic action for this patient, also without wearing the device.

5.3.3 Patient #2

Patient #2: Personalisation of the orthosis

A complex orthosis (Fig. 5.7) was constructed for this patient aiming both to limit his tendency to stabilise the left limb by hyperextending the elbow joint and alleviate the very strong flexion of the wrist and fingers. Therefore, the pseudoelastic elements were used to (1) generate a flexion torque that was driving the elbow towards a reference angle of around 70° of flexion, without fixing its position and (2) extend the wrist and hand to a neutral resting position. (3) The forearm was kept at a neutral angle of prono-supination. The device imparts a torque that is approximately 70% the torque necessary to sustain the forearm and around 4-5% the maximal voluntary isometric contraction moment. The patient wore the orthosis for a month, 7 hours a day, with good acceptance.

Patient #2: Results

The clinical scales reported a slight variation in MAS (pre: 10; post: 9 – overall values for the upper limb) and an increase in MULA (pre: 25.9%; post: 31.9%). The results coming from the kinematic analysis are reported in Figures 5.8, 5.9 and 5.10. Concerning the thorax, the main improvement is seen in the forward flexion: at T1, the orthosis has an instantaneous stabilising effect; at T2, the patient appears to have gained a better average posture compared to normality (Fig. 5.8). As for the shoulder, the main improvements are in the reduction of the exaggerated quasi-fixed adduction: especially without the orthosis, the average posture reaches almost normal values at T2. There are also

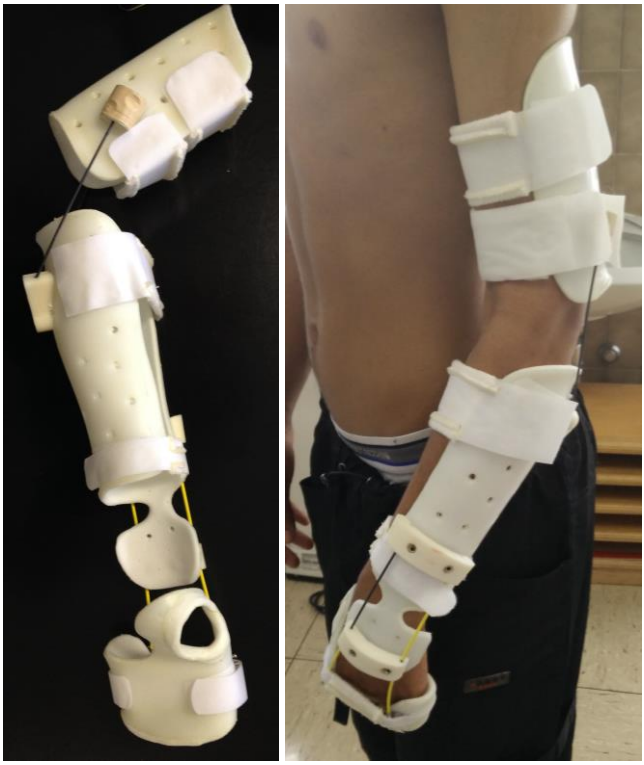

Figure 5.7 On the *left,* the multi-joint upper limb orthosis designed and constructed for the specific needs of Patient #2 (left). On the *right* the picture shows the posture assumed by Patient #2, while wearing the orthosis for the first time.

improvements in flexion/extension, with an increase in the effective range of motion (Fig. 5.9). Looking at the elbow joint, while the range of motion is small and irregular at T1, by T2 it has much improved, becoming larger and more coherent with the task repetitions. At the same milestones, the instantaneous effect of wearing the orthosis is to make motion steadier (Fig. 5.10). The wrist shows a better radial/ulnar inclination after the treatment (especially without the orthosis), while the initial hyperextension is converted into a large flexion (Fig. 5.10). In

general terms, the sequence of five movement repetitions is carried out faster, and the fingertip reaches closer to the target (Fig. 5.10). The kinematic analysis also provided interesting results (cf. Table 5.4, 5.5, 5.6); in particular, the parameters *Ic* decreased and *NMU* remained slightly stable between *T1* and *T2* in both condition: *with* and *without* the orthosis. The patient reported being comfortable with the device apart from some sweating in the heat of summer and noticed some general improvement in posture, while wearing the orthosis and some softening of the hand rigidity.

Table 5.4 *Mean values of the temporal (tT, tN, tTt, tTm), and spatial parameters (D, S, V) for Patient #2. The kinematic parameters shown are the mean values across the 5 repetitions of the reaching target task: pre- and post- one-month's treatment, and with and without the orthosis. In the bottom row, the corresponding values for the healthy population enrolled in the study of Chapter 4. The definitions of these parameters are found in Chapter 4.*

ID	cond.	tT	tN	tTt	tTm	D	S	V
#2	T1	15,98	1,51	0,90	15,12	65,28	369,59	249,48
	T1ort	11,77	1,13	0,62	11,17	58,93	337,82	336,68
	T2	19,23	1,15	4,88	14,22	144,47	392,61	459,90
	T2ort	10,64	1,16	0,30	10,17	106,83	319,37	302,70

ID	tT	tN	tTt	tTm	D	S	V
Healthy	12,41	0,91	0,26	10,47	17,97	357,12	409,56

Table 5.5 *ROMs of the angular and linear parameters resulting from the kinematic analysis for the patient #2. The kinematic parameters shown are the mean values across the 5 repetitions of the reaching target task: pre- and post-one-month treatment, and with and without the orthosis. In the bottom row, the corresponding values for the healthy population enrolled in the study of Chapter 4. The definitions of these parameters are found in Chapter 4.*

ID	cond.	ShF	ShA	ShI	ElF	ElP	WrF	WrU	ThX	ThY	ThZ	ThLF	ThT	ThFF
#2	T1	20,60	20,07	15,79	20,02	13,62	6,28	9,25	176,31	64,50	54,87	11,43	6,25	20,13
	T1ort	21,53	18,04	19,41	10,23	5,20	5,61	8,70	115,86	55,87	38,42	12,78	4,77	16,30
	T2	32,52	31,42	41,60	34,69	36,50	9,16	8,59	41,41	56,86	26,39	11,17	5,37	9,29
	T2ort	19,40	27,46	28,08	21,31	21,91	11,15	8,40	84,18	72,25	31,87	12,55	4,83	14,47

ID	ShF	ShA	ShI	ElF	ElP	WrF	WrU	ThX	ThY	ThZ	ThLF	ThT	ThFF
Healthy	45,09	21,87	23,08	41,64	12,31	12,06	7,14	16,19	5,74	17,83	3,23	3,02	11,57

Table 5.6 *Indices Ic (index of curvature) and NMU (number of movement units) for the patient #2. The kinematic parameters shown are the mean values across the 5 repetitions of the reaching target task: pre- and post- one-month treatment, and with and without the orthosis. In the bottom row, the corresponding values for the healthy population enrolled in the study of Chapter 4. The definitions of these parameters are found in Chapter 4.*

ID	cond.	Index	Max	Min	Mean	StDev	Index	Max	Min	Mean	StDev	Nrep
#2	T1	Ic	1,86	1,39	1,60	0,18	NMU	3,00	1,00	2,00	0,71	5,00
	T1ort	Ic	1,69	1,22	1,42	0,24	NMU	2,00	1,00	1,20	0,45	5,00
	T2	Ic	3,19	1,07	1,67	0,88	NMU	4,00	1,00	1,80	1,30	5,00
	T2ort	Ic	1,68	1,10	1,44	0,27	NMU	4,00	1,00	2,00	1,22	5,00
Healthy		Ic	1,12	1,03	1,06	0,05	NMU	1,07	1,00	1,01	0,05	5,00

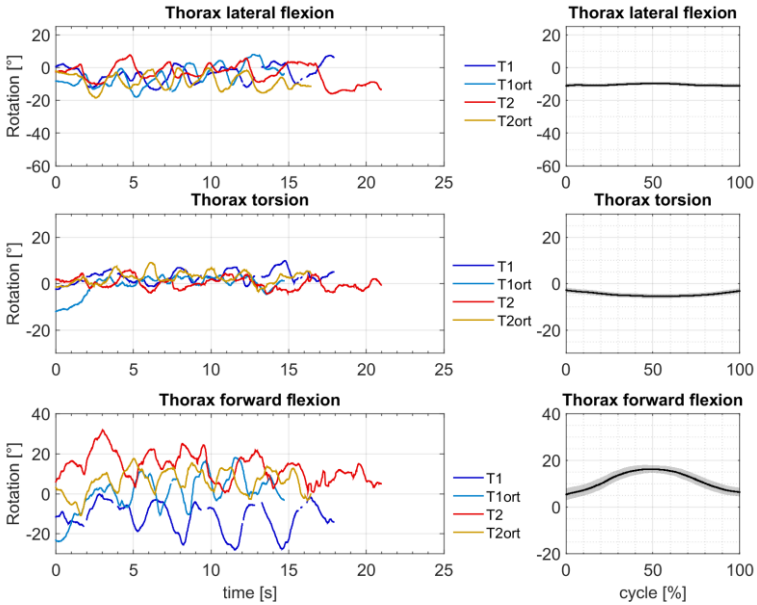

Figure 5.8 The graphs report, for Patient #2, the tracings of the angular kinematics of the *Thorax* during the pointing-forward task. The timecourses for the different degrees of freedom (*left side*) are compared with normal trends of

the same parameters (*on the right* – average ± st. dev. over the subjects, against normalised repetition time, i.e. % of the cycle). The Thorax lateral flexion (*top*) is the oscillation right (negative) and left (positive) of the upper body; the Thorax torsion (*middle*) is the motion around the vertical axis of the body (positive rightwards) and the Thorax forward flexion (*bottom*) is the back (negative) and forth (positive) motion of the upper body.

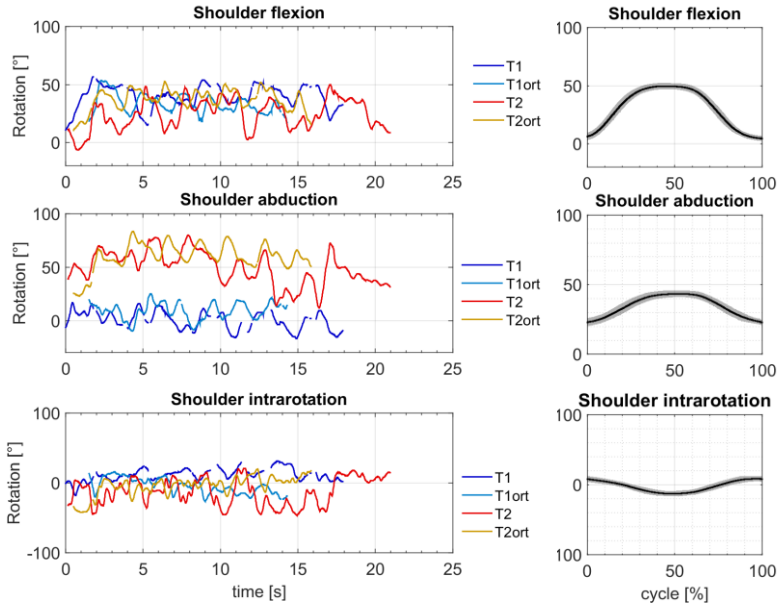

Figure 5.9 The graphs report, for Patient #2, the tracings of the angular kinematics of the *Shoulder* during the pointing-forward task. The timecourses for the different degrees of freedom (*left side*) are compared with normal trends of the same parameters (*on the right* – average ± st. dev. over the subjects, against normalised repetition time, i.e. % of the cycle). The Shoulder flexion (*top*) is the back (negative) and forth (positive) flexion of the shoulder joint; the Shoulder abduction (*middle*) is the motion that brings the arm from closer (negative) to the body to far (positive) from it laterally; and the Shoulder intrarotation (*bottom*) is the motion of the arm around its longitudinal axis (positive towards the body midline).

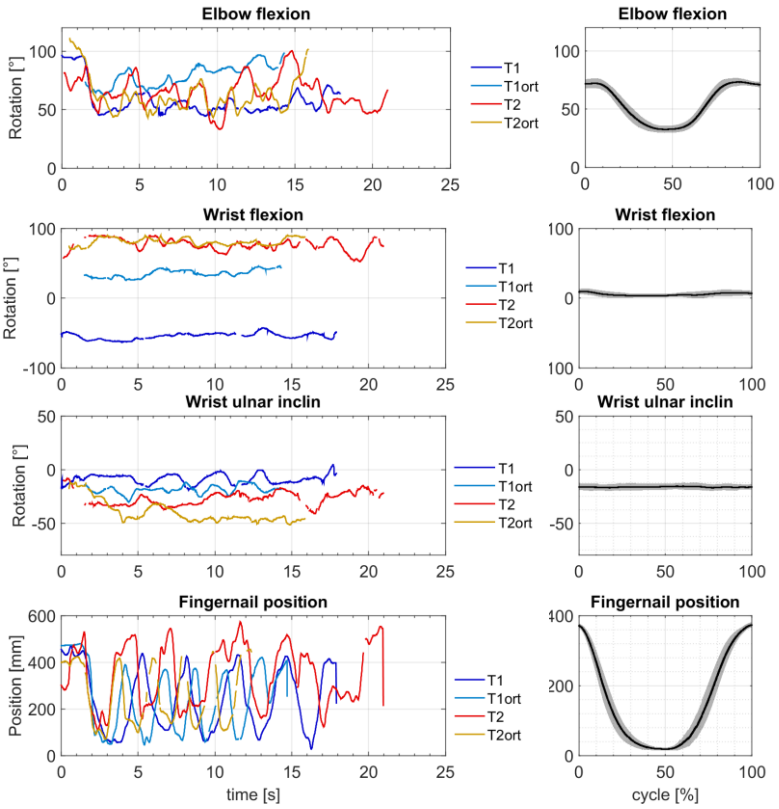

Figure 5.10 The graphs report, for Patient #2, the tracings of the angular kinematics of the *Elbow* and *Wrist*, and the *Distance of the Fingernail from the target* during the pointing-forward task. The timecourses for the different degrees of freedom (*left side*) are compared with normal trends of the same parameters (*on the right* – average ± st. dev. over the subjects, against normalised repetition time, i.e. % of the cycle). The Elbow flexion (*top*) is the rotating motion (flexion positive) around the joint centre of rotation in the plane of the humerus and forearm; the Wrist flexion (*second from the top*) is the rotating motion (volar positive) around the axis linking the radial and ulnar styloid and the Wrist ulnar inclin (*third*) is the medial/lateral deviation of the wrist joint (positive towards the ulnar side). The Fingernail distance from target (*bottom*) is always positive and decreases getting close to the target.

Patient #2: Discussion

For Patient #2, the orthotic treatment produced a change in the approach and movement strategies employed to carry out the task. The initial scheme was based mainly on exploiting macroscopic back and forth thorax motion, as the shoulder always remained very tightly adducted and the elbow was used very little. Many different movement parameters were modified after the treatment: the kinematic analysis showed a better thorax stabilisation, the reduction of the shoulder adduction, as well as an increase in the ranges of motion of the shoulder, elbow and wrist flexion. Although the patient was now combining and effectively controlling a far larger number of degrees of freedom, the net result was nonetheless a faster execution of the same number of repetitions, and a slight improvement in reaching closer to the target. Looking at the clinical scales, it can be observed that the use of this type of dynamic orthosis did not produce any increase in hypertone, but instead a slight decrease; that is consistent with the fact that joint control is not obtained by fixing its position, but rather through the application of mild forces. Considering the MULA score, it can be argued that the changes in the motor scheme suggested by the kinematic analysis did translate into a better functional ability to carry out a number of different standardised tasks (+23%). The observed variations in the kinematic parameters *Ic* and *NMU* suggest that wearing orthosis had an instantaneous effect both at T1 and T2: this effect is produced especially with the device on. These results suggest that small oscillations are compensated more at the beginning of the orthotic treatment rather than at the end; although this patient was able to carry out the task both at the before and after the treatment, the best stabilisation was always observed while using the orthosis.

5.3.4 Patient #3

Patient #3: Personalisation of the orthosis

The orthosis for this patient was constructed aiming to support primarily the left elbow joint, which was generally not completely under control, although used in a relative voluntary manner coordinated with the task objective (Fig. 5.11 *top*). The pseudoelastic elements in this case were not used to reposition the limb, because no fixed joint posture was present during the movements. The approach adopted was to choose a reference angle similar to the physiological neutral elbow angle of 110°-120° and to use pseudoelasticity and damping to generate both a mild flexion and extension torque around that position, just to provide sensory feedback (Fig. 5.11 *bottom*). The device imparts a torque that is approximately 200% the torque necessary to sustain the forearm and around 5-6% the maximal voluntary isometric contraction moment. The patient wore the orthosis for a month, 8/9 hours a day, with good acceptance especially during daily activities.

Patient #3: Results

The clinical scales reported no variation in MAS (pre: 0; post: 0 – overall values for the upper limb) and a small decrease in MULA (pre: 69.8%; post: 63.8%). The results of the kinematic analysis are reported in Figures 5.12, 5.13 and 5.14. Concerning the thorax, the main variations are seen in the lateral flexion and torsion: from T1 to T2 the average value of those tracings remain similar to normality although the oscillation around the average increases in a task-related way; another effect visible on the thorax parameters is the reduction of the high frequency noise superimposed to the signal (Fig. 5.12). Looking at the shoulder parameters the execution is generally correct and task-related, especially for the flexion; the average value of the shoulder abduction stays higher than normality but is always task related. The shoulder intrarotation increases its phasing to the overall movement at T2,

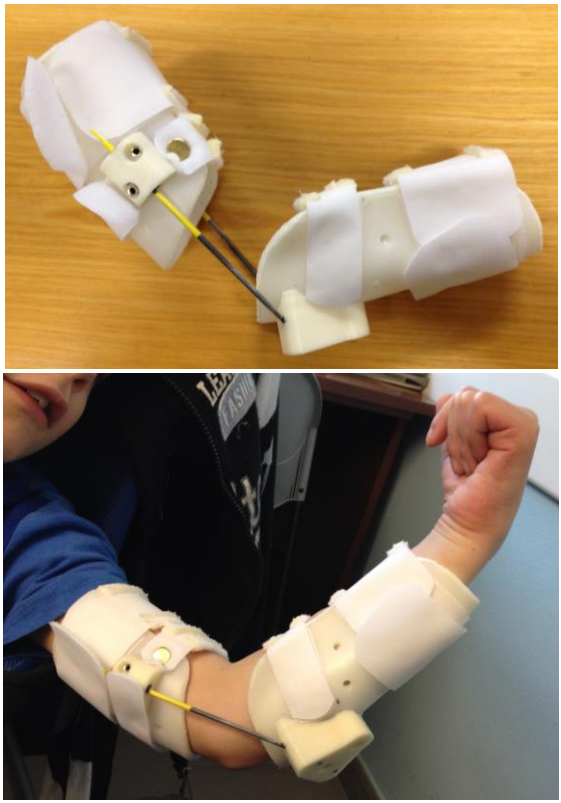

Figure 5.11 *Top,* the orthosis designed and constructed for Patient #3. *Bottom*, the orthosis worn by the patient: it can be noticed how the NiTi bars are aligned with the joint centre without touching the limb, to prevent any possible discomfort. This was achieved by carefully designing customised wire fixtures (Chapter 3).

especially without the orthosis, although a superimposed high frequency noise persist (Fig. 5.13).

Looking at the elbow joint, while the range of motion without the orthosis is quite large and similar between T1 and T2 (reaching slightly larger extension angles after the treatment), the ROM with the orthosis

is a little smaller with a reduction in the extension. The wrist shows a smaller radial/ulnar ROM after the treatment (both with and without the orthosis), while the initial small ROM in the wrist flexion/extension is converted into a larger ROM, both with and without the orthosis (Fig. 5.14). In general terms, the sequence of five movement repetitions is carried out more slowly after the treatment (Fig. 5.14). The patient reported being comfortable with the device especially for some particular daily activities, such as playing videogames and feeding himself. His mother reported that the child was asking to wear the orthosis for those activities. The videos taken by caregivers in a more familiar environment, the comments reported by therapists together with our videos taken during the kinematic analysis, were all coherent in suggesting that the patient seemed to get helped by the device. In particular, his parents reported that he was more comfortable in feeding himself, playing, and handling the videogames controller, after one month of treatment and especially using the orthosis; moreover his therapist reported an improvement in some items of the MULA when done with the orthosis on and also during a specific sports activity, i.e. fencing, where he was able to control the sword better with the orthosis.

Table 5.7 *Mean values of temporal (tT, tN, tTt, tTm), and spatial parameters (D, S, V) for Patient #3. The kinematic parameters shown are the mean values across the 5 repetitions of the reaching target task: pre- and post- one-month treatment, and with and without the orthosis. In the bottom row, the corresponding values for the healthy population enrolled in the study of Chapter 4. The definitions of these parameters are found in Chapter 4.*

ID	*cond.*	*tT*	*tN*	*tTt*	*tTm*	*D*	*S*	*V*
#3	T1	25,70	1,34	7,87	13,23	17,55	300,44	233,41
	T1ort	31,76	1,75	12,90	13,22	18,76	246,57	185,66
	T2	22,79	1,11	7,92	9,52	18,81	214,20	210,60
	T2ort	34,15	1,34	14,32	9,42	15,79	219,80	202,70

ID	*tT*	*tN*	*tTt*	*tTm*	*D*	*S*	*V*
Healthy	12,41	0,91	0,26	10,47	17,97	357,12	409,56

Table 5.8 *ROMs of the angular and linear parameters resulting from the kinematic analysis for the patient #3. The kinematic parameters shown are the mean values across the 5 repetitions of the reaching target task: pre- and post-one-month treatment, and with and without the orthosis. In the bottom row, the corresponding values for the healthy population enrolled in the study of Chapter 4. The definitions of these parameters are found in Chapter 4.*

ID	cond.	ShF	ShA	ShI	ElF	ElP	WrF	WrU	ThX	ThY	ThZ	ThLF	ThT	ThFF
#3	T1	55,61	29,13	39,71	67,12	32,95	44,52	28,76	11,66	9,24	28,42	4,25	8,27	11,25
	T1ort	36,95	23,73	42,19	32,57	18,11	21,80	36,51	34,30	14,23	26,30	8,22	6,74	15,08
	T2	17,01	22,77	53,43	13,87	45,53	63,41	19,84	35,55	12,37	29,09	11,13	7,10	15,19
	T2ort	27,40	23,09	37,84	41,63	18,75	44,04	15,59	56,60	19,67	31,90	10,28	6,06	11,95

ID	ShF	ShA	ShI	ElF	ElP	WrF	WrU	ThX	ThY	ThZ	ThLF	ThT	ThFF
Healthy	45,09	21,87	23,08	41,64	12,31	12,06	7,14	16,19	5,74	17,83	3,23	3,02	11,57

Table 5.9 *Indices Ic (index of curvature) and NMU (number of movement units) for the patient #3. The kinematic parameters shown are the mean values across the 5 repetitions of the reaching target task: pre- and post- one-month treatment, and with and without the orthosis. In the bottom row, the corresponding values for the healthy population enrolled in the study of Chapter 4. The definitions of these parameters are found in Chapter 4.*

ID	cond.	Index	Max	Min	Mean	StDev	Index	Max	Min	Mean	StDev	Nrep
#3	T1	Ic	2,07	1,21	1,48	0,34	NMU	3,00	2,00	2,20	0,45	5,00
	T1ort	Ic	4,42	1,28	2,19	1,28	NMU	5,00	2,00	3,20	1,64	5,00
	T2	Ic	2,08	1,14	1,62	0,35	NMU	3,00	1,00	2,20	0,84	5,00
	T2ort	Ic	3,26	1,03	1,81	0,86	NMU	7,00	1,00	3,20	2,39	5,00

Healthy	Ic	1,12	1,03	1,06	0,05	NMU	1,07	1,00	1,01	0,05	5,00

Patient #3: Discussion

Looking at the general execution of the motor task proposed to this hyperkinetic patient, it seems that the instantaneous effect of the orthosis was to "hinder" his capability to perform a movement or a sequence that he was already able to carry out with his initial motor skills. Also the condensed kinematic indices *Ic* and *NMU* (increased) were

negatively affected by the use of the orthosis before and after the treatment (cf. Table 5.9). However, for this patient, the informal reports by family and caregivers, were not in line with those quantitative observations. Furthermore, after checking the videos shot during the kinematic assessment, we observed that the patient showed a greater ease in carrying out the motor task, which was evident in spite of the longer total time spent in executing the motor task repetitions, and

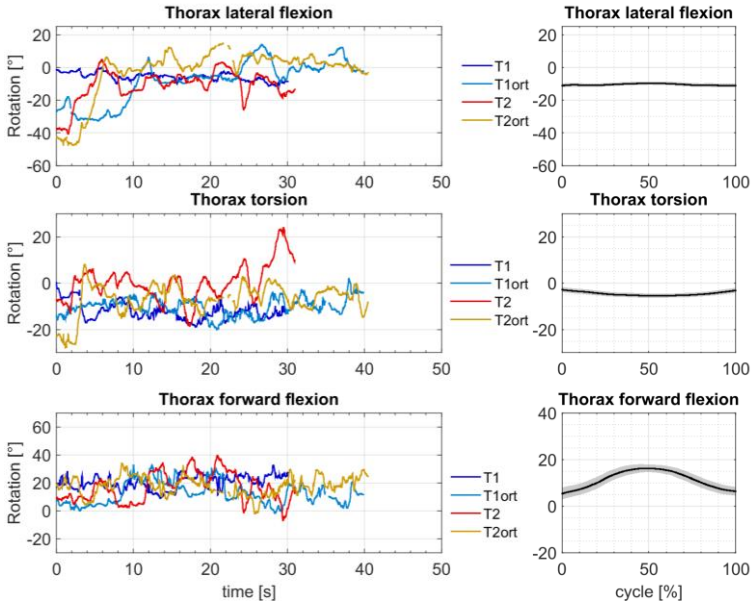

Figure 5.12 The graphs report, for Patient #3, the tracings of the angular kinematics of the *Thorax* during the pointing-forward task. The timecourses for the different degrees of freedom (*left side*) are compared with normal trends of the same parameters (*on the right* – average ± st. dev. over the subjects, against normalised repetition time, i.e. % of the cycle). The Thorax lateral flexion (*top*) is the oscillation left (negative) and right (positive) of the upper body; the Thorax torsion (*middle*) is the motion around the vertical axis of the body (positive leftwards) and the Thorax forward flexion (*bottom*) is the back (negative) and forth (positive) motion of the upper body.

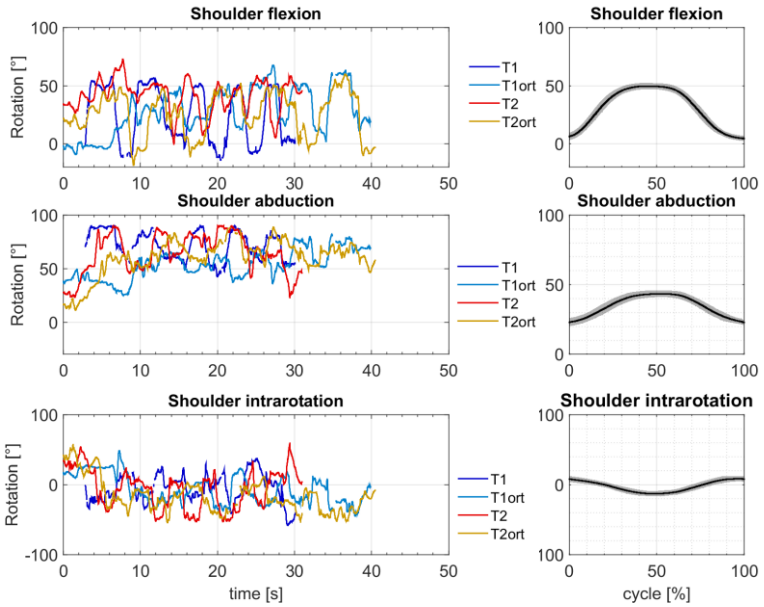

Figure 5.13 The graphs report, for Patient #3, the tracings of the angular kinematics of the *Shoulder* during the pointing-forward task. The timecourses for the different degrees of freedom (*left side*) are compared with normal trends of the same parameters (*on the right* – average ± st. dev. over the subjects, against normalised repetition time, i.e. % of the cycle). The Shoulder flexion (*top*) is the back (negative) and forth (positive) flexion of the shoulder joint; the Shoulder abduction (*middle*) is the motion that brings the arm from closer (negative) to the body to far (positive) from it laterally; and the Shoulder intrarotation (*bottom*) is the motion of the arm around its longitudinal axis (positive towards the body midline).

almost an attempt to show off his capabilities: in fact, the longer execution time was not because of a slower motion speed altogether, but because of a much longer time spent on the target (cf. Fig. 5.14 *bottom*), which for hyperkinetic patients is quite a difficult exercise. The lack in measurable quantitative improvements during the tests could be explained inferring that if a subject presents with a kinematic picture in

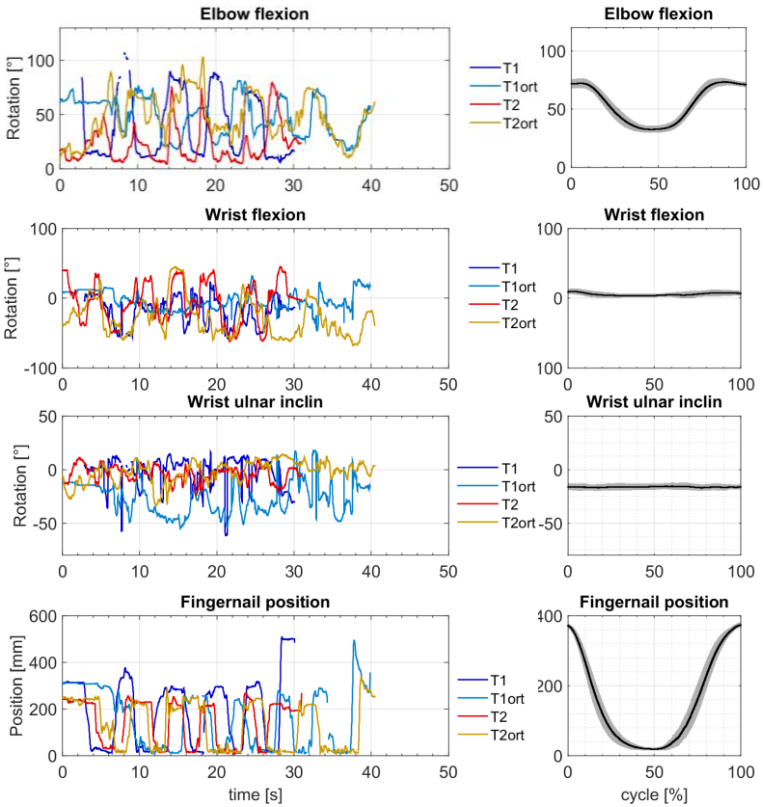

Figure 5.14 The graphs report, for Patient #3, the tracings of the angular kinematics of the *Elbow* and *Wrist*, and the *Distance of the Fingernail from the target* during the pointing-forward task. The timecourses for the different degrees of freedom (*left side*) are compared with normal trends of the same parameters (*on the right* – average ± st. dev. over the subjects, against normalised repetition time, i.e. % of the cycle). The Elbow flexion (*top*) is the rotating motion (flexion positive) around the joint centre of rotation in the plane of the humerus and forearm; the Wrist flexion (*second from the top*) is the rotating motion (volar positive) around the axis linking the radial and ulnar styloid and the Wrist ulnar inclin (*third*) is the medial/lateral deviation of the wrist joint (positive towards the ulnar side). The Fingernail distance from target (*bottom*) is always positive and decreases getting close to the target. *Bottom*: the

T2 tracings (*red* and *yellow*) are longer because the flat parts are longer: this depends on the finger being held around the target for a longer time, rather than a slower motion, which would be represented (and is not) by a less steeper slope of the non-flat parts of the tracings.

which there are no degrees of freedom that are functionally blocked, the orthosis will not produce any postural change. While initially the added force field could be felt to act against the already existent motor skills it is possible that eventually it may help handle dynamic tasks more precisely or stabilise the endpoint of movement (like in touching the target or wielding a sword).

5.3.5 Patient #4

Patient #4: Personalisation of the orthosis

The orthosis for the fourth patient was constructed aiming to support and drive the right elbow joint, which was not controlled or used in a precise and voluntary way during motion (Fig. 5.15 *top*). In fact, the subject tended to keep the elbow joint generally extended (but not completely fixed), without using it appropriately during the movement execution, and rather compensating with the thorax motion. Considering those results, the pseudoelastic elements were shape-set to impart a sufficient force not to be too high as to prevent voluntary motion, but high enough to impart a mild and continuous torque and thus be clearly perceived. The approach adopted was to choose a reference angle similar to the physiological neutral elbow angle of 110°-120° and to use pseudoelasticity and damping to generate the flexion and extension torque around that position (Fig. 5.15 *middle*). The device imparts a torque that is approximately 200% the torque necessary to sustain the forearm and around 6-8% the maximal voluntary isometric contraction moment. The patient wore the orthosis for a month, 8/9 hours a day, with good acceptance, with only some issues due to the heat localised under the valves (the rehabilitation month has been

unluckily planned in July/August).

Patient #4: Results

The clinical scales reported no variation in MAS (pre: 1; post: 1 – overall values for the upper limb) and a strong increase in MULA (pre: 7.3%; post: 16.4%). The results coming from the kinematic analysis are reported in Figures 5.16, 5.17 and 5.18.

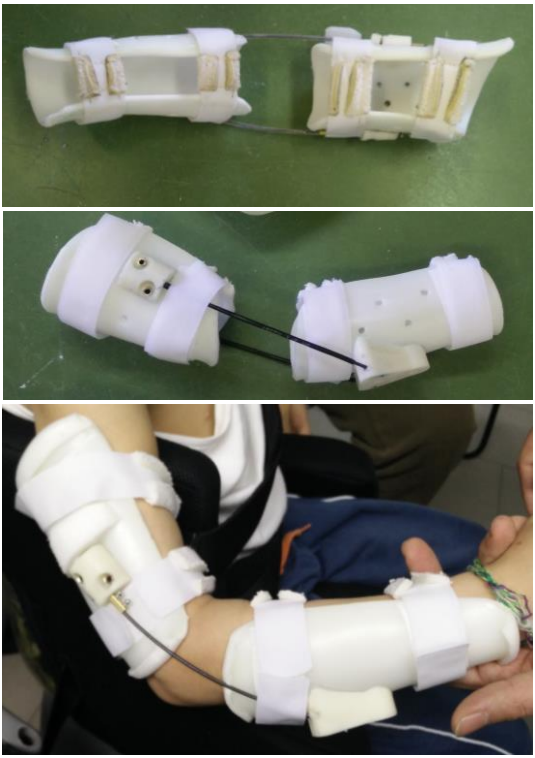

Figure 5.15 *Top* and *middle* are shown the top and lateral view of the orthosis designed and customised for Patient #4. *Bottom*, the instantaneous repositioning effect of the orthosis on the affected upper limb: naturally and gently the orthosis imparts a force field that acts pushing the limb towards a more physiological resting posture.

Overall, the target is never reached. Concerning the thorax, the main variations are seen in the torsion and forward flexion, whose ROMs decrease from T1 to T2 towards normality values (these trends can be seen especially without the orthosis, due to the severe and unrecoverable loss in the thorax pool of markers during the T2ort kinematic assessment). Looking at the shoulder joint, the traces of abduction and intrarotation did not vary largely, but they remained in the range of normality. On the other hand, the shoulder flexion/extension ROM increased in term of baseline, towards a more physiological value and in terms of variations; in fact, while at T1 there is no effective attempt at reaching the target, at T2 a certain motor task correlation can be appreciated with some distinguishable repetitions although blurred and affected by high frequency noise. The elbow flexion/extension tracing did not reveal any particular variation, remaining in the range of 0° of flexion; also the wrist flexion ROM and ulnar deviation remained still during the kinematic assessment but in almost physiological ranges. For this patient it was not possible to calculate any synthetic index, because the movement repetitions could not be segmented. In addition to the presented results, some interesting videos shot by the family and caregivers became available during the month of treatment, which recorded important improvements in the patient's ability to control the upper limb in daily activities. For the sake of clarity and brevity they are described and commented in the discussion, next.

Patient #4: Discussion

The very severe condition of this patient precluded the possibility to acquire and collect a good dataset, so tracings are severely affected by lacunae and many losses due to his unpredictable and uncontrollable movements (see Fig. 5.19). Nonetheless, the results coming from the clinical scales and the videos taken by his parents are quite impressive: not only has he been able to use his arm more functionally but also to

control the involuntary movements. After one month of treatment with the pseudoelastic orthosis, besides the positive comments and improvements reported by teachers at the primary school, the videos taken by the therapist during a rehabilitation session in the swimming pool (Fig. 5.20) revealed an increased capability in a real-life *reaching task* similar to the one proposed during kinematic assessment, even though the precision of the performance was not completely good.

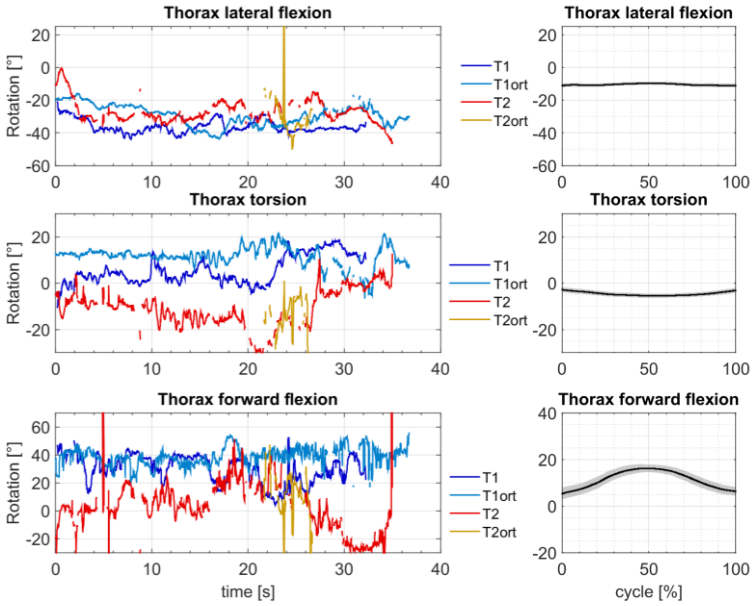

Figure 5.16 The graphs report, for Patient #4, the tracings of the angular kinematics of the *Thorax* during the pointing-forward task. The timecourses for the different degrees of freedom (*left side*) are compared with normal trends of the same parameters (*on the right* – average ± st. dev. over the subjects, against normalised repetition time, i.e. % of the cycle). The Thorax lateral flexion (*top*) is the oscillation left (negative) and right (positive) of the upper body; the Thorax torsion (*middle*) is the motion around the vertical axis of the body (positive leftwards) and the Thorax forward flexion (*bottom*) is the back (negative) and forth (positive) motion of the upper body.

Even more surprising were the videos taken at the end of the one-month treatment with the new orthotic device: the two videos, whose screenshots are reported in Fig. 5.21 show the patient feeding himself, first using his hand (a task that he had never been able to do before), and few minutes later using a fork, which definitely requires a higher precision and control.

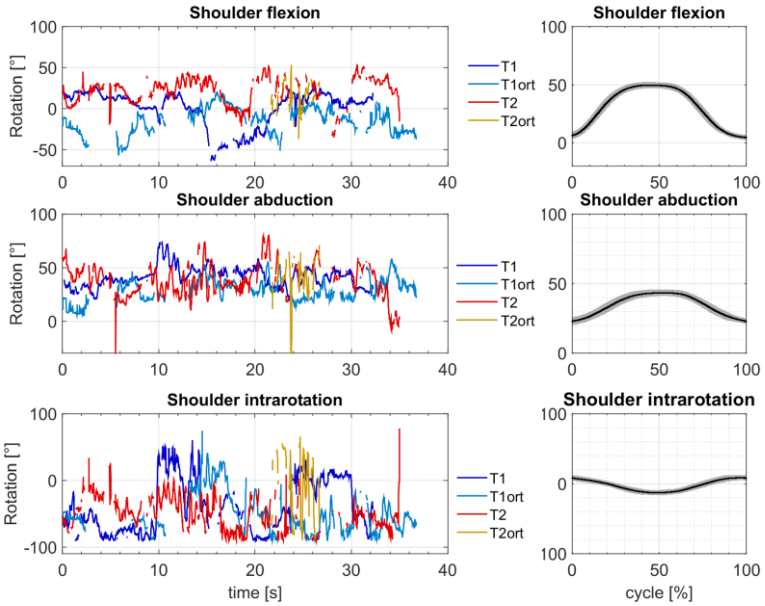

Figure 5.17 The graphs report, for Patient #4, the tracings of the angular kinematics of the *Shoulder* during the pointing-forward task. The timecourses for the different degrees of freedom (*left side*) are compared with normal trends of the same parameters (*on the right* – average ± st. dev. over the subjects, against normalised repetition time, i.e. % of the cycle). The Shoulder flexion (*top*) is the back (negative) and forth (positive) flexion of the shoulder joint; the Shoulder abduction (*middle*) is the motion that brings the arm from closer (negative) to the body to far (positive) from it laterally; and the Shoulder intrarotation (*bottom*) is the motion of the arm around its longitudinal axis (positive towards the body midline).

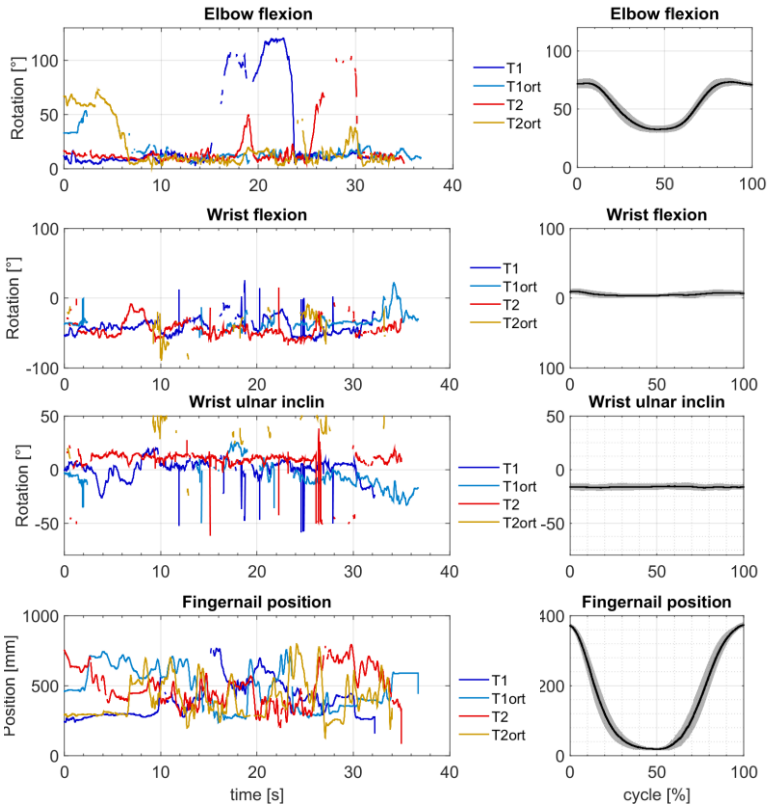

Figure 5.18 The graphs report, for Patient #4, the tracings of the angular kinematics of the *Elbow* and *Wrist*, and the *Distance of the Fingernail from the target* during the pointing-forward task. The timecourses for the different degrees of freedom (*left side*) are compared with normal trends of the same parameters (*on the right* – average ± st. dev. over the subjects, against normalised repetition time, i.e. % of the cycle). The Elbow flexion (*top*) is the rotating motion (flexion positive) around the joint centre of rotation in the plane of the humerus and forearm; the Wrist flexion (*second from the top*) is the rotating motion (volar positive) around the axis linking the radial and ulnar styloid and the Wrist ulnar inclin (*third*) is the medial/lateral deviation of the wrist joint (positive towards the ulnar side). The Fingernail distance from target (*bottom*) is always positive and decreases getting close to the target.

Furthermore, these goals were carried out without wearing the device. An explanation of these results could come from considering the high level of participation that this patient always showed. He could understand the tasks quite well and really struggled very hard to reach the target during the tests, however, being in an unfamiliar environment, such as the laboratory, with many people staring, if he gradually got tired and was unable to start the movement well, his general motivation tended to wane and thus the outcome could be affected in a drastic way. Possibly a friendlier environment was one of the factors producing the best performances at home or at the pool.

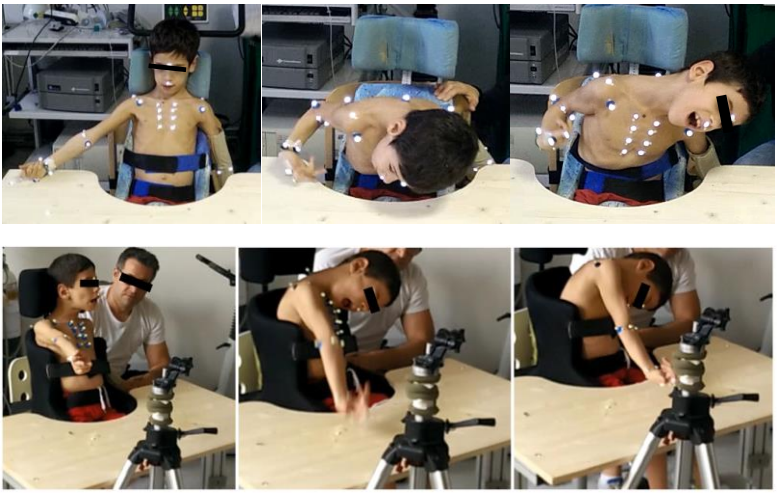

Figure 5.19 Screenshots of the video taken during the preliminary kinematic assessments (T1) of Patient #4, during hand-to-mouth (*top*) and pointing-forward (*bottom*) tasks. It is evident from the 3 consecutive instant how the random, large and unpredictable movements of the thorax and limbs strongly affect the markers visibility in the FOV of the optoelectronic system cameras and thus the possibility to reconstruct their spatial position, whatever the position of the markers and cameras. The global motion of the trunk and upper limb is completely ineffective, and the hand never reaches close to the goals (mouth or target).

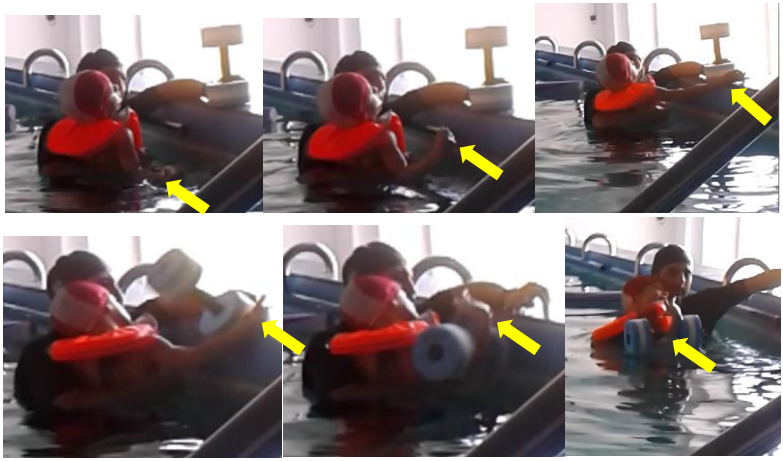

Figure 5.20 Screenshots taken during a hydrokinesitherapy session of Patient #4's. The *yellow arrows* highlight the hand position during the action of reaching a buoy. It is worth to notice how the task is carried out quite well, despite the particular environment, even if the final grasp is still lacking.

Figure 5.21 Screenshot sequence shows patient #4 during **autonomous** feeding action: it is quite astonishing to see how a task, which has never been possible before (see Fig. 5.19 *top*), is now doable, even with the fork (*red circle*), which definitely adds an extra difficulty. In particular, notice that the trunk is completely upright and steady, in comparison with Figure 5.19, above.

5.3.6 Patient #5

Patient #5: Personalisation of the orthosis

The procedures used for Patient #5 have been the same as for the others: the orthosis for this patient was constructed aiming to support the left elbow joint, which was generally not completely under control, and often held in a hyperflexion scheme, together with a mild supination of the forearm. Due to the extremely delicate behavioural condition of the little girl, the pseudoelastic elements in this case were used to favour the limb repositioning, but not imparting a too high force field, that could easily be perceived as a constraint more than a sensory stimulation by the patient. We chose a reference angle similar to the physiological neutral elbow angle of 110°-120° and we fixed the pseudoelastic wires asymmetrically on the shells to impart a mild torsion on the forearm valve with respect to the one of the upper arm. In this manner we imparted an initial torque towards pronation to recover a more physiological condition. As for the previous devices presented above, the pseudoelasticity and damping generated also a mild flexion and extension torque around the neutral position (Fig. 5.22). The device imparts a torque that is approximately 200% the torque necessary to sustain the forearm and around 6-7% the maximal voluntary isometric contraction moment.

Patient #5: Results and Discussion

Despite the really severe behavioural problems of this patient, which precluded the possibility to carry out longer kinematic evaluations or administer the clinical scales, with the methods devised for the surfaces acquisition (cf. Chapter 3), we have been able to collect sufficient data to reconstruct the geometry of the arm (Fig. 5.23) and thus design a fully customised orthosis. The patient wore the orthosis for a month, 4/6 hours a day, with quite good acceptance (considering her general

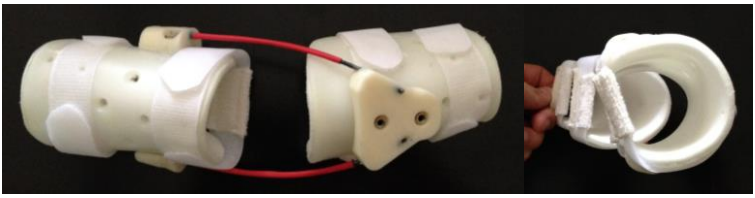

Figure 5.22 The personalised orthosis designed and constructed for patient #5. On the right, it is important to notice the relative rotation between the two valves, which is introduced to impart an initial pronation, to correct also the excessive supination of the forearm.

Figure 5.23 The screenshot, from the video taken during the preliminary tentative evaluation of Patient #5, shows the evident problems related to the low collaborative level of the little girl, while evaluating her upper limb kinematics. Nevertheless the protocol devised for the upper limb surface reconstruction (cf. Ch. 3), allowed to collect sufficient data in really little time (just one frame is enough), to design the customised valves of the orthosis.

Figure 5.24 The two photographs depict Patient #5 using the personalised orthosis, during daily-life activities, despite her generally low acceptance of any kind of devices (either wearable or not).

condition) (Fig. 5.24), especially during daily activities, i.e. playing and drawing, with also positive comments from the parents and caregivers at school. We were not able to conduct any kinematic acquisition in the standardised tasks or a scoring of MULA due to the very low compliance of the child. As a consequence, quantitative results are not available.

5.4 General discussion

5.4.1 Customisation of the orthoses

Generally, all patients reported a high level of comfort, being able to wear the devices for more than the minimal number of hours prescribed by the physicians. We believe the full customisation of the orthosis (geometrical and functional) produces important results in terms of better acceptability, comfort, and hence usability. The methods used to design the valves allowed to obtain a perfect adaptation to the anatomical surfaces of the patient's limb; the selection of the metallic

elements to place on the device (size, strength, pseudoelastic behaviour) together with the assembling procedure including a personalised tuning of the connections of the pseudoelastic elements onto the valves, allowed reducing the friction on the skin, by avoiding undesired movements between the valves and the limb surface. In this manner, the corrective forces imparted by the pseudoelastic elements could be transferred to the body in an effective way. Also the use of optoelectronic stereophotogrammetry as a very rapid and non-invasive system to acquire limb surfaces (as well as kinematics) did improve the general management of the surface acquisition, because the patients' involuntary motor patterns did not have to be constrained during long and boring acquisitions, which would have reduced the final quality of the available datasets. This has been of great importance for all the patients, and in particular for Patient #5, because, considering her very low compliance to be touched or handled, without this particular approach we would not have been able to acquire any data to design and construct the personalised device for the treatment.

5.4.2 Methods of assessment

The methods of assessment chosen for the present study were found quite balanced and helpful in providing an affordable pool of data to quantify the modification of the motor pattern and thus evaluating the patients before and after the treatment period. In fact, while the clinical scales are a standardised and easily-sharable tool, the kinematic analysis can provide a very fine detail of segmental motion, thus enabling disentangling of the components of functional changes, which was deemed essential for the present work. A similar use of this technique was in fact applied to other paediatric neurologic conditions of interest (Jasper et al. 2011; Butler et al. 2010; Reid et al. 2010). In addition, including interviewing, which was done both by PedsQL™, and more importantly informally, was useful to record effects not easily detectable by assessing patients at set time points only, and in a non-completely-

familiar environment. The experimental procedure devised for analysing the dystonic and hyperkinetic patients did present some difficulties however, specifically linked to the very nature of the movement disorder with its day-to-day ups and downs superimposed on the clinical evolution to be assessed.

The availability of direct accounts by the patients about the one-month experience, helped confirm some of the results obtained by quantitative kinematics, while the clinical scales sometimes depicted a worse-than-real scenario because they were scored on a “bad day”. Direct reports, were often more informative than PedsQL. In fact, the clinicians reported low reliability for the PedsQL score, due to the not completely coherent comments given by the patients or their caregivers, probably related also to the short rehabilitation time of one month.

The optoelectronic movement analysis proved a robust tool, showing detailed variations reliably. The main problem observed was connected to the unpredictability of the movements that the patients involuntarily make, which sometimes interfered with the possibility to obtain a complete dataset because the reflective markers got blocked out from the cameras. To avoid this, it was very useful to include some marker redundancy on the skin, and devise a specific algorithm to exploit that redundancy to minimise the data loss and the lacunae in the final datasets. Patient #4 can be considered as a limit case in relation to the use of our kinematic acquisition and analysis protocol: the tracings are corrupted but can be interpreted qualitatively; the severity of this patient’s hyperkinesia and the resulting inability to carry out proper repetitions of the task produced the practical impossibility to extract quantitative information and synthetic indices.

Overall, we found that using a multi-modal and multi-scale approach was important to provide a pool of data as complete as possible, and offer a more affordable evaluation not only of the new treatment proposed, but also of the clinical status of the patients.

5.4.3 Overall clinical considerations

The great differences in patients' presentations and their limited number were the main reasons for the single-case trial scheme chosen for the study. Individual results have been discussed. We shall now try to group some effects and discuss patients in comparison, without attempting any statistical analysis.

Four children made gains on at least one clinical scale (viz. MAS and/or MULA), The results of movement analysis indicated that (1) the two children with dystonic traits improved proximal stability in pointing and smoothness in arm movements, one of them also retained the improvements without the device; (2) the two children with hyperkinetic problems had smaller evidence in terms of ROM variations in proximal or distal districts, although parents and therapists reported a great improvement in the general stability and specific use of the limb in daily activities.

From a specifically quantitative kinematic perspective, the results suggest that the functional benefit of dynamic pseudoelastic NiTi-based devices could be greater for dystonic patients than hyperkinetic ones.

This difference could be explained inferring that if a subject presents with a kinematic picture in which there are degrees of freedom functionally blocked in terms of task-related ROM (as with more dystonic patients), the orthosis could act to improve his capabilities by initially releasing those degrees of freedom and changing the reference posture; on the other hand, if the joints are already all active during the task, but poorly controlled (a case mainly visible in the hyperkinetic subjects, especially #3) the force field does not have any repositioning action, but just a stabilising one.

The choice to treat only the joint(s) most affected revealed to be appropriate, because it was shown that local improvements tended to

irradiate to all the upper limb districts (very evident for Patient #1, and also Patient #2), with useful segmental changes in the involvement of joints far from the ones the orthosis was designed for and directly applied to. As a consequence, control schemes tended to become more complex and multi-joint. A possible interpretation of this behaviour, to be verified by extending the number of observations, is that limb control in secondary dystonia could be improved by acting with a coupled biomechanical-repositioning and proprioceptive action localised at one or more focal points in the kinematic chain. Removing or reducing in that way the adherence to a stiff postural scheme (often resorted to by the patients, as if to minimise the number of degrees of freedom to be controlled – cf. elbow extension in Patients #1, #2 and #4, shoulder adduction in Patient #2, etc.), and substituting it by a mild feedback action generated by the pseudoelastic elements in response to movement, it is possible that we are providing the patient with a reference viscoelastic force field, in which stabilising posture and motion becomes more affordable. In fact, the dynamic constraint induced by the orthosis, by providing some containment, might be sufficient to alleviate for the muscles the burden to continuously keep joints rigid and free them for functional use.

Coming to the videos and observations by the patients, parents and physiotherapists, despite the limitation of not being quantitative information and thus not providing measurable data, they showed, in many cases, how patients gained the ability to execute some simple actions that they were not able to do properly (such as drawing and holding the game controller during playing) and in 2 cases that they had never done before (feeding oneself independently, also with a fork; and reaching a buoy, stretching the arm in the swimming pool during a physiotherapy session). Those observations were made in particular for the hyperkinetic patients, and interpreted as a capacity of the orthosis to improve limb control stability. At least for Patient #4, the strong improvement in MULA over the period of study, is a confirmation of the

functional improvements achieved also in hyperkinesia. It is very unfortunate that those same observations could not be made quantitatively in the experimental setting of the kinematic laboratory. It is recognised, however, that for these patients, the emotional aspects must be taken into account in a very accurate manner, because they can strongly affect the assessment results (Gimeno et al. 2013; Koy et al. 2016), and this could be the case.

5.5 Conclusions of the study and future perspective.

With the quantitative and qualitative data reported in this study, and aware of the evident limitations of drawing conclusions from barely four/five single case studies, we can interpret the results of the present pilot trials to be in line with the rationale of the experiment. We observed variations in the movement strategies employed by two mainly dystonic patients and two mainly hyperkinetic patients, while carrying out the pointing-forward task. Those variations were dissimilar for the two "groups" of patients in that the more dystonic included a transition from an initial execution characterised by widespread stiffening of the limb, towards one involving a collaborative use of several joints; on the other hand, the mainly hyperkinetic patients displayed a different conditioning due to the orthosis: in particular, they reported a better control in the use of the limb, especially during the execution of various functional motor task, even if the kinematic analysis did not show any remarkable variation. Our present interpretation is that the repositioning of one or more joints in the kinematic chain by a dynamic force providing augmented proprioceptive feedback could help free the muscles from merely delivering stabilisation through stiffening, and allow their functional use in a more synergistic control scheme, especially when the initial status is characterised by a hypertone and resulting rigidity to one or more joints. When the initial picture is not characterised by one or more degrees of freedom being functionally

blocked, the orthosis does not seem to produce any measurable postural change, but, in the functional domain, control can become more stable, possibly due to the dynamic quality of the force field, namely the viscous component.

Especially for the hyperkinetic patients, with all-active degrees of freedom, the residual voluntary motion should not be hindered by the force field imparted, and thus this study suggests that the viscous component should be maximised, while the strength should probably low, in order to offer just a sensory stimulation and a proprioceptive enhancement. For the hypertonic patients, there is also a reason to keep corrective moments low, that is to reduce the risk to arouse an excessive stretch-reflex response. This working hypothesis should be tested on a larger cohort of dystonic and hyperkinetic patients.

In conclusion, all these findings suggest that the use of the new personalised dynamic pseudoelastic devices can affect in a positive and effective way the rearrangement of the motor scheme, leading from individually-different initial statuses to an overall more physiological condition.

5.6 References

Butler, E. E., Ladd, A. L., LaMont, L. E., & Rose, J. (2010). Temporal–spatial parameters of the upper limb during a reach & grasp cycle for children. *Gait & posture*, *32*(3), 301-306.

Butler, E. E., Ladd, A. L., Louie, S. A., LaMont, L. E., Wong, W., & Rose, J. (2010). Three-dimensional kinematics of the upper limb during a Reach and Grasp Cycle for children. *Gait & posture*, *32*(1), 72-77.

Gimeno, H., Gordon, A., Tustin, K., & Lin, J. P. (2013). Functional priorities in daily life for children and young people with dystonic movement disorders and their families. *european journal of paediatric neurology*, *17*(2), 161-168.

Hidecker, M. J. C., Paneth, N., Rosenbaum, P. L., Kent, R. D., Lillie, J., Eulenberg, J. B., ... & Taylor, K. (2011). Developing and validating the Communication Function Classification System for individuals with cerebral palsy. *Developmental Medicine & Child Neurology*, *53*(8), 704-710.

Jaspers, E., Desloovere, K., Bruyninckx, H., Klingels, K., Molenaers, G., Aertbeliën, E., ... & Feys, H. (2011). Three-dimensional upper limb movement characteristics in children with hemiplegic cerebral palsy and typically developing children. *Research in developmental disabilities*, *32*(6), 2283-2294.

Koy, A., Lin, J. P., Sanger, T. D., Marks, W. A., Mink, J. W., & Timmermann, L. (2016). Advances in management of movement disorders in children. *The Lancet Neurology*, *15*(7), 719-735.

Reid, S., Elliott, C., Alderson, J., Lloyd, D., & Elliott, B. (2010). Repeatability of upper limb kinematics for children with and without cerebral palsy. *Gait & posture*, *32*(1), 10-17.

Sanger, T. D. (2006). Arm trajectories in dyskinetic cerebral palsy have increased random variability. *Journal of Child Neurology*, *21*(7), 551-557.

Conclusions

Nowadays, one of the most relevant issues in the management of patients affected by Childhood Dyskinesia is the lack of valid, effective and always applicable solutions, which can account for the high variability of the patients' clinical pictures. In this respect, in the present thesis, the initial aim of probing the possible help and support given by a new passive dynamic and fully customised wearable orthotic device has been developed trying to cover all the aspect connected to this target. The literature research, through a goal-oriented analysis of the neurophysiological bases of the clinical problem, allowed us to identify the main impairing features and characteristics that could, on one side, be approached with orthotic treatments and, on the other side, should be overcome to make a difference in patients' life quality. The findings revealed the complexity of the problem, and also inspired the requirements of foremost technical relevance that had to be considered. Exploiting this preliminary result, we addressed the topic of selecting functional materials able to achieve the target, and in particular the deploy of appropriate therapeutic forces. The study of the materials characteristics, and the consequent selection of the NiTi-based alloys, have demonstrated to be a good choice in terms of accomplishment of the requests: the possibility to tune the material properties during thermomechanical shape setting, and thus broaden the range of the useful material characteristics, was exploited in the construction of the dynamic elements, i.e. the functional core of the devices. The decision to employ the optoelectronic system not only for the kinematic assessments, but also for the limb surface reconstruction, proved very valuable. In fact, despite the problems encountered with the patients' variability on the clinical and behavioural sides (strictly related to their pathological conditions), the method we devised has been efficient and provided affordable and reliable results that allowed us to design and

construct the personalised valves and fixtures of the customised orthoses. On the other hand, even if the optoelectronic system is a fairly standard tool employed for motion analysis, in the present application, it showed some peculiar aspects together with some limitations. In particular, this type of motion analysis did provide in general an objective methodology to characterise and to assess upper-limb dystonia and hyperkinesia in an experimental setting. However, while the specific protocol devised allowed to collect in a precise way the healthy subjects, in few cases, there have been some limitations for the patients: the large, random and unpredictable movements of the upper limb and thorax during the acquisitions limited the marker visibility during the execution of the requested motor tasks, sometimes preventing the reconstruction of their position in space for several consecutive timeframes. These problems encouraged us to develop a specialised method to reconstruct the data, limiting data loss; the achievement of this objective together with all the subroutines written *ad hoc* for the kinematic analysis of the data coming from the subjects, are part of the collateral results of the present thesis. These methods in fact, provided the data used to quantify the clinical changes connected with the use of the new wearable device during the one-month treatment of the patients.

The kinematic analysis reported for the patients, who took part to the study, showed that the repositioning of one or more joints in the kinematic chain by a dynamic force providing also augmented proprioceptive feedback could help free the muscles from merely delivering stabilisation through stiffening, and allow their functional use in a more synergistic control scheme, especially when the initial status is characterised by a hypertone and resulting rigidity to one or more joints. For the hypertonic patients, there is a reason to keep corrective moments low, that is to reduce the risk to arouse an excessive stretch-reflex response. When the initial picture is not characterised by one or

more degrees of freedom being functionally blocked, the orthosis does not seem to produce any measurable postural change, but, in the functional domain, control can become more stable, possibly due to the dynamic quality of the force field, namely the viscous component. The quantitative and qualitative results coming from the more hyperkinetic children suggested that if they displayed all-active degrees of freedom, the residual voluntary motion should not be hindered by the force field imparted, and thus this study suggests that the viscous component should be maximised, while the strength should probably be kept low, in order to offer just a sensory stimulation and a proprioceptive enhancement. The design of the trials in the form of a series of single-case studies, found its reason in the limited number of patients enrolled and analysed. This is on the one hand, a limitation because the general quantitative and qualitative findings cannot afford a general validity, but should only be regarded as a help and an initial guideline to plan future investigations on larger cohorts of subjects. On the other hand, the extreme heterogeneity displayed by the subjects enrolled has been a great challenge for the entire system devised to study this specific class of diseases, extract the requirements, design the concept of the new wearable solution, construct, test and evaluate it.

The general conclusions of the thesis are that the presented orthotic solution could be a valid adjunct in the rehabilitation treatment of young patients affected by Childhood Dyskinesia, because, based on the data analysed, they appear to act by repositioning the limb and rearranging the motor scheme, leading from individually-different initial statuses to an overall more physiological condition.

Acknowledgements

The possibility to tackle the extreme heterogeneity of topics presented in the thesis has been the result of a valuable collaboration with many different national and international partners, who helped me in carrying out the project, covering many of the technical aspects during these three-years' work. The project is the product of a collaboration proposed by the research Institute CNR ICMATE (National Research Council of Italy – Institute of Condensed Matter Chemistry and Technologies for Energy, Lecco), to the University Politecnico di Milano (DEIB – Department of Electronics Information and Bioengineering, Milan) and the IRCCS Neurological Institute Carlo Besta (Institute for Scientific Research and Care, Milan).

In particular, at the CNR, where I work as a research fellow, I have done the main part of the research from the technical experimentation on the materials and the design of the orthosis, to the analysis of the data coming from the kinematic analysis, under the supervision and the fundamental help of Dr. Simone Pittaccio, who took part in all the steps of this thesis being not only the advisor, but also a valuable help and advice in all the activities. During the study of the material properties, the preparation and the analysis of the samples I collaborated with the technicians Giordano Carcano and Enrico Bassani both belonging to the CNR – ICMATE, UOS Lecco coordinated by the researcher Dr. Francesca Passaretti.

The Politecnico di Milano is the University which gave me the possibility to carry out the PhD project from a formal point of view. Furthermore, in its LARes laboratory (Laboratory for the Analysis of Breathing) directed by Prof. Andrea Aliverti, I have carried out all the tests with the optoelectronic system, both on the healthy subjects and the patients, in

order to acquire and collect the kinematic data foreseen by the experimental protocol, collaborating in particular with Ms. Antonella LoMauro, who is in charge of the technical aspects of the optoelectronic system.

The Neurological Institute Carlo Besta is the hospital, which has been involved in the project. In particular, the Neurodevelopmental Unit directed by Dr. Daria Riva (later Dr. Chiara Pantaleoni, *ad interim*), participated for the patients' enrolment. Thanks to the work of Dr. Manuela Pagliano, Dr. Giovanni Baranello, and the help of the therapists Maria Teresa Arnoldi, Riccardo Zanin, and doctor in training Giorgia Aprile, we designed the clinical part of the project, we developed the clinical protocol, then submitted to the Ethical Committee of the Hospital. Additionally, these same people selected and enrolled the 5 patients for the study, and evaluated them at the three milestones planned by the study. They were also useful partners for discussions and focussing on the clinical aspects of the study.

To construct the new fully-customised wearable device for every patient enrolled, I exploited the technical know-how of the COE (Centro Ortopedico Emiliano, Reggio nell'Emilia – Italy) which is an orthopaedic factory, affiliate of Ottobock Italia, particularly expert in the manufacturing and construction of orthotic devices. There, thanks to the advice of Bruno Bassi and the technical help of Miguel Ferrari and Loredana Costi, I learnt the techniques to build the personalised orthoses and I assembled all the devices.

For the analysis of the kinematic dataset and an initial key to their interpretation, I received positive and helpful advice from the research group at the Department of Biomechanical Engineering, Faculty of Mechanical Engineering, Delft University of Technology (TU DELFT – The

Netherlands), where I spent some months collaborating with Prof. Frans van der Helm and Dr. Winfred Mugge.

At the beginning of this thesis, I had the opportunity to discuss the initial concept of the new wearable orthosis with Prof. Arjan Buis and Prof. Roy Bowers from the Biomedical Department of Strathclyde University (Glasgow – UK), receiving some comments about the requirements needed for my project and some positive criticism about the methods I should develop.

I also had the opportunity to present the investigation on the neurophysiological basis of the Childhood Dyskinesia and the general rational of the approach, to a recognised expert in this field: Prof. John Rothwell, head of Physiology and Pathophysiology of Human Motor Control at the UCL Institute of Neurology (University College of London – UK), receiving positive comments about the hypothesis of the project and the new possible approach developed in the thesis.